

DAMAGE IDENTIFICATION, PROGRESSION, AND CONDITION RATING OF  
BRIDGE DECKS USING MULTI-MODAL NON-DESTRUCTIVE TESTING

By

BRIAN M. PAILES

A Dissertation submitted to the

Graduate School-New Brunswick

Rutgers, The State University of New Jersey

in partial fulfillment of the requirements

for the degree of

Doctor of Philosophy

Graduate Program in Civil and Environmental Engineering

written under the direction of

Dr. Nenad Gucunski

and approved by

---

---

---

---

New Brunswick, New Jersey

May 2014

## ABSTRACT OF THE DISSERTATION

Damage Identification, Progression, and Condition Rating of Bridge Decks Using Multi-Modal  
Non-Destructive Testing

by BRIAN M. PAILES

Dissertation Director:

Dr. Nenad Gucunski

Bridges are an important part of the nation's infrastructure and due to the limited budgets available to keep them properly maintained, the methods of evaluation and damage identification must improve in accuracy and cost-effectiveness. For the industry of bridge evaluation and damage identification the research area that provides the greatest potential is multi-modal non-destructive testing (NDT). A multi-modal NDT approach to condition assessment allows for the identification of several different deterioration states, in turn providing a more complete condition assessment. Research was conducted to develop a methodology and program to convert multi-modal NDT data from bare reinforced concrete bridge decks into a condition-based assessment. The NDT methods utilized were electrical resistivity (ER), half-cell potential (HCP), ground penetrating radar (GPR), impact echo (IE), and chain drag (CD). Data for each of these methods was collected on 12 bridge decks located in various geographic locations. Correlations were identified between the NDT methods so as to better understand the relationship between the methods and concrete deterioration. Some of the identified correlations include a strong association of low cover depth with deterioration, ER and HCP measurements being highly related, and GPR attenuation associated with locations of deterioration identify by ER, HCP, and CD. The identified correlations were used to develop a statistics-based approach to threshold identification for ER, HCP, and GPR. Threshold values are highly relative; therefore, a statistical approach provides a more effective and robust threshold identification methodology. Using the

identified thresholds, the multi-modal NDT data was fused and converted into a deterioration-based condition assessment that identifies locations of corrosive environment, active corrosion, delamination/lateral cracking, and severe delamination. The condition assessment program also rates the bridge decks using established and federally mandated rating systems created by the National Bridge Inventory and American Association of State Highway and Transportation Officials. This research resulted in a more effective multi-modal NDT condition assessment of bridge decks. Improved multi-modal NDT will provide bridge owners and maintenance personnel an improved tool to assess bridge decks and to make decisions regarding their maintenance.

## ACKNOWLEDGMENTS

I would like to thank my advisor, Dr. Nenad Gucunski, for providing me with immeasurable amounts of guidance and support. I would like to also thank my thesis committee members, Dr. Ali Maher, Dr. Hao Wang, and Dr. Michael Brown.

I would also like to acknowledge the help of Arezoo Imani, Farhad Fetrat, Hooman Parvardeh, Sabine Krushchwitz, Shane Mott, Chris Mazzotta, Ken Lee, Francisco Romero, Erica Erlanger, Ronald Guillen, Insung Hwang, Daniel Guillen, Kevin Clark, Michael Morales, Rich Szatkowski, and Daniel Usher for their help in data collection. I would also like to thank Jeffery Milton, Dave Meggers, and Jim Leaden for taking time out of their schedules to discuss how departments of transportation use and apply federally mandated bridge rating systems.

I would also like to thank my parents, Lawrence and Goldie Pailes, who have provided me with love and support. Without them, I would have never become the person that I am today.

Last, but not least, I would like to thank “The Crew,” Ben, Da, Derek, Kyle, Nils, and Zack.

## TABLE OF CONTENTS

Abstract of the Dissertation .....	ii
Acknowledgments.....	iv
Table of Contents .....	v
List of Tables .....	viii
List of Figures.....	x
List of Equations .....	xiv
Symbols and Abbreviations .....	xv
Introduction.....	1
Objectives .....	5
Literature Review.....	6
Corrosion of Reinforced Concrete .....	6
Electrical Resistivity (ER) .....	8
Half-Cell Potential .....	10
Ground Penetrating Radar.....	12
Impact Echo .....	14
Chain Drag.....	16
Non-Destructive Testing Data Fusion.....	17
Methods and Materials.....	21
Non-Destructive Testing Methods.....	21
Equipment Details.....	23

Data Collection .....	25
Data Comparisons.....	27
Threshold Analysis .....	27
Condition Assessment.....	28
Condition Rating.....	30
Presentation of Deck Condition .....	34
Data Agreement Rating.....	35
Alternate Grid Spacing .....	40
Non-Destructive Test Method Survey .....	41
Results and Discussion .....	41
Data Comparisons.....	41
Comparisons between Electrical Resistivity and Half-Cell Potential.....	41
Ground Penetrating Radar.....	44
Impact Echo .....	47
Cover Depth.....	52
Spatial Comparisons .....	56
Comparisons with Time.....	59
Threshold Analysis .....	67
Half-Cell Potential Threshold Analysis.....	68
Electrical Resistivity Threshold Analysis.....	72
Ground Penetrating Radar Threshold Analysis.....	74

Application on Other Structures .....	79
Condition Assessment.....	84
Condition Rating.....	88
Data Agreement Rating.....	90
Multi-Modal Condition Assessment Program .....	92
Alternate Grid Spacing .....	94
Findings .....	105
Conclusions.....	106
Recommendations.....	108
Future Work.....	109
References.....	112
Acknowledgement of Previous Publication.....	114
Appendices.....	115
Appendix 1 – Non-Destructive Test Method Survey.....	116
Appendix 2 – MATLAB Code for Multi-Modal Condition Assessment .....	119
Appendix 3 – Sample Output from Condition Assessment Code.....	158
Appendix 4 –Condition Plots of Evaluated Bridges .....	161

## LIST OF TABLES

Table 1: Interpretation of concrete resistivity (Feliu, Gonzalez and Andrade 1996).....	10
Table 2: Details and descriptions of the structures involved in this research .....	26
Table 3: Description and importance of identified damage states .....	29
Table 4: National Bridge Inspection Standards (Ryan, et al. 2006).....	31
Table 5: AASHTO Bridge Element rating system (AASHTO 2011).....	31
Table 6: NBIS rating criteria based on multi-modal NDT results .....	33
Table 7: Multi-modal NDT data agreement rating tables .....	37
Table 8: Situations of complete NDT data agreement.....	39
Table 9: Agreement and disagreement between IE and CD results.....	48
Table 10: Comparison of severe delamination identification between CD and IE .....	49
Table 11: Average NDT measurement based on impact echo signal rating .....	50
Table 12: Average cover depth for various condition states.....	53
Table 13: Average cover depth for impact echo signal ratings.....	53
Table 14: Spatial agreement in condition between all methods, in percentage .....	58
Table 15: Spatial agreement in condition between all methods, in percentage, HCP scaled to 100%,.....	59
Table 16: Change in percentage of agreement from general threshold to individual thresholds...	59
Table 17: Average resistivity based on changing half-cell potential values (Haymarket, Virginia) .....	61
Table 18: Comparison of GPR threshold values with average GPR amplitude.....	79
Table 19: Threshold analysis results.....	80
Table 20: Nonduplicating condition quantities.....	86
Table 21: Duplicating damage quantities.....	87
Table 22: NBIS rating according to NDT analysis .....	89
Table 23: AASHTO condition rating results .....	90

Table 24: NDT data agreement rating and percentage of complete agreement .....	92
Table 25: Sample input file for the condition assessment program .....	93
Table 26: Percent reduction in amount of test points for various grids .....	105

## LIST OF FIGURES

Figure 1: Ground penetrating radar survey (Haymarket, Virginia) .....	4
Figure 2: Half-cell potential survey (Haymarket, Virginia).....	4
Figure 3: Typical corrosion reaction.....	7
Figure 4: Relative size of iron and its oxides (Pilling-Bedworth Ratio) (McCafferty 2010).....	8
Figure 5: Four-point Wenner resistivity probe measurement and setup .....	9
Figure 6: Half-cell potential measurement and setup .....	11
Figure 7: Collection and analysis of ground penetrating radar data .....	13
Figure 8: GPR waveform (A-scan).....	14
Figure 9: Collection and analysis of impact echo data - after (Gucunski, Slabaugh, et al. 2007) .	16
Figure 10: Progression of bridge deck deterioration and methods of evaluation – after (Gucunski, Feldmann, et al., Multimodal condition assessment of bridge decks by NDE and its validation 2009) .....	22
Figure 11: Non-destructive testing of a bridge deck, A) electrical resistivity, B) half-cell potential, C) ground penetrating radar, D) chain drag, E & F) impact echo.....	24
Figure 12: Various data presentation method (Haymarket, Virginia).....	35
Figure 13: Relative half-cell potential based on resistivity.....	42
Figure 14: Cumulative frequency distribution of half-cell potentials based on resistivity for all 12 bridges.....	44
Figure 15: Comparison of average relative GPR amplitude to ER.....	45
Figure 16: Comparison of average relative GPR amplitude to HCP .....	46
Figure 17: HCP overlaid with relative GPR amplitude (Haymarket, Virginia).....	47
Figure 18: Cumulative frequency distribution of resistivity based on impact echo signal rating..	50
Figure 19: Cumulative frequency distribution of half-cell potential based on impact echo signal rating .....	51

Figure 20: Cumulative frequency distribution of relative GPR amplitude based on impact echo signal rating.....	52
Figure 21: Average cover depth for distribution of half-cell potentials.....	54
Figure 22: Average cover depth for distribution of relative amplitudes .....	55
Figure 23: Average cover depth for distribution of resistivity.....	56
Figure 24: Areas of the 2009 ER and HCP surveys below 40 kohm·cm and –350 mV CSE (Haymarket, Virginia).....	57
Figure 25: Distribution of half-cell potentials based on electrical resistivity for various years (Haymarket, Virginia).....	60
Figure 26: Areas of ER surveys in 2009 and 2011 below 40 kohm·cm (Haymarket, Virginia)....	62
Figure 27: Areas of HCP surveys in 2009 and 2011 below –350 mV CSE (Haymarket, Virginia) .....	63
Figure 28: Areas of GPR surveys in 2009 and 2011 below –20 dB (Haymarket, Virginia) .....	64
Figure 29: Areas of IE surveys in 2009 and 2011 with a signal rating of 3 or 4 (Haymarket, Virginia).....	65
Figure 30: Areas of CD surveys in 2009 and 2011 with a severe delamination (Haymarket, Virginia).....	66
Figure 31: Influence of surrounding location’s 2009 condition on the central test location’s 2011 condition (Haymarket, Virginia).....	67
Figure 32: Cumulative frequency distribution of HCP data filtered according to resistivity (Haymarket, Virginia).....	69
Figure 33: Slope of the cumulative frequency distribution of filtered HCP data (Haymarket, Virginia).....	70
Figure 34: Cumulative frequency distribution of ER data filtered according to HCP data (Haymarket, Virginia).....	73
Figure 35: Delta curve of filtered ER cumulative frequency data (Haymarket, Virginia).....	74

Figure 36: Cumulative frequency distribution of GPR amplitude filtered by ER and HCP data (Haymarket, Virginia).....	76
Figure 37: Cumulative frequency distribution of GPR amplitude filtered by ER and CD data (Haymarket, Virginia).....	77
Figure 38: Cumulative frequency distribution of GPR amplitude filtered by ER, HCP, and CD data (Haymarket, Virginia).....	77
Figure 39: GPR threshold analysis delta curves (Haymarket, Virginia).....	78
Figure 40: Slope of the cumulative frequency distribution of filtered HCP data (Sandstone, Minnesota).....	81
Figure 41: Slope of the cumulative frequency distribution of HCP data filtered according to resistivity (Elkton, Maryland).....	82
Figure 42: Delta curve of filtered ER cumulative frequency data (Almond, New York).....	83
Figure 43: GPR threshold analysis delta curves (Sandstone, Minnesota).....	83
Figure 44: GPR threshold analysis delta curves (Upper Freehold Township, New Jersey).....	84
Figure 45: Condition assessment of Route 15 Bridge in Haymarket Virginia.....	85
Figure 46: Input information for the condition assessment code.....	93
Figure 47: Analysis of ER and HCP measured values for changing survey grid spacing.....	95
Figure 48: Quantities of damage area based on grid spacing.....	96
Figure 49: ER survey results using various grid spacings (Rt. 18 Neptune, New Jersey).....	97
Figure 50: HCP survey results using various grid spacings (Rt. 18 Neptune, New Jersey).....	98
Figure 51: Percent change in detection area of electrical methods for various square grid spacings.....	99
Figure 52: Percent change in detection area of electrical methods for various rectangular grid spacings.....	100
Figure 53: Percent change in detection area of acoustic methods for various square grid spacings.....	101

Figure 54: Percent change in detection area of acoustic methods for various rectangular grid spacings.....	101
Figure 55: Percent change in average measurements due to various grid spacings.....	102
Figure 56: ER survey results using various grid spacings (Haymarket, Virginia).....	103
Figure 57: HCP survey results using various grid spacings (Haymarket, Virginia).....	104
Figure 58: Condition assessment of I-495 South Bridge in Wilmington, Delaware.....	162
Figure 59: Condition assessment of I-195 East Bridge in Upper Freehold, New Jersey.....	162
Figure 60: Condition assessment of Pequea Boulevard Bridge in Conestoga, Pennsylvania.....	163
Figure 61: Condition assessment of School House Road Bridge in Middletown, Pennsylvania.	163
Figure 62: Condition assessment of Route 123 Bridge in Sandstone, Minnesota .....	164
Figure 63: Condition assessment of Route 15 Bridge in Haymarket, Virginia .....	164
Figure 64: Condition assessment of Route 18 Bridge in Neptune, New Jersey.....	165
Figure 65: Condition assessment of Route 21 Bridge in Almond, New York.....	165
Figure 66: Condition assessment of Route 273 Bridge in Elkton, Maryland .....	166
Figure 67: Condition assessment of Route 47 Bridge in Deptford Township, New Jersey.....	166
Figure 68: Condition assessment of Route 93 Bridge in Sumner, Iowa .....	167
Figure 69: Condition assessment of West Bangs Ave Bridge in Neptune, New Jersey .....	167

## LIST OF EQUATIONS

Resistivity equation.....	9
Variance-covariance equation.....	19
Correlation equation.....	19
Centered finite difference formula.....	71

## SYMBOLS AND ABBREVIATIONS

a.....	Resistivity probe spacing
AASHTO .....	American Association of State Highway and Transportation Officials
BAM .....	Germany's Federal Institute for Materials Research and Testing
CD.....	Chain drag
CSE .....	Copper sulfate electrode
DOT .....	Department of transportation
ER .....	Electrical resistivity
FHWA.....	Federal Highway Administration
GPR.....	Ground penetrating radar
HCP.....	Half-cell potential
HSCP .....	Human Subjects Certification Program
I .....	Electrical current, amperes
IE.....	Impact echo
IRB.....	Institutional Review Board
KDOT .....	Kansas Department of Transportation
LTBP.....	Long Term Bridge Performance
NBIS .....	National Bridge Inspection Standards

NDT .....Non-destructive testing

NJDOT .....New Jersey Department of Transportation

$\rho$  .....Resistivity, ohm·cm

R.....Resistance, ohm

UE .....Ultrasonic echo

USW.....Ultrasonic Surface Wave

V.....Voltage, v

VDOT .....Virginia Department of Transportation

## INTRODUCTION

Bridges are an important part of the nation's infrastructure and due to the limited budgets available to keep them properly maintained, the methods of evaluation and damage identification must improve in accuracy and cost-effectiveness. At the forefront of bridge evaluation and damage identification is non-destructive testing (NDT). NDT is an effective form of condition assessment that continues to advance through increases in accuracy while time requirements and costs decrease. There are many different NDT methods capable of evaluating and identifying different types of damage in reinforced concrete structures. These NDT methods include, but are not limited to, ground penetrating radar (GPR), impact echo (IE), half-cell potential (HCP), electrical resistivity (ER), surface wave testing, ultrasonic wave testing, infrared thermography, and many others. Each of these methods uses a unique physical principal of the bridge materials to identify locations of deterioration. For example, HCP is able to identify active corrosion by measuring the electrical potential difference between the steel reinforcement and a reference electrode. IE locates delaminations by impacting the concrete surface and evaluating the frequency of the reflecting waves. Unfortunately, there is no single NDT technology that is capable of identifying all of the various deterioration phenomena that can affect a bridge deck. To get a complete understanding of a bridge deck's condition, NDT practitioners have started surveying bridge decks using a multi-modal NDT approach. Using a multi-modal NDT approach allows for the identification of several different damage states, resulting in a more complete understanding of a deck's condition.

While a multi-modal NDT approach provides a more complete understanding of a bridge deck's condition, this approach also creates several difficulties. The practitioner must deal with significantly more data, understand how to properly fuse that data, and interpret the data fusion. It is the aim of this research to develop methodologies and protocols for the data analysis and

presentation of multi-modal NDT data so that it provides a more complete condition assessment of a bridge deck.

There are four primary gaps in the practice of multi-modal NDT that this research is aimed at addressing;

1. Results of NDT testing are commonly provided to bridge owners and maintenance personnel in the form of contour plots based on the NDT measurement scale.

Current practice when providing a bridge owner with NDT results is to provide those results in the form of a contour plot. The contour scale is based on the units and measurement range of the NDT device, in which colors are used to indicate the areas of deterioration and sound concrete. Figure 1 is the result of a GPR survey on a bridge deck in Haymarket, Virginia. The contour scale is in decibels of signal attenuation. Most bridge owners and maintenance personnel are not familiar with GPR nor signal attenuation, therefore, this scale has no tangible meaning to them. The only way for them to identify areas of damage would be through reading any supplemental report accompanying the figure and referencing the color scheme. It is typical to assume that warm colors, red and yellow, indicate damage and cool colors, blues and greens, indicate sound concrete. However, what kind of damage do these warm colors indicate? What is the difference in damage between red and yellow? A plot like Figure 1 creates more questions than answers for a person without an NDT background. NDT Results based on the scale of the measurement device is not the most effective way of presenting NDT results to people responsible for bridge maintenance and operation. These results do not provide a bridge owner or maintenance personnel with information that they can directly use in decision-making.

2. When multiple NDT methods are performed on a structure, results of each method are typically presented separately. True data fusion between the multiple methods is not being conducted.

A GPR survey of a reinforced concrete bridge deck alone is not enough information to accurately identify every deterioration state. Therefore, a multi-modal NDT approach is taken to provide a more complete condition assessment. The current practice when conducting a multi-model NDT survey is to provide each method's results in an individual plot. Besides some qualitative assessment typically provided in an accompanying report, there is no true data fusion between the NDT methods, nor is there a quantitative analysis. Each NDT method measures a different parameter in the deck; therefore, they can sometimes give differing results, which if presented in different plots to a person untrained in NDT will indicate conflicting results. Figure 1 and Figure 2 are the results of GPR and HCP surveys conducted on the same bridge deck in Haymarket, Virginia. These two methods measure completely different parameters in the bridge deck; therefore, the areas of agreement and disagreement between the warm colors do not necessarily indicate the accuracy of the surveys. To someone untrained in NDT, they could interpret areas of disagreement as incorrect or conflicting results. In actuality, that is not the case because each method is identifying different condition states. The true condition of the bridge can only be identified through the fusion of these two survey results.

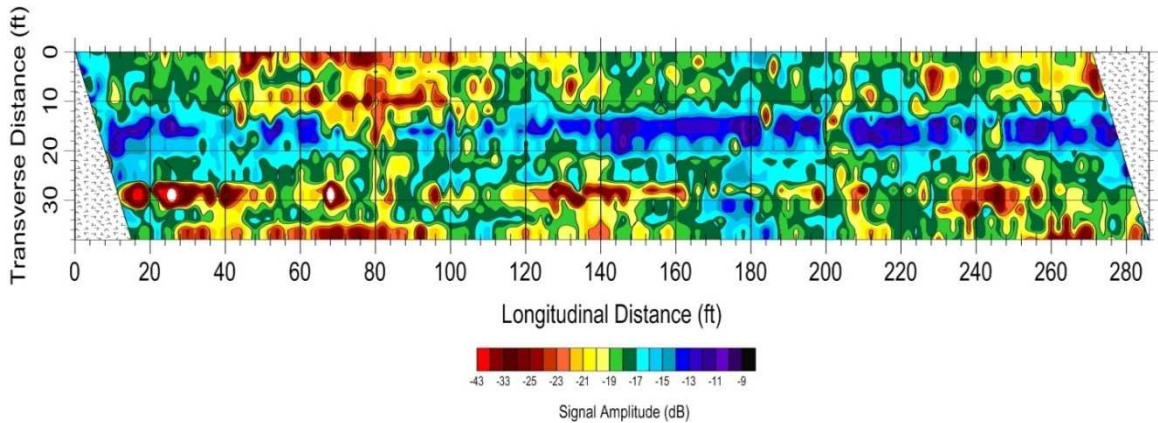


Figure 1: Ground penetrating radar survey (Haymarket, Virginia)

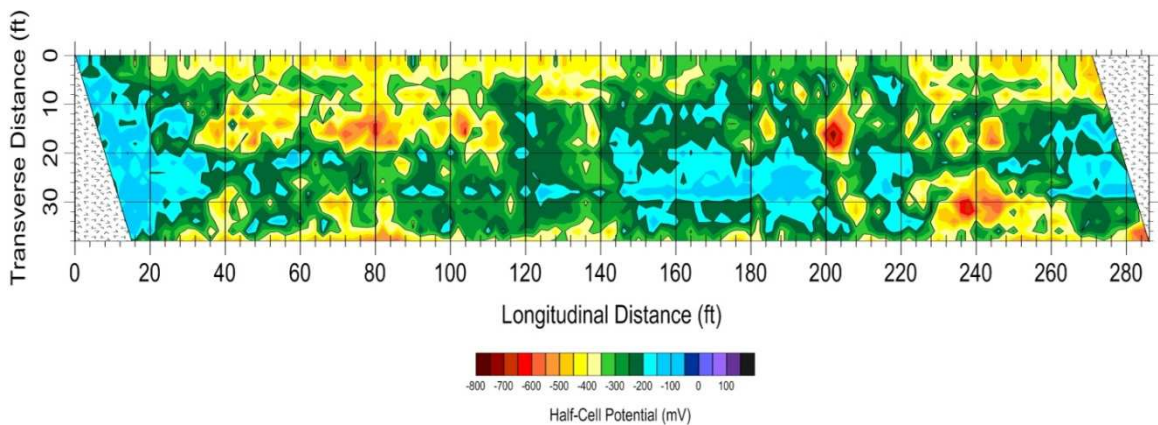


Figure 2: Half-cell potential survey (Haymarket, Virginia)

3. Multi-modal NDT results are not commonly being used to understand how damage will progress in the future.

With the application of multi-modal NDT and periodic monitoring of individual structures, more research needs to be focused at understanding where damage will spread and how fast. Each NDT method describes a different aspect of reinforced concrete degradation. By understanding what methods detect which stage of deterioration and how these stages progress, a better understanding of bridge deterioration will be gained. For instance ER detects a corrosive environment, while HCP measures potential to identify if corrosion is active. Areas identified in

the ER survey as corrosive environment, which are passive in the HCP survey, could indicate that these locations corrosion will activate in the near future. Associations like this could lead to more accurate predictions regarding the future condition of a bridge.

4. Overall, NDT as a decision-making tool for bridge owners and maintenance operations is limited because of several gaps in the multi-modal NDT practice.

Solutions to the first three gaps in the NDT practice will make NDT a more efficient and effective decision-making tool for bridge owners and maintenance personnel. The reason that NDT condition surveys are performed on structures is to identify deterioration processes and locate damage, so that bridge owners can make decisions regarding maintenance. The goal of NDT practitioners should be to direct NDT methods towards what bridge owners and maintenance operations need.

## OBJECTIVES

The four primary problems with the current NDT practice were outlined in the Introduction. To solve these problems, several research objectives were established. The primary research objective is to develop an automated condition assessment program that will take post-processed NDT data and convert it into a damage-based condition assessment.

This primary objective is a large and very broad goal. In order to complete this primary objective, there are several secondary objectives that will need to be accomplished, as follow:

- Identify trends and correlations in the multi-modal NDT data.
- Develop a statistics-based approach to threshold identification.
- Convert NDT data into a condition-based assessment.
- Convert the multi-modal NDT condition assessment into a rating using already established and federally mandated rating systems.

- Present the condition of the deck in an accurate and genuine way.
- Identify the strength of agreement in damage identification between the NDT methods.
- Validate the current sampling procedures and identify if larger NDT sampling can be used to more quickly establish general deck condition.
- Drive NDT surveys and results to be focused more on meeting the needs of bridge owners and maintenance operations.

## LITERATURE REVIEW

As a part of this research, an in-depth literature review was conducted on the corrosion process of reinforced concrete, the different NDT methods being implemented, and the fusion of multi-modal NDT data. The focus of this research is NDT to identify concrete deterioration caused by chloride-induced corrosion. Chloride-induced corrosion is not the only deterioration mechanism that affects reinforced concrete decks; it is, however, the most common (ACI Committee 222 2001). Other deterioration mechanisms that can occur in reinforced concrete bridge decks include, but are not limited to, carbonation, alkali-silica reaction, freeze-thaw, and mechanical distress (Ryan, et al. 2006).

## CORROSION OF REINFORCED CONCRETE

Corrosion is an electrochemical reaction involving iron, water, and oxygen. In the presence of water and oxygen, iron will release two electrons and combine with oxygen and hydrogen to create ferric oxide at the anodic region of the corrosion reaction (Figure 3). At the cathodic region of the reaction, the free electrons will combine with oxygen and water to create hydroxide. Iron will only release its electrons if there are elements willing to accept the freed electrons, resulting in a balanced reaction. Concrete normally provides a highly alkaline environment, with pH of approximately 13.5 (Rapa and Hartt 1999), in which steel is naturally passive (Broomfield

2007). The passivity of steel in a highly alkaline environment is due to the formation of a protective oxide film (Funahashi 1990). The protective oxide film is formed along the surface of the steel and protects the steel from more severe corrosion (Funahashi 1990). However, chloride or carbon dioxide, which can diffuse into the concrete matrix from the external environment, can lower a concrete's pH and depassivate the steel (Poulsen and Mejlbro 2006). Corrosion of concrete reinforcement creates a progression of damage, starting with section loss, formation of iron oxide, concrete cracking, delamination, and eventual spalling. The concrete damage that results from corrosion activity is due to the accumulation of ferric oxide beneath the concrete surface. Ferric oxide molecules are larger than the original iron (Figure 4); therefore, as they form, there is an increase in material volume at the steel level. This increase in volume creates expansive forces inside the concrete that result in the formation of concrete tensile stresses. Concrete, which is relatively weak in tension, will eventually crack due to these stresses and lead to delamination and an eventual spall.

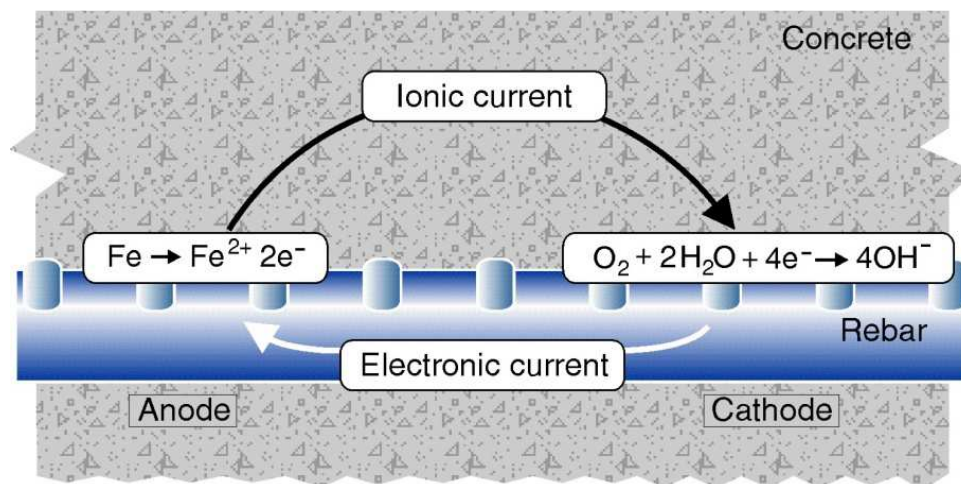


Figure 3: Typical corrosion reaction

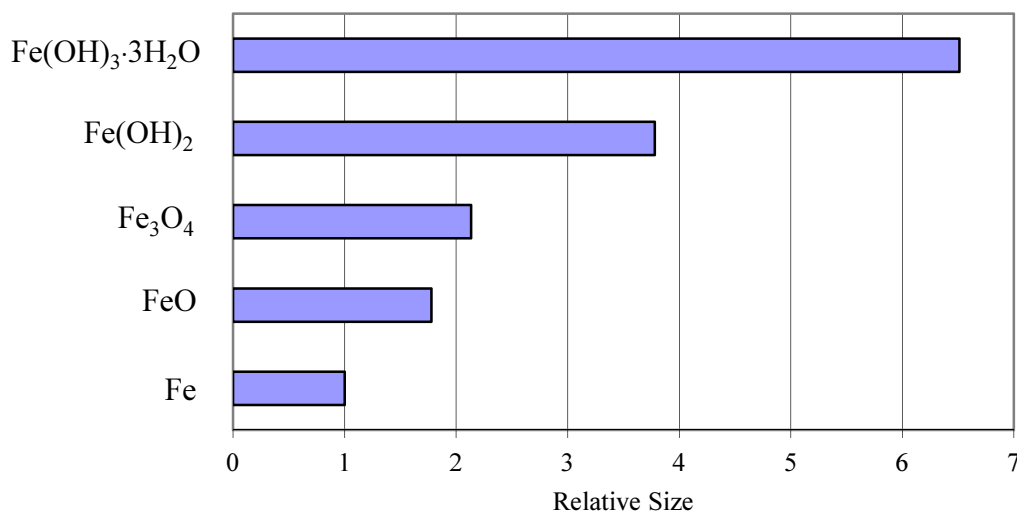


Figure 4: Relative size of iron and its oxides (Pilling-Bedworth Ratio) (McCafferty 2010)

The deterioration process of reinforced concrete can be identified and monitored through the use of many different NDT methods. The NDT methods used to identify the condition of bridge decks for this research are; ER, HCP, GPR, IE, and chain drag (CD). These methods were specifically selected due to their combined ability to capture the full spectrum of concrete deterioration with regard to corrosion activity.

#### ELECTRICAL RESISTIVITY (ER)

Electrical resistivity is an NDT method that measures the concrete's ability to pass electrical current. Concrete's ability to support current flow is an important factor in deterioration, because corrosion is an electrochemical reaction requiring current flow. If the concrete is highly resistive, then that limits the ability of ions to move between the cathodic and anodic regions of the corrosion reaction. If the concrete has a low resistivity, then the corrosion reaction will have no difficulty in passing current, allowing for the corrosion reaction to occur quite rapidly and over a larger area. The resistivity of concrete is highly dependent on the concrete's moisture content, permeability, chloride content, and temperature (Elkey and Sellevold 1995). The ability of the concrete to pass current increases as water and free ions accumulate in the concrete matrix and

the concrete pores increase in size and continuity. The corrosion reaction is highly dependent on the presence of water, chlorides, and current flow; therefore, areas in which the resistivity is low indicate an environment that is conducive to corrosion activity. There are several methods to measure concrete resistivity; however, the most common method in civil engineering applications is the four-point Wenner method (Kessler, et al. 2008). The four-point Wenner method involves passing of current between two exterior probes and measuring the potential between two intermediate probes, all spaced at equal intervals,  $a$  (Figure 5). Equation (1) is used to calculate resistivity ( $\rho$ , kohm·cm) using the parameters measured by the Wenner method; current ( $I$ , amperes), potential ( $V$ , volts), resistance ( $R$ , kohm), and probe spacing ( $a$ , inches).

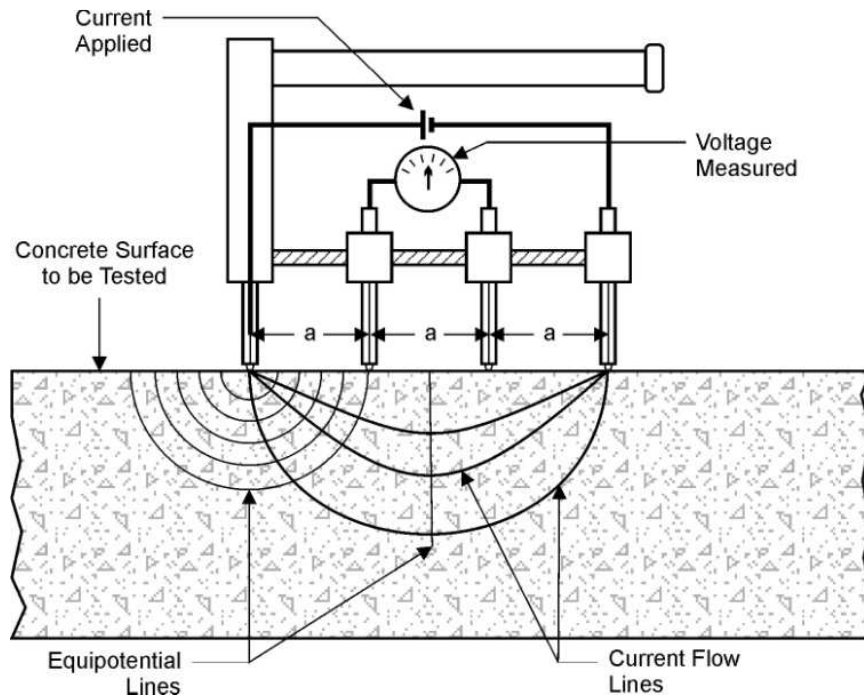


Figure 5: Four-point Wenner resistivity probe measurement and setup

$$\rho = \frac{2\pi aV}{I} \quad (1)$$

In the literature, there have been several interpretations of resistivity measurements made on reinforced concrete. Table 1 provides a general interpretation of resistivity values with respect to risk of corrosion. Most studies agree that a concrete resistivity less than 10 kohm·cm is associated with a very high risk of steel corrosion activity (Elkey and Sellevold 1995) (Malhotra and Carino 2004) (Feliu, Gonzalez and Andrade 1996). However, there has been much variation and debate in identifying at what resistivity value the risk of corrosion is low. Resistivity values above which risk of corrosion is low have been given as 10 kohm·cm (Elkey and Sellevold 1995), 20 kohm·cm (Bungey 1989), 30 kohm·cm (Morris, et al. 2002), and 50 kohm·cm (Feliu, Gonzalez and Andrade 1996).

Table 1: Interpretation of concrete resistivity (Feliu, Gonzalez and Andrade 1996)

Concrete Resistivity (kohm·cm)	Risk of Corrosion
< 10	High
10 – 50	Moderate
50 – 100	Low
> 100	Negligible

## HALF-CELL POTENTIAL

Half-cell potential is an NDT method capable of identifying locations of active corrosion in reinforced concrete. HCP measurements are conducted by electrically connecting a reference electrode to the steel reinforcement and measuring the potential difference between them (

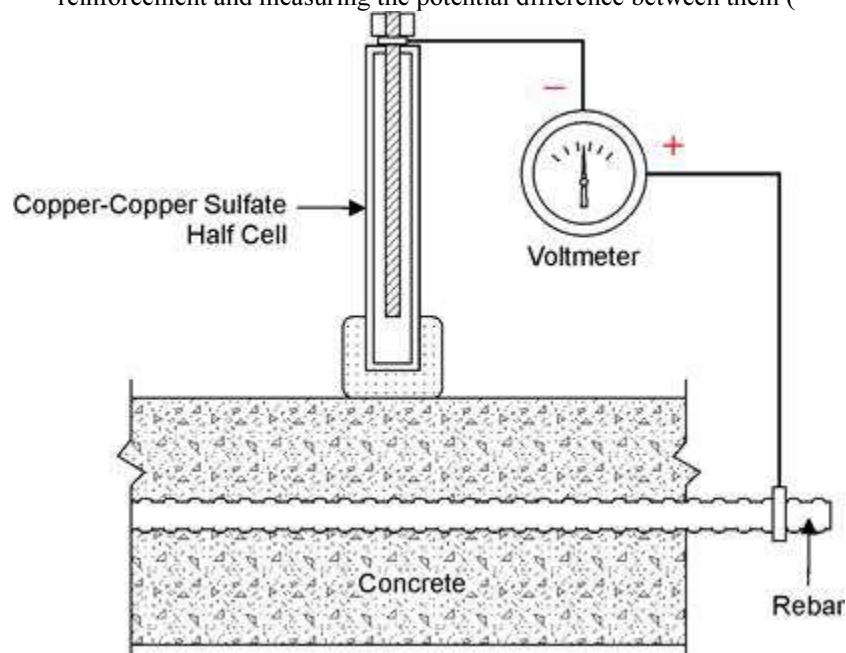


Figure 6). In most civil engineering applications, the reference electrode is a copper/copper sulfate electrode (CSE) (ACI Committee 222 2001), comprised of a copper rod inside a saturated solution of copper sulfate. HCP measurements are a probabilistic measurement, in that they indicate the probability of active corrosion. ASTM C876-09, the *Standard Test Method for Corrosion Potentials of Uncoated Reinforcing Steel in Concrete* (ASTM 2009) indicates that when the HCP is less than  $-350$  mV CSE, the probability of active corrosion is 90%. When the potential is greater than  $-200$  mV CSE, there is a 90% probability of a passive condition, and between those ranges corrosion activity is uncertain. The threshold values provided by ASTM C876-09 are not absolute and are not applicable in every situation (Elsener, et al. 2003). HCP threshold values can shift depending on several factors. These factors include concrete temperature, moisture and oxygen content, resistivity, presence of ions, surface treatments, stray currents, and corrosion-inhibiting admixtures (Gu and Beaudoin 1998). The concrete's concentration of moisture and oxygen has a significant effect on potential measurements. An increase in moisture content will cause a negative shift in potential and a decrease in oxygen content will also cause a negative shift in the potential (Gu and Beaudoin 1998).

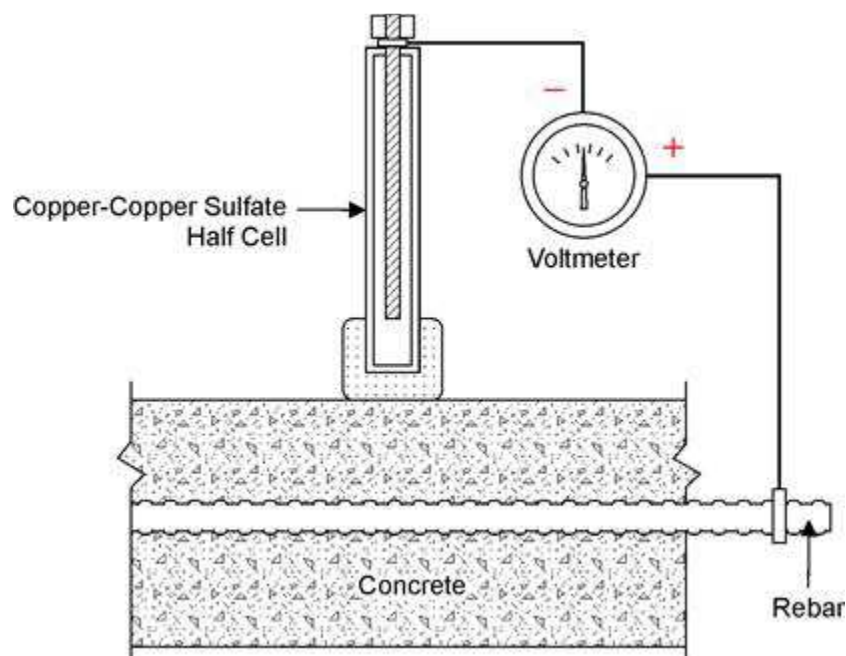


Figure 6: Half-cell potential measurement and setup

## GROUND PENETRATING RADAR

Ground penetrating radar is an electromagnetic NDT method used to qualitatively assess the condition of reinforced concrete structures through the evaluation of radar (electromagnetic) waves reflected from different interfaces, most commonly reinforcing steel (Figure 7). Figure 7 provides a picture of the GPR cart along with two images of the resulting B-scan from a GPR survey. The B-scans are of a bridge deck, and the brighter white dots are the reflections that result from the reinforcement. In the lower image of the B-scan there is an area of rebar that is not as bright and clear as the rest. This is the result of signal attenuation caused by increased moisture and chloride concentrations in the concrete. Radar waves that are transmitted into concrete will reflect when encountering changes in dielectric permittivity of materials (Daniels 2004). When radar waves encounter reinforcing steel in concrete, strong reflections are created due to the large difference in relative dielectric permittivity (dielectric constant) between concrete (4 to 11) and steel, (a conductor; mathematically infinity) (Huston, Fuhr, et al. 2002). Moisture which has a large effect on the dielectric constant of concrete has a dielectric value of 80. Through the evaluation of the steel reinforcement reflections, a condition assessment of the concrete can be conducted by spatially comparing the relative variation in reflected signal amplitudes (Parrillo and Roberts 2006). Attenuation in the radar waves is caused by travel distance (cover depth), the concrete's moisture and ion concentrations, cross-sectional area of the steel, presence of ferric oxide, and if there is significant concrete cracking or delamination which can scatter a signal (Parrillo and Roberts 2006). The effect of cover depth on the signal attenuation can be corrected for in the post-processing of the GPR data. The factors associated with signal attenuation are also strongly associated with concrete deterioration. These are for instance high concentrations of free ions and moisture which lead to an environment that is favorable for corrosion activity. Attenuation is also caused from scattering of the GPR signal due

to large amount of cracking and delamination. The steel cross-section also influences the magnitude of the GPR reflections. If the steel cross-section is compromised by corrosion then that along with the formation of large amounts of ferric oxide can decrease the magnitude of the reflection. This allows for the GPR amplitude evaluation to provide insight into the condition state of a bridge deck.

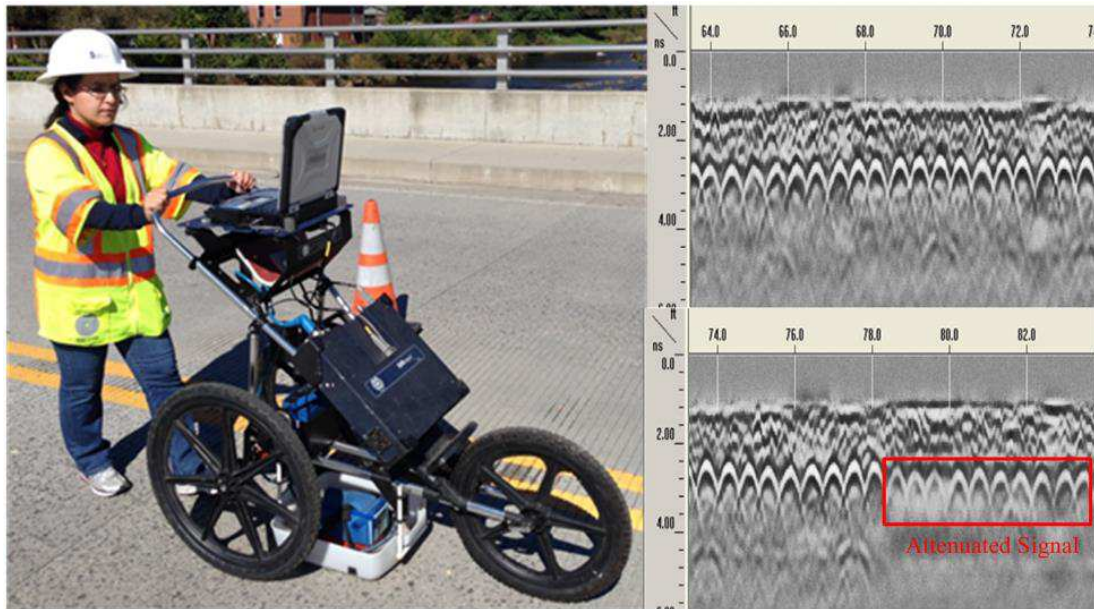


Figure 7: Collection and analysis of ground penetrating radar data

Figure 8 provides a GPR waveform; also known as the A-scan. A GPR survey collects A-scans at the defined sampling increments. These A-scans are then combined to form a B-scan. The B-scan colors are the result of a gray scale being applied to the distribution of amplitudes. In order to analyze the GPR data it must go through several processing steps so that the amplitude of the wave at the concrete/rebar interface can be determined. These corrections include background removal, time-zero correction, migration, and depth correction. Time-zero correction accounts for the small bit of air the GPR wave must travel through before it reaches the concrete surface. Migration corrects the GPR waveforms from the error caused by the motion of the antenna. In Figure 7 the rebar reflections look like parabolas; which is the result of the antenna's motion

during data collection. Once the GPR data has been corrected, the software tries to identify the peaks in the data caused by the rebar reflections. The user must then verify all of the software's selections since the program will miss peaks and make incorrect selections. The automated picking is used as an initial pass. Once the proper peaks have been selected then the amplitude at those locations along with distance measurements are imported into a spreadsheet for analysis.

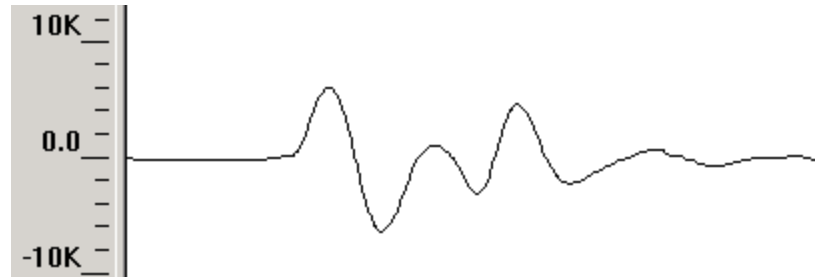


Figure 8: GPR waveform (A-scan)

## IMPACT ECHO

Impact echo is an acoustic NDT method used to identify lateral cracks and delaminations beneath the concrete surface. IE identifies damage by mechanically striking the concrete surface and recording the resulting response of the deck. Typically the mechanical impact is caused by striking a steel bearing or solenoid on the surface of the concrete (Ryan, et al. 2006). The impact creates stress waves that reflect off of the bottom of the deck and/or intermediate damage interface (Gucunski, Slabaugh, et al. 2007). A recording device, like a piezoelectric transducer or accelerometer, is coupled to the surface of the concrete and records the velocity or acceleration of the response. The recorded signal is captured in the time-domain and converted into the frequency-domain using the fast Fourier transform. The frequency-domain identifies the energy levels for the spectrum of frequencies recorded. If the stress wave is reflecting off of the bottom of a sound deck, then the wave energy will be at a frequency relating to the thickness of the deck (Figure 9) (Gucunski, Slabaugh, et al. 2007). If there are intermediate reflectors in the deck, like delaminations or lateral cracks, then there could be secondary peaks in the frequency spectrum or

the primary peak could be shifted to a frequency associate with the impeding intermediate interface (Gucunski, Slabaugh, et al. 2007). This depends if the damage is completely or partially reflecting the wave energy. If there is a partial reflection, then there will be a primary peak at the frequency corresponding to the full deck thickness, and a peak corresponding to the intermediate damage (Gucunski, Slabaugh, et al. 2007). If the damage is so significant that it reflects all of the wave energy, then the primary peak will be shifted, higher for a delamination, and lower for large near surface delamination (Gucunski, Slabaugh, et al. 2007). The lower frequency caused by a large near surface delaminations is a result of the IE device recording the movement of the delamination when it is impacted. The delamination acts like a beam in flexure as opposed to a slab.

In the analysis of IE data a numerical value is assigned to each of the conditions identified in Figure 9. A signal rating of 1 indicates “good condition,” signal rating of 2 indicates “fair condition,” signal rating of 3 indicates “poor condition,” and a signal rating of 4 indicates “serious condition.”

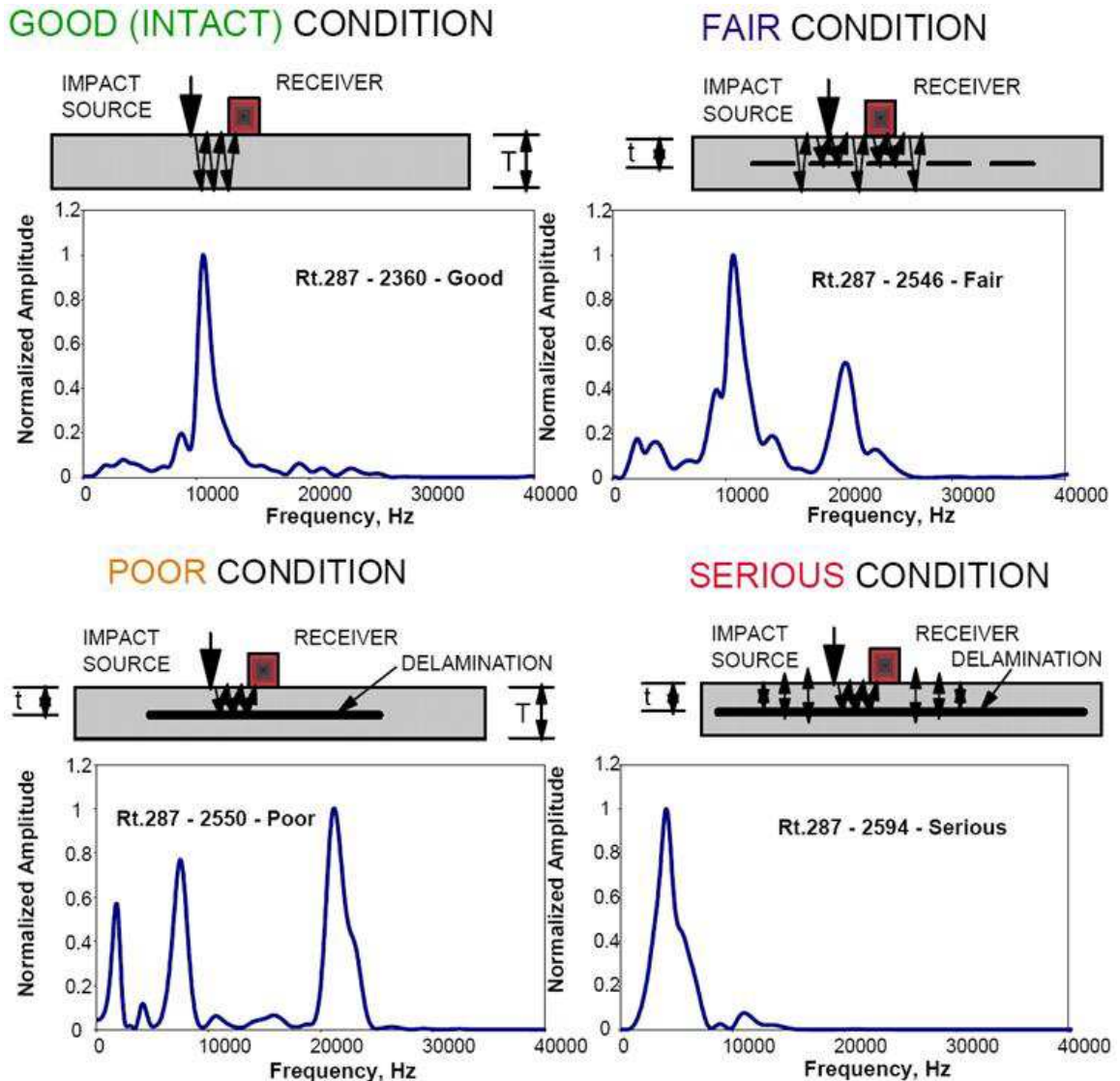


Figure 9: Collection and analysis of impact echo data - after (Gucunski, Slabaugh, et al. 2007)

## CHAIN DRAG

Chain drag is an NDT method that is less sophisticated than the previous NDT methods; however, it is highly effective at identifying large near-surface delaminations (ASTM 1992). CD uses large steel chains that are dragged along the surface of a bridge deck to identify large late-stage delaminations. The CD operator listens to the sound that is created by the chain and when the pitch of the sound changes to a hollow sound, which is usually of lower pitch than that of the

chains on sound concrete; this identifies the location of a delamination (ASTM 1992). In general, the lower the pitch, the larger the delamination, as with a drum head. When the chains are dragged over a large late-stage delamination, the flexural vibrations of the delamination cause the change in sound frequency (ASTM 1992). When the chains are dragged over a section that is not delaminated, they create a clear ringing sound caused by the chain itself (ASTM 1992). ASTM D4580, the *Standard Practice for Measuring Delaminations in Concrete Bridge Decks by Sounding* covers the operations and specifications to conduct a CD survey (ASTM 1992). The reason that CD can only find large late-stage delaminations is that the test is dependent on human hearing. Only large late-stage delaminations create a sound in the audible frequency range, typically 1 to 4 kHz (Gucunski, Imani, et al. 2013). Therefore, the operators' skill in detecting a delamination using CD is highly dependent on their hearing ability and the surrounding ambient noise level (Henderson, Dion and Costley 1999).

#### NON-DESTRUCTIVE TESTING DATA FUSION

It is critical to this research to understand each NDT method, how it operates, and how to properly fuse the results from these different methods together. Horn (Horn 2006) presents an overview of NDT reliability with regard to the combination of multiple NDT methods. The focus of the work was on eddy current and ultrasonic testing in the aerospace industry, but the overarching ideas of the paper are very applicable to data fusion of any technologies in any field. Horn describes the difference between repeat measurements and using multiple methods to evaluate a sample. Performing repeat measurements increases the "statistical precision" of the results, while the use of multiple techniques can allow for each method to reveal phenomena that the other methods many not be able to detect (Horn 2006). This is a very important statement and the reason why the use of multi-modal NDT methods is important. The use of several different methods allows for the detection of different damage states or conditions that would not be

identified if only one method was used. Multi-modal NDT provides a more complete assessment of the test subject.

Research by Horn (Horn 2006) and Gros et al. (Gros, Bousigue and Takahashi 1999) discussed different ways to fuse the results of two different NDT methods conducted on the same material/structure. The objective of their work was to combine the results of multiple NDT methods so that detection errors, like unidentified damage and false damage identification, were minimized. The methods of fusion included, logical operators “and” and “or”, summation, maximum amplitude, averaging, weighted averaging, Bayes’ theorem, and Dempster-Shafer theory (Horn 2006) (Gros, Bousigue and Takahashi 1999). An important step in both Horn (Horn 2006) and Gros’s (Gros, Bousigue and Takahashi 1999) work is that when they were fusing the NDT results, the data was in the same scale. In Horn’s work, the two different NDT methods provided results in the same data format, wave amplitude, and Gros’s work used the image pixels that resulted from the data processing. In both situations, the data being fused had the same scale. If the data did not have the same scale, the fusion of the data would not produce meaningful information.

Work done by Huston et al. in 2010 (Huston, Cui, et al. 2010) investigated combining the results of HCP, GPR, IE, and CD to better understand the condition of a bridge deck in Virginia. Huston et al. took a purely statistical approach to the fusion of the four NDT results. In order to fuse the data together, they linearly normalized the results of each method to a 0-1 scale so that each method had the same scale. Huston et al. plotted the linearized results, which resulted in 660,000 pixels, representing the deck surface. The pixel values were then used to make comparisons between the different methods. Huston et al. also used pixel blocks as another way to compare the NDT results. The blocks were taken as 50 x 50 pixel segments and assigned the average value of the pixels contained in each segment. Huston et al. created a variance-covariance matrix (Equation (2)) to compare each data point, pixel, and block value of all four test methods. The

magnitude of  $\sigma_{ij}$  indicates the degree to which methods i and j are related to each other. A negative value of  $\sigma_{ij}$  indicates that as the value of i increases, the value of j decreases, and a positive value indicates that as i increases, j also increases.

$$\sigma_{ij} = \frac{1}{N-2} \sum_{k=1}^N (x_{ik} - \bar{x}_i)(x_{jk} - \bar{x}_j) \quad (2)$$

Along with variance-covariance, Huston et al. also created a correlation matrix (Equation (3)), which is similar to the covariance analysis in that it assesses if the i and j variable are related. Huston et al. reported that the statistical correlation of the NDT methods was “relatively weak.”

$$\rho_{ij} = \frac{\sigma_{ij}}{(\sigma_{ii}\sigma_{jj})^{1/2}} \quad (3)$$

Huston et al. also produced several plots of the combined data in order to understand visually observed correlations and agreement in the data. By taking a mean value of condition estimates for each method and plotting on a grey scale, black indicated agreement between the methods in detection of damage and white indicated agreement between the methods in identification of no damage. The plots indicated that there was better agreement in identifying damage than agreement in identifying no damage. There were many areas where all of the methods indicated damage; however, there was a limited area in which all the methods agreed there was no damage. There was also a significant amount of area that indicated no agreement between the methods about the condition state.

Huston et al. concluded that the agreement in condition of the four methods was not strong. However, they state that the combination of several different NDT methods could allow for a better assessment of bridge deck condition. The conclusion that the four different NDT methods

do not have strong correlation is not surprising, since each method is identifying a different condition, deterioration process, or damage type. This work by Huston et al. shows the importance of understanding how each NDT method is related and unrelated. Huston et al. were trying to combine the data without evaluating if these methods have strong correlations based on their physical principals of operation. For instance, it is expected that HCP and CD have poor statistical correlation, since HCP is identifying active corrosion and CD identifies large near-surface delaminations. The statistical correlation of these results is going to be weak, since active corrosion is an early stage condition compared to delaminations, which are late-stage. Additionally, delaminations can result from several different deterioration processes, not just corrosion.

Germany's Federal Institute for Materials Research and Testing (BAM) conducted multi-modal NDT research using GPR and ultrasonic echo (UE) in the evaluation of a reinforced concrete slab and a concrete box girder bridge (Maierhofer, et al. 2008) (Kohl and Streicher 2006). The results of the work showed that GPR and UE complemented each other due to the differences in investigation depth and reinforcement detection. GPR signals have difficulty penetrating past dense reinforcing grids, however, are excellent at evaluating the condition of the first layer of concrete reinforcement. This makes the investigation of anything past the top layer of reinforcement difficult for GPR. UE is able to evaluate the concrete cross-section; however, UE is unable to differentiate between the concrete and steel reinforcement. Through the combination of GPR and UE data sets, a complete evaluation of the reinforced concrete specimens was obtained. This work demonstrates how two complementary NDT methods can produce excellent results when the data is properly merged.

A review was also conducted of work done at Rutgers University regarding the use of multi-model NDT to evaluate bridge decks (Gucunski, Feldmann, et al. 2010), (Gucunski, Feldmann, et al. 2009), (Gucunski, Imani, et al. 2013), (Gucunski, Romero, et al. 2010). The deck surveys

were conducted using a wide array of NDT methods: ER, HCP, GPR, ultrasonic surface wave (USW), IE, and CD. The research provides evidence for the benefits of using multiple NDT methods to evaluate a bridge deck. The different methods provide a complete evaluation of the bridge deck by identifying damage at varying stages of deterioration. The work also indicated that each of the different NDT methods indicated similar areas of damage, which improved the confidence in the overall results. The following is a sampling of the results from these papers; areas of high GPR attenuation are also associated with HCP indicating active corrosion (Gucunski, Feldmann, et al. 2010); a deck with no areas of corrosive environment indicated no areas of active corrosion (Gucunski, Romero, et al. 2010); areas of high GPR attenuation were verified as damage through coring (Gucunski, Feldmann, et al. 2009); and IE was able to more completely identify delaminations when compared to CD (Gucunski, Romero, et al. 2010). This work demonstrates that a more complete evaluation of a bridge deck can be done by using a multi-modal NDT approach. One overarching step that was missing from this work, however, was that there was no true fusion of the NDT results. Each NDT result was presented in a separate plot and none of the results were combined to improve the overall bridge assessment. All the comparative analyses were done qualitatively, based on a visual assessment of the plots.

## METHODS AND MATERIALS

### NON-DESTRUCTIVE TESTING METHODS

The five NDT methods used to survey and assess the condition of the bridge decks for this research are ER, HCP, GPR, IE, and CD. ER and HCP are electrical methods that are capable of identifying a corrosive environment in concrete and the probability of active corrosion, respectively. GPR is an electromagnetic method that is able to identify, mostly in qualitative terms, various types of concrete degradation, which include corrosion, high moisture and chloride contents, significant cracking and delaminations to a limited degree. IE and CD are acoustic

methods that are capable of identifying delaminations and lateral cracking in varying degrees. These NDT methods were selected because each method is capable of identifying a different damage state in the progression of concrete deterioration. Figure 10 depicts the progression of reinforced concrete deterioration as a result of chloride-induced corrosion. Initially, there is the infiltration of moisture and chlorides into the concrete matrix, then the initiation of corrosion, then cracking, and eventual delamination, which leads to spalling. At each stage along this progression, there is a different NDT technology that is best suited to identifying that condition state. Assessing the condition of a deck simultaneously with these NDT methods provides a more complete assessment of the deck's condition, since each stage of the deterioration process can be identified. There is also some overlap of the technologies, like ER and GPR, which provide the ability to verify results between different technologies.

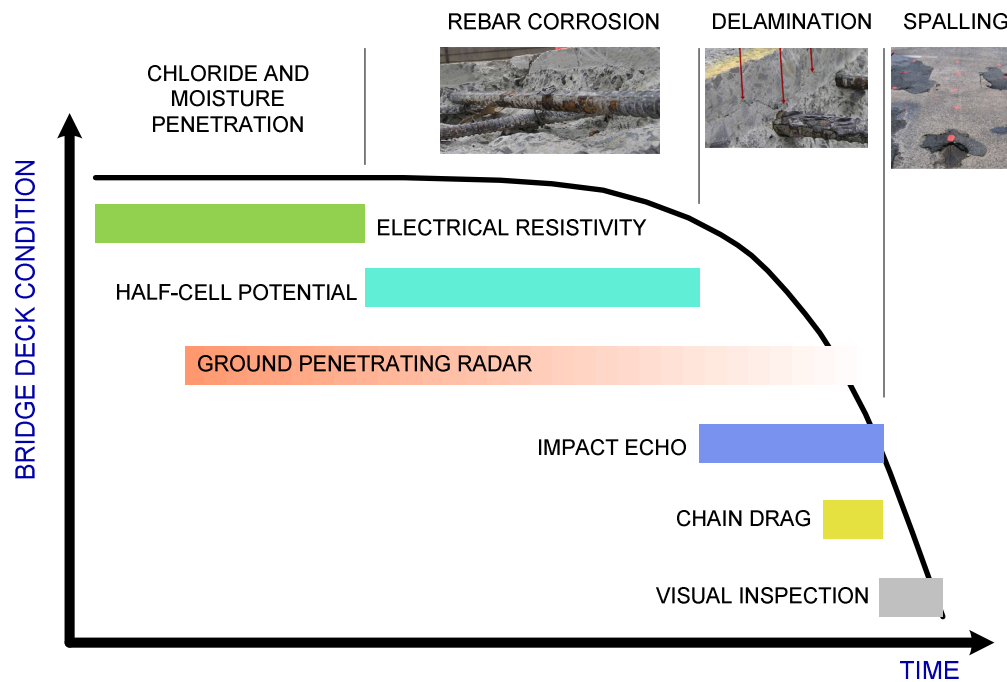


Figure 10: Progression of bridge deck deterioration and methods of evaluation – after (Gucunski, Feldmann, et al. 2009)

### *Equipment Details*

The ER surveys (Figure 11-A) were conducted using a four-point Wenner probe connected to a data logger. The ER electrode spacing was set at 1.5 in. Water was applied to the concrete surface prior to ER testing to improve the electrical couple between the probes and concrete surface. The surface layer of a concrete deck is typically drier than the deck thickness as a whole. This is due to surface moisture evaporation caused by exposure to the sun and wind. Wetting the deck surface prior to testing helps to remove this dry layer and improve coupling between the electrode and concrete.

The HCP measurements were collected (Figure 11-B) using a copper/copper sulfate reference electrode connected to a data logger. Data collection with HCP was done in accordance to ASTM C876-09. Each bridge deck's reinforcing steel was verified to be electrically continuous prior to data collection. Water was applied to the concrete surface prior to HCP testing to aid in creating an electrical couple between the reference electrode and the concrete.



Figure 11: Non-destructive testing of a bridge deck, A) electrical resistivity, B) half-cell potential, C) ground penetrating radar, D) chain drag, E & F) impact echo

The GPR survey was conducted using a ground-coupled 1.5 GHz antenna collecting at 60 scans per foot. The antenna was attached to a push cart that was used to scan the surface of the bridge deck in lines that were perpendicular to the direction of the top layer of reinforcing steel (Figure 11-C). The top layer of steel was in the transverse direction (relative to traffic flow and the length of the spans) for all of the bridges in this research. Therefore, the GPR survey lines were conducted in the longitudinal direction.

The IE survey was conducted using an automated IE device called Stepper (Figure 11-E & F). The device has an array of three IE probes that autonomously progressed across the deck to collect IE data. The impact source was a steel ball bearing and the recording device was a piezoelectric transducer. The IE data was analyzed and converted into a numerical scale, 1

through 4, according to the analysis outlined in Figure 9. A result of good was rated as 1, fair-2, poor-3, and serious-4.

The CD survey was conducted using 4 steel chains connected to a steel pipe (Figure 11-D). These chains were dragged over the surface of the deck to identify locations of delaminations. In conjunction with the CD survey, hammer sounding was done to delineate the extent of each delamination that was identified in the CD survey. Data collection with CD was done in accordance to ASTM D4580.

#### DATA COLLECTION

The data for this research was collected on twelve bridge decks throughout the United States of America. It is not the aim of this dissertation to discuss the details of each bridge, since they are all unique, having different dimensions, load bearing systems, exposure environments, and geographic locations. While each bridge is unique, they are all similar in that they all have bare reinforced concrete decks with electrically continuous steel reinforcement. Table 2 provides a brief overview of the structures that were surveyed as a part of this research. All of these structures, except the structure in Iowa, are a part of the Long Term Bridge Performance (LTBP) Program funded by the Federal Highway Administration (FHWA).

Table 2: Details and descriptions of the structures involved in this research

Carries	Crossing	Location	Bridge Type	Number of Spans	Deck Area (ft <sup>2</sup> )
I-495 South	Route 13	Wilmington, DE	Continuous Steel Girder	2	13,716
I-195 East	Sharon Station Rd.	Upper Freehold Township, NJ	Simply Supported Steel Girder	1	3,420
Pequea Boulevard	Pequea Creek	Conestoga, PA	Simply Supported Prestressed Concrete Girder	2	6,952
School House Road	State Route 283	Middletown, PA	Continuous Steel Girder	2	10,296
State Route 123	Kettle River	Sandstone, MN	Deck Truss	4	6,400*
State Route 15	Interstate 66	Haymarket, VA	Continuous Steel Girder	2	10,420
State Route 18	State Route 66	Neptune, NJ	Simply Supported Prestressed Concrete Girder	2	6,800
State Route 21	Karr Valley Creek	Almond, NY	Adjacent Box Beam	3	4,930
State Route 273	Little Elk Creek	Elkton, MD	Continuous Steel Girder	2	4,508
State Route 47	State Route 55	Deptford Township, NJ	Continuous Steel Girder	3	12,580
State Route 93	Natural Steam	Sumner, IA	Simply Supported Steel Girder	1	2,980
West Bangs Ave	State Route 18	Neptune, NJ	Simply Supported Prestressed Concrete Girder	2	5,940

\* This represents area tested, not the total deck area

Data collection with each NDT method followed a defined protocol that was used on all of the bridge decks. While each individual NDT method has its own testing protocols, the focus of this section will be on the overall data collection procedure. On each deck, a 2 ft × 2 ft grid was laid out using chalk or water-soluble spray paint. The point measurement methods (ER, HCP, and IE) collected data at each of these grid locations. GPR, which performs scans instead of point measurements, conducted scans perpendicular to the direction of the top reinforcing steel. The GPR scans were performed in the longitudinal direction since the transverse reinforcement was the top layer of reinforcement. The longitudinal GPR scans were spaced 2 ft transversely, in conjunction with the testing grid. The CD survey was conducted over the entire deck and the

results of the survey were discretized at each grid location to indicate whether or not there was a delamination at the grid location.

On every bridge, all of the NDT methods were surveyed at the same time to ensure that the environmental conditions were consistent for each method.

#### DATA COMPARISONS

To describe a bridge deck's condition through the use of multi-modal NDT, a complete understanding of NDT data and how each method is related and unrelated is important. It is necessary to identify trends and correlations in the data that could be used to help define thresholds and determine the level of confidence in the results. The NDT results from each method will be quantitatively compared to identify relationships between the data of the various NDT methods. For example, do locations of corrosive environment identified by ER correspond well to areas of active corrosion identified by HCP? Do areas of low concrete cover correspond to areas of damage? How well do IE and CD agree about the location of delaminations? These are the types of questions that can be answered by looking at comparisons in the data and then used to help establish thresholds and confidence values for the condition assessment.

#### THRESHOLD ANALYSIS

The proper identification of damage through NDT requires an understanding of what value in the NDT measurement scale indicates a specific condition, known as the threshold value(s). For instance, when collecting HCP data, what voltage (potential) indicates active corrosion? What resistivity value(s) in an ER survey indicates an environment that facilitates corrosion activity? Thresholds need to be identified for ER, HCP, and GPR, because each of these methods provides results in the form of a distinct, continuous scale of measured values. In contrast, CD and IE do not need threshold values, because they provide results directly related to the delamination condition. As indicated in the literature review, various threshold values for the different NDT

methods have been presented throughout the literature. However, these thresholds are not absolute and can shift due to many factors. An objective of this research will be to create a statistically based approach to threshold identification that provides a robust threshold identification methodology that will work in a variety of situations. The results of the data comparisons will be used to help establish the threshold identification methodology for each of the NDT methods. The goal will be to produce a threshold analysis methodology that can be automated and combined into a condition assessment program.

It is important that the term *threshold value* be defined, as it will be used extensively throughout this research and can be interpreted differently by different people. Threshold value has a different meaning for ER, HCP, and GPR. In ER, there is typically one threshold value provided and it indicates that when the resistivity is less than or equal to the ER threshold, the concrete provides an environment conducive to corrosion activity. When the resistivity is greater than the threshold value, the concrete environment hinders corrosion activity. In HCP, there are commonly two threshold values identified: an active and passive threshold. The active threshold indicates that when a potential is less than or equal to the active threshold, there is a high probability that the steel being measured is actively corroding. The passive threshold indicates that when the potential is greater than or equal to the passive threshold, there is a high probability that the steel is in a passive state. In a GPR analysis, there is typically only one threshold value provided. The GPR threshold value indicates that when the relative amplitude is less than or equal to the threshold amplitude, the concrete is in a state of degradation. When the relative amplitude is greater than the threshold amplitude, the concrete is not in a state of degradation.

#### CONDITION ASSESSMENT

Once the threshold values have been defined, then the NDT results for each method can be broken into descriptions regarding the deterioration process or damage state of the bridge deck. The condition states that will be defined on the bridge deck are: severe delamination,

delamination/lateral cracking, active corrosion, corrosive environment, and sound deck (Table 3). These damage states are listed in the order of their importance; the more severe damage being of greater importance.

Table 3: Description and importance of identified damage states

<b>Damage Type</b>	<b>Identification Method</b>	<b>Rating</b>
Severe Delamination	Chain Drag or Impact Echo (IE = 4)	4
Delamination/Lateral Cracking	Impact Echo Signal Rating 3 or 2	3
Active Corrosion	Half-Cell Potential	2
Corrosive Environment	Electrical Resistivity or Ground Penetrating Radar	1
Sound Deck	Negative Result from All Systems	0

The condition assessment will be conducted using an automated program that evaluates each point and assigns a condition based on the results of the multi-modal NDT survey. Severe delaminations (condition rating 4) will be identified by CD or an IE signal rating of 4. An IE rating will only be accepted if ER, HCP, or GPR are also below their respective threshold values. The reasoning behind this is due to a lack of confidence in the IE data, due to findings discussed in the *Results/Data Comparisons* section. An accepted IE signal rating of 2 or 3 will be considered delamination/lateral cracking (condition rating 3). Active corrosion (condition rating 2) will be identified when HCP is below its threshold value. If either GPR or ER is below its threshold value, then the corrosive environment condition will be assigned to that location (condition rating 1). If no deterioration exists at a location, then it will be identified as sound (condition rating 0).

During the condition assessment, a single location can be affected by more than one damage type. For instance, a location with a severe delamination can also be actively corroding. However, the active corrosion is not of primary concern, since the severe delamination is of greater significance. The severe delamination is going to lead to serviceability issues and requires maintenance, while the active corrosion condition is an indication as to the delamination's cause. Therefore, the severe delamination will be indicated on the final condition assessment at that

location and not the active corrosion. At each location on the deck, only the highest order of damage will be identified, since this is the damage of the greatest importance. However, any secondary condition state at a location will be recorded for future use in the plotting of the damage, and determination of data agreement.

#### CONDITION RATING

With the damage in the bridge deck identified, the deck will be given an overall condition rating based on the already established and federally required National Bridge Inspection Standards (NBIS) (Table 4) and Bridge Element Inspection procedures defined by the American Association of State Highway and Transportation Officials (AASHTO) (Table 5). The implementation of an already established and federally required bridge rating methodology allows for this multi-modal NDT condition assessment to be more easily understood and implemented by bridge owners and maintenance personnel. There are two primary challenges when converting multi-modal NDT data into the NBIS and AASHTO rating systems: 1) the rating systems were designed with mostly visual inspection in mind; 2) the NBIS rating is a qualitative system while the multi-modal NDT assessment is a quantitative analysis. Multi-modal NDT primarily evaluates the interior condition of the deck, which provides a different condition assessment when compared to a purely visual assessment. Multi-modal NDT identifies deterioration processes at a much earlier state than visual inspection. There will also be significant challenges in relating qualitative and quantitative assessments. To overcome these challenges, the author contacted bridge inspection personnel at the Kansas Department of Transportation (KDOT), New Jersey Department of Transportation (NJDOT), and the Virginia Department of Transportation (VDOT) to learn how they apply the NBIS and AASHTO ratings. These discussions aided in developing a condition rating methodology that will aid in bridging the gap between visual and NDT inspection.

Table 4: National Bridge Inspection Standards (Ryan, et al. 2006)

Code	Description
N	Not Applicable
9	Excellent Condition
8	Very Good Condition - no problems noted
7	Good Condition - some minor problems
6	Satisfactory Condition - structural elements show some minor deterioration
5	Fair Condition - all primary structural elements are sound but may have minor section loss, cracking, spalling or scour
4	Poor Condition - advanced section loss, deterioration, spalling or scour.
3	Serious Condition - loss of section, deterioration of primary structural elements. Fatigue cracks in steel or shear cracks in concrete may be present
2	Critical Condition - advanced deterioration of primary structural elements. Fatigue cracks in steel or shear cracks in concrete may be present or scour may have removed substructure support. Unless closely monitored it may be necessary to close the bridge until corrective action is taken.
1	"Imminent" Failure Condition - major deterioration or section loss present in critical structural components or obvious vertical or horizontal movement affecting structure stability. Bridge is closed to traffic but corrective action may put it back in light service.
0	Failed Condition - out of service; beyond corrective action

Table 5: AASHTO Bridge Element rating system (AASHTO 2011)

Defect	Condition State 1	Condition State 2	Condition State 3	Condition State 4
Cracking	None to hairline	Narrow size or density, or both	Medium size or density, or both	The condition is beyond the limits established in condition state three (3), warrants a structural review to determine the strength or serviceability of the element or bridge, or both.
Spalls Delaminations Patched Areas	None	Moderate spall or patch areas that are sound	Severe spall or patched area showing distress	
Efflorescence	None	Moderate without rust	Severe with rust staining	
Load Capacity	No reduction	No reduction	No reduction	

In discussions with the various departments of transportation (DOT), and by reading through their bridge inspection manuals (Kansas Department of Transportation Bureau of Local Projects Bridge Team 2012), (New Jersey Department of Transportation 2009), (Virginia Department of

Transporation 2012), (Virginia Department of Transportation 2007), and (Krauss, Lawler and Steiner 2008), a better understating of how they apply the NBIS and AASHTO ratings was gained. The primary cross-over between the NDT condition assessment and the visual inspections are the percentages of severe delaminations. Severe delaminations are the only type of deterioration identified in both visual and NDT inspections. Visual inspections, despite the name, also include CD and hammer sounding, which are used to identify severe delaminations. The rating of a deck using multi-modal NDT will begin by identifying the percentage of the deck that is severely delaminated and associating that percentage level with an NBIS rating according to Table 6. The distribution of severe delamination percentages in Table 6 is based on current DOT practices and procedures. Then the percentage of the deck that is in a state of delamination/lateral cracking, actively corrodng, and corrosive environment will be summed, and if that area is larger than the *Area of Other Deterioration* then the NBIS rating will be decreased by one. For instance, if 15% of the bridge deck area is severely delaminated and the other deterioration states sum to 30%; e.g. delamination/lateral cracking (15%), actively corrodng (10%), and corrosive environment (5%), then the deck will be rated 7. If 15% of the bridge deck area is severely delaminated and the other deterioration states sum to 45%, then the deck will be rated 6. The severe delaminations are the primary driver for the NBIS rating. The other deterioration states define the severity of unseen damage and decrease the rating if that unseen damage is of a significant level. Some DOT practices associate much smaller areas of severe delaminations with each condition state. However, their inspection processes are typically not as detailed as a multi-modal NDT survey and thus a multi-modal NDT survey of a visually inspected bridge will typically turn up greater quantities of severe delamination. Therefore, the values in Table 6 are aligned with DOT practices, even though the delamination quantities may seem inflated. NBIS condition states 2, 1, and 0 are levels of damage that are so severe that they cannot be assessed by a multi-modal NDT survey.

Table 6: NBIS rating criteria based on multi-modal NDT results

NBIS Condition	Area of Severe Delamination (%)		Area of Other Deterioration (%)
	$\geq$	<	<
9	0	0	10
8	0	5	20
7	5	10	30
6	10	20	40
5	20	40	40
4	40	60	40
3	60	N/A	N/A
2	N/A	N/A	N/A
1	N/A	N/A	N/A
0	N/A	N/A	N/A

N/A – Not applicable

The AASHTO Bridge Element Rating, for bridge element 12 (bare reinforced concrete decks), will be defined by the square footage of deck area that falls into each AASHTO condition state category. AASHTO condition state 1 will be the amount of deck area that receives a condition state of sound deck and corrosive environment (damage states 0 and 1, Table 3). AASHTO condition state 2 will be the amount of deck area that is identified as actively corroding and delamination/lateral cracking (damage states 2 and 3, Table 3). AASHTO condition state 3 will be the deck area that is severely delaminated (damage state 4, Table 3). AASHTO condition state 4 will not be defined, since it is outside of the scope of the multi-modal NDT assessment.

The NBIS and AASHTO Ratings will be produced as an output of the condition assessment program. This will allow for bridge owners and maintenance personal to easily apply this NDT condition assessment to their existing condition evaluation procedures, standards, and documentation.

While the conversion of the multi-modal NDT results into NBIS and AASHTO is not perfect, the larger objective of this exercise is to get NDT practitioners thinking about how to better relate

NDT results to bridge owners' and maintenance personnel's' needs. Also it is important to get the people behind the NBIS and AASHTO ratings to be thinking about how these ratings can be changed to better suit NDT surveys.

#### PRESENTATION OF DECK CONDITION

To produce a condition assessment that is an effective decision-making tool, it is critical that the condition be accurately depicted. Current plotting techniques of NDT data create unverified data transitions, because the contouring software automatically assumes the data is continuous.

Contouring software creates smooth data transitions according to the selected interpolation scheme. The primary plot in Figure 12 is a depiction of the Haymarket, Virginia deck condition, in which the condition state for each test location is provided to the contouring software in a comma-delimited list of discrete values within a single data file. Each condition state is numerically identified in the contouring software based on its condition hierarchy (Table 3).

Using this information, the software produces a contour plot in which all of the data points have smooth (interpolated) transitions based on the value of the surrounding test locations. For instance, if adjacent test locations have a condition of 4-severe delamination and 1-corrosive environment, the software will assume that the conditions 3 and 2 exist between these two locations. This transition does not necessarily exist in the actual structure and can provide a false sense of data continuity. As a way to limit the software from creating false transitions, each damage type can be plotted individually and each location is only given one condition state; the complete plot is assembled by overlaying nonduplicating condition assessments. The software will not be able to interpolate between the different conditions and there will be no transitions at all. This is the other extreme in the data presentation. Each data set becomes independent; therefore, any transitions that did exist are no longer presented, thereby creating large gaps of "sound concrete" between adjacent locations of differing condition (Figure 12). The most reliable method between these two extremes is by overlaying duplicating areas of condition

assessment (Figure 12). If a test location is severely delaminated and actively corroding, then both of those conditions are recorded for that location and each condition type has a separate grid file. The distribution of each condition state is then plotted individually and overlaid according to the hierarchy (Table 3). At each location the highest order of damage afflicting that location is shown; however, if a transition exists between two locations, it can be properly shown without creating unverified data.

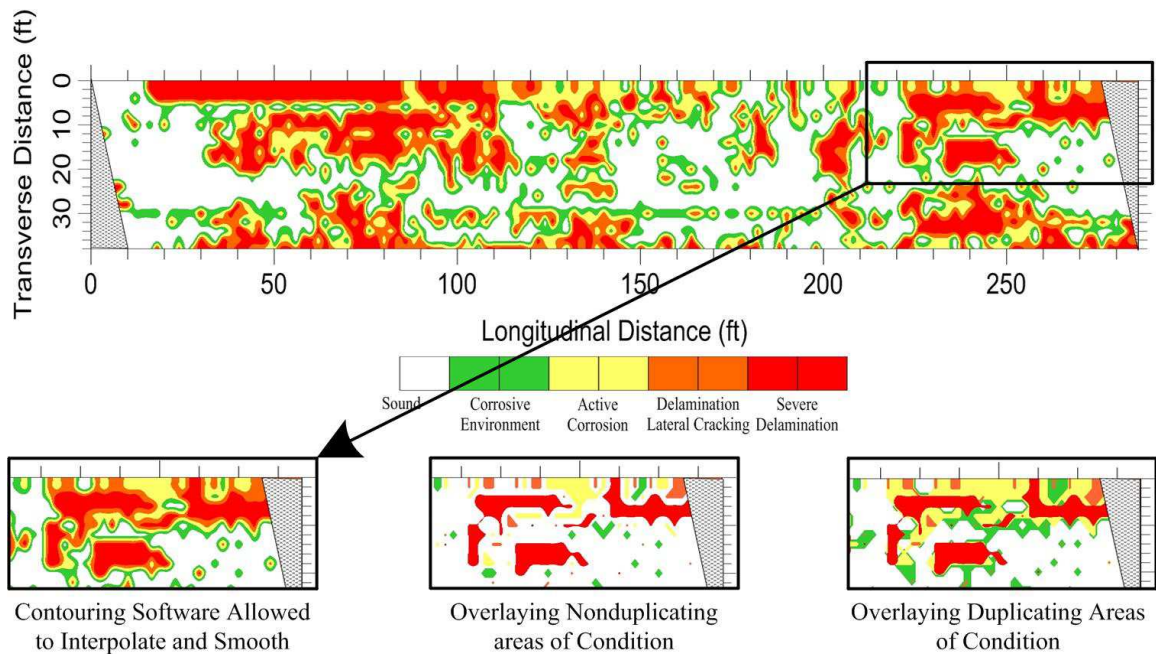


Figure 12: Various data presentation method (Haymarket, Virginia)

#### DATA AGREEMENT RATING

The multi-modal NDT approach to concrete deck assessment allows for the ability to identify whether the various NDT methods agree or disagree about concrete deterioration at each test location. For example, if GPR indicates concrete degradation and HCP indicates active corrosion at a given test location, the confidence that there is corrosion activity is much higher than if just HCP was below its threshold. Every possible permutation of multi-modal NDT result scenarios was determined and an agreement level rating for each scenario was established (Table 7). This

allows for a rating to be calculated according to the level of agreement in the multi-modal NDT data. At this time, the rating values are based on the literature review, the researcher's experience, and results of this work. Results obtained from the data comparisons made as a part of this research were used to help establish the percentage values. The data comparisons identified specific relationships between the different NDT methods, which were used to help establish the level of agreement between the various methods. In order to provide statistical backing to these values, autopsies and coring of the decks must take place, which is outside the scope of this work. At each test location on a deck, a rating is determined based on Table 7 and then the average rating over the entire deck is calculated. The higher the rating, the more agreement regarding deterioration exists between the different NDT methods.

Table 7: Multi-modal NDT data agreement rating tables

Condition State	Agreement Level	CD	IE	HCP	GPR	ER
<b>Severe Delamination</b>	100%	1	4	≤ Thres.	≤ Thres.	≤ Thres.
	99%	1	3	≤ Thres.	≤ Thres.	≤ Thres.
	95%	1	2	≤ Thres.	≤ Thres.	≤ Thres.
	90%	1	1	≤ Thres.	≤ Thres.	≤ Thres.
	85%	0	4	≤ Thres.	≤ Thres.	≤ Thres.
	90%	1	4	≤ Thres.	≤ Thres.	>Thres.
	89%	1	3	≤ Thres.	≤ Thres.	>Thres.
	85%	1	2	≤ Thres.	≤ Thres.	>Thres.
	80%	1	1	≤ Thres.	≤ Thres.	>Thres.
	80%	0	4	≤ Thres.	≤ Thres.	>Thres.
	90%	1	4	≤ Thres.	>Thres.	≤ Thres.
	89%	1	3	≤ Thres.	>Thres.	≤ Thres.
	85%	1	2	≤ Thres.	>Thres.	≤ Thres.
	80%	1	1	≤ Thres.	>Thres.	≤ Thres.
	80%	0	4	≤ Thres.	>Thres.	≤ Thres.
	90%	1	4	>Thres.	≤ Thres.	≤ Thres.
	89%	1	3	>Thres.	≤ Thres.	≤ Thres.
	85%	1	2	>Thres.	≤ Thres.	≤ Thres.
	80%	1	1	>Thres.	≤ Thres.	≤ Thres.
	80%	0	4	>Thres.	≤ Thres.	≤ Thres.
	80%	1	4	≤ Thres.	>Thres.	>Thres.
	79%	1	3	≤ Thres.	>Thres.	>Thres.
	75%	1	2	≤ Thres.	>Thres.	>Thres.
	70%	1	1	≤ Thres.	>Thres.	>Thres.
	70%	0	4	≤ Thres.	>Thres.	>Thres.
	80%	1	4	>Thres.	≤ Thres.	>Thres.
	79%	1	3	>Thres.	≤ Thres.	>Thres.
	75%	1	2	>Thres.	≤ Thres.	>Thres.
	70%	1	1	>Thres.	≤ Thres.	>Thres.
	70%	0	4	>Thres.	≤ Thres.	>Thres.
	80%	1	4	>Thres.	>Thres.	≤ Thres.
	79%	1	3	>Thres.	>Thres.	≤ Thres.
	75%	1	2	>Thres.	>Thres.	≤ Thres.
	70%	1	1	>Thres.	>Thres.	≤ Thres.
70%	0	4	>Thres.	>Thres.	≤ Thres.	
70%	1	4	>Thres.	>Thres.	>Thres.	
69%	1	3	>Thres.	>Thres.	>Thres.	
65%	1	2	>Thres.	>Thres.	>Thres.	
60%	1	1	>Thres.	>Thres.	>Thres.	
50%	0	4	>Thres.	>Thres.	>Thres.	

Condition State	Agreement Level	CD	IE	HCP	GPR	ER
Delamination/Lateral Cracking	100%	0	3	≤ Thres.	≤ Thres.	≤ Thres.
	100%	0	2	≤ Thres.	≤ Thres.	≤ Thres.
	90%	0	3	≤ Thres.	≤ Thres.	>Thres.
	90%	0	2	≤ Thres.	≤ Thres.	>Thres.
	90%	0	3	≤ Thres.	>Thres.	≤ Thres.
	90%	0	2	≤ Thres.	>Thres.	≤ Thres.
	80%	0	3	>Thres.	≤ Thres.	≤ Thres.
	80%	0	2	>Thres.	≤ Thres.	≤ Thres.
	75%	0	3	≤ Thres.	>Thres.	>Thres.
	75%	0	2	≤ Thres.	>Thres.	>Thres.
	70%	0	3	>Thres.	≤ Thres.	>Thres.
	70%	0	2	>Thres.	≤ Thres.	>Thres.
	60%	0	3	>Thres.	>Thres.	≤ Thres.
	60%	0	2	>Thres.	>Thres.	≤ Thres.
	40%	0	3	>Thres.	>Thres.	>Thres.
	40%	0	2	>Thres.	>Thres.	>Thres.
Active Corrosion	100%	0	1	≤ Thres.	≤ Thres.	≤ Thres.
	75%	0	1	≤ Thres.	>Thres.	≤ Thres.
	70%	0	1	≤ Thres.	≤ Thres.	>Thres.
	50%	0	1	≤ Thres.	>Thres.	>Thres.
Corrosive Environment	100%	0	1	>Thres.	≤ Thres.	≤ Thres.
	75%	0	1	>Thres.	>Thres.	≤ Thres.
	75%	0	1	>Thres.	≤ Thres.	>Thres.
Sound Deck	100%	0	1	>Thres.	>Thres.	>Thres.

In addition to the data agreement level rating, which is based on highly subjective rating values, the percentage of the deck that is in total agreement between the different NDT methods will also be evaluated. Situations of total agreement for each damage state indicate that all of the auxiliary NDT methods are in agreement about deterioration at that location (Table 8). For example, when

there is a corrosive environment condition, that condition can be identified by either GPR or ER being below their respective thresholds. However, for complete agreement, they both need to be below threshold.

Table 8: Situations of complete NDT data agreement

Condition	Chain Drag	Impact Echo	Half-Cell Potential	Ground Penetrating Radar	Electrical Resistivity
<b>Severe Delamination</b>	1	4	<=Thres	<=Thres	<=Thres
<b>Delamination/Lateral Cracking</b>	0	3 or 2	<=Thres	<=Thres	<=Thres
<b>Active Corrosion</b>	0	1	<=Thres	<=Thres	<=Thres
<b>Corrosive Environment</b>	0	1	>Thres	<=Thres	<=Thres
<b>Sound Deck</b>	0	1	>Thres	>Thres	>Thres

The percentage of the deck in complete agreement along with the data agreement rating will provide a quantitative way to assess the effectiveness of the multi-modal NDT condition assessment along with providing a level of confidence in the results. A high percentage of the deck that is in complete agreement will equate to a high level of confidence in the condition assessment. This analysis can also be used to help identify the deterioration mechanism afflicting the bridge deck. If there is high data agreement, this could indicate chloride-induced corrosion, while poor agreement could indicate carbonation-induced corrosion or mechanical damage. For instance, during carbonation-induced corrosion the resistivity of the concrete will increase substantially. Therefore, ER will not be able to identify areas of corrosive environment and thus will not correlate well with areas of severe delaminations. An example of mechanical damage could be debonding of an overlay; this form of deterioration cannot be identified by ER or HCP, but would be identified by IE and CD. Therefore, there would not be strong agreement between the various NDT methods.

The focus of this work has been the use of five NDT technologies, simultaneously implemented on a bridge deck. In practical application, all of these methods may not be able to be

implemented. However, the understanding gained through this research will help to better understand data from bridges that are surveyed using a limited multi-nodal NDT approach. While a condition assessment can be obtained from fewer NDT methods, the assessment would not be as complete as the approach identified in this research.

#### ALTERNATE GRID SPACING

A 2 ft × 2 ft sampling grid was used throughout this research because the NDT surveys were collected as a part of the LTBP Program. The LTBP Program has established data collection protocols for which the 2 ft × 2 ft grid spacing was specified. To understand the affect this grid spacing has on the NDT survey results, an analysis was conducted to evaluate the effectiveness of a 2 ft × 2 ft grid and how it compares to different grid spacings. To identify if a 2 ft × 2 ft grid accurately identifies damage, a randomly selected section of the Rt. 18 over Rt. 66 deck in Neptune, New Jersey was surveyed using a 0.5 ft × 0.5 ft grid. The overall dimensions of this area were 6 ft transversely by 16 ft longitudinally. An evaluation with a grid using 0.5-ft increments allowed for various combinations of grid spacing to be evaluated, 0.5 ft × 0.5 ft, 1 ft × 1 ft, 1.5 ft × 1.5 ft, and 2 ft × 2 ft. In the analysis, the researcher evaluated what effect the different grid spacing had on the average measured values and quantity of area identified as damaged.

An analysis was also conducted to identify what effect a grid spacing larger than 2 ft × 2 ft would have on the measured values and damage quantities. Since the analysis was conducted on previously collected data, only multiples of the 2 ft × 2 ft grid spacings associated with the original data could be evaluated. Grid spacings of 2 ft × 2 ft, 4 ft × 4 ft, all the way up to 20 ft × 20 ft were evaluated for each bridge. Rectangular grid spacings were also evaluated, since they are proportionally more similar to bridge deck dimensions. The rectangular grid spacings evaluated were 2 and 4 ft in the transverse direction and 2, 4, 6, 8, and 10 ft in the longitudinal direction.

## NON-DESTRUCTIVE TEST METHOD SURVEY

An important objective of this work is to make NDT a better tool for bridge owners and maintenance personnel. To accomplish this goal, it is important to know what bridge owners and maintenance personnel think about NDT condition assessment and their level of familiarity with it. A short two-page survey was designed to learn more about how NDT is viewed, understood, and applied by bridge owners and maintenance personnel (Appendix 1 – Non-Destructive Test Method Survey).

Page one of the survey focused at understanding what NDT background the bridge owners and maintenance personnel have. Do they use NDT?; what methods?; does their agency own NDT equipment?; and do they think NDT methods are effective? Page two of the survey focused on understanding what bridge owners and maintenance personnel understand from standard NDT plots. Page 2 also focused at understanding what kind of information they would like to learn from an NDT survey. Learning how bridge owners and maintenance personnel view, understand, and apply NDT will allow for NDT to become a better decision-making tool.

## RESULTS AND DISCUSSION

### DATA COMPARISONS

The following section provides the results of the correlations and data comparisons made between the multi-modal NDT data.

#### *Comparisons between Electrical Resistivity and Half-Cell Potential*

The ER and HCP data were analyzed to identify if a relationship between concrete resistivity and the state of corrosion activity existed. For each bridge deck, the HCP data was filtered according to the resistivity measured at the same location, in increments of 5 kohm·cm. The average HCP (and variance) was calculated for each increment and then compared to the average HCP for the

entire bridge to determine a relative average potential. The relative average potential for each increment was determined for all 12 bridges and then combined to produce Figure 13. The relative potential was used because each bridge has a distinct range of potentials, along with shifting threshold values. This makes comparisons of the measured potentials between different bridges not as informative as relative potentials. Analysis of Figure 13 indicates that when the resistivity is below 40 kohm·cm, the slope of the curve steepens significantly. Low resistivities are associated with potentials that are significantly below average (i.e., more active). Above 40 kohm·cm, the curve levels off and has potentials that are above average. There is a clear relationship between low resistivity and low potential. The bridges in this study are strongly affected by chloride-induced corrosion, which is a strong factor as to why the ER and HCP relationship exists. In environments with minimal chloride exposure, this relationship may be different or non-existent.

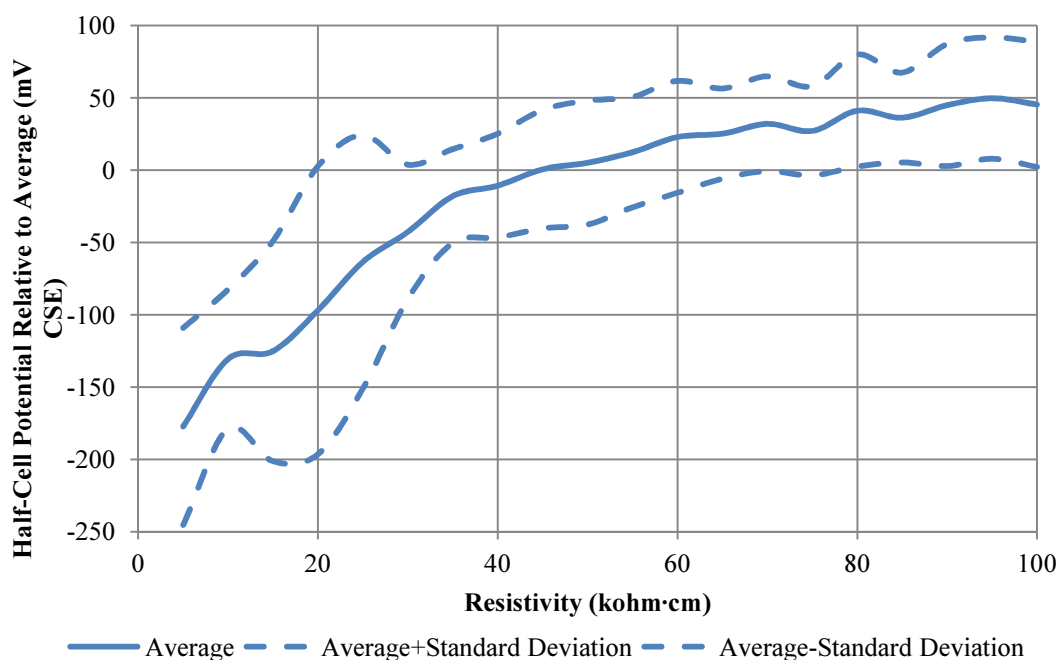


Figure 13: Relative half-cell potential based on resistivity

Figure 14 shows the cumulative frequency distribution of the HCP measurements which have been filtered according to the resistivity measurement made at the same location for all 12 bridges. The HCP data has been separated into two groups, locations of corrosive environment,  $ER \leq 30 \text{ kohm}\cdot\text{cm}$ , and non-corrosive environment,  $ER \geq 70 \text{ kohm}\cdot\text{cm}$ . The values of 30 and 70  $\text{kohm}\cdot\text{cm}$  were selected because these limits are well within the corrosive and non-corrosive environments for all of the bridge decks in this study. As will be presented in the threshold identification section; the ER thresholds for the entire sampling of bridges shift between 30 and 53  $\text{kohm}\cdot\text{cm}$ . Therefore, to insure that a corrosive environment is represented on all of the bridges,  $\leq 30 \text{ kohm}\cdot\text{cm}$  has been selected as a corrosive environment. To insure that a non-corrosive environment is represented for all of the bridges, locations with a resistivity  $\geq 70 \text{ kohm}\cdot\text{cm}$  were selected as a non-corrosive environment. The distribution of potentials for the two environments differs significantly from each other. When the resistivity indicates a corrosive environment, 74.0% of the time the potential at those locations is less than  $-350 \text{ mV CSE}$ . When the resistivity indicates a non-corrosive environment, 89.1% of the locations have a potential that is greater than  $-350 \text{ mV CSE}$ . Only 6.3% of the corrosive environment test locations have a potential greater than  $-200 \text{ mV CSE}$ . This indicates a clear relationship between ER and HCP measurements.

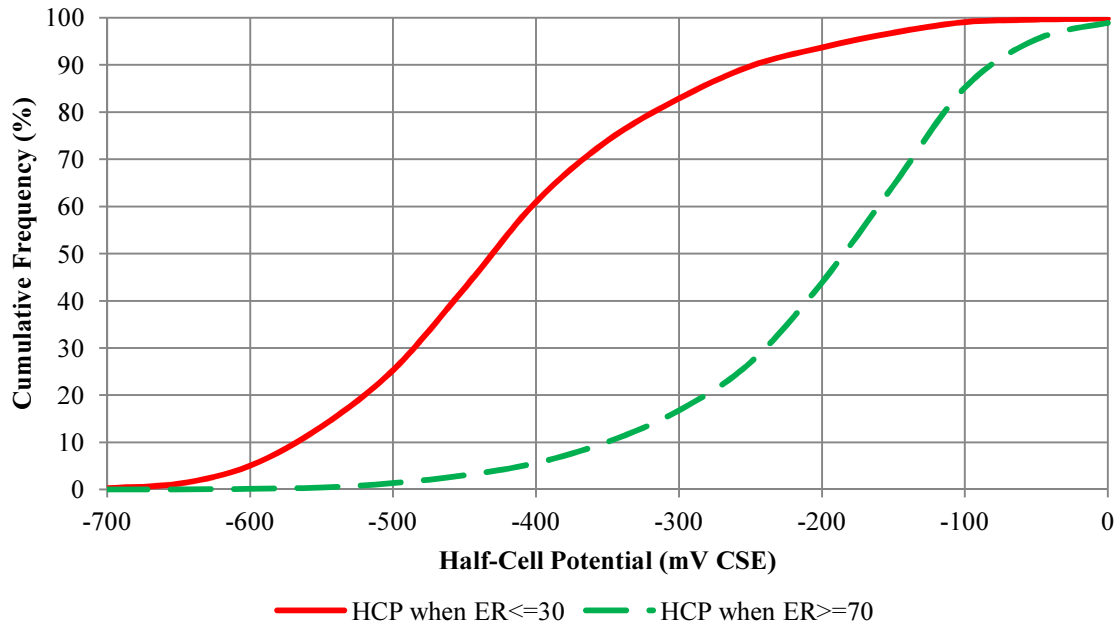


Figure 14: Cumulative frequency distribution of half-cell potentials based on resistivity for all 12 bridges

Figure 13 and Figure 14 show a clear relationship between the ER and HCP data collected on the bridge decks in this study. Concrete resistivity is closely associated with the concentration of moisture and chloride in the concrete. Increased levels of moisture and chloride provide an environment in concrete that is conducive to corrosion activity. Therefore, it is reasonable to expect that on bridge decks in situations of low concrete resistivity associated with moisture and chloride, there will be a high probability of active corrosion at that location.

#### *Ground Penetrating Radar*

Correlations were identified between the results of GPR amplitude analysis and the other NDT methods utilized in this study. GPR is a highly relative measurement, in that the range of amplitudes for each bridge deck is unique to that deck due to the deck's dielectric and geometric properties. Therefore, to be able to combine the GPR data from all 12 bridges, each GPR data set must be converted into a consistent measurement scale (i.e., normalized). That scale will be the

relative average, which for the GPR amplitude is its difference in amplitude from the average amplitude for the bridge deck as a whole.

Figure 15 provides a comparison of the average relative GPR amplitude to the electrical resistivity measured at the same location. For the distribution of resistivity values, in increments of 5 kohm·cm, the average relative amplitudes were determined. There is a clear trend of decreasing amplitudes associated with low resistivity values. At approximately 50 kohm·cm, the curve's slope starts to increase significantly in the direction of lower resistivities. Above 50 kohm·cm, the curve is relatively level and the relative amplitude is above average. Figure 15 shows that when the resistivity of concrete decreases, the attenuation of the GPR amplitude increases. ER and GPR are both affected by the electrical properties of the concrete that is being measured. It is expected that the concrete's dielectric and resistivity, measured by GPR and ER respectively, will correlate because they are both electrical parameters.

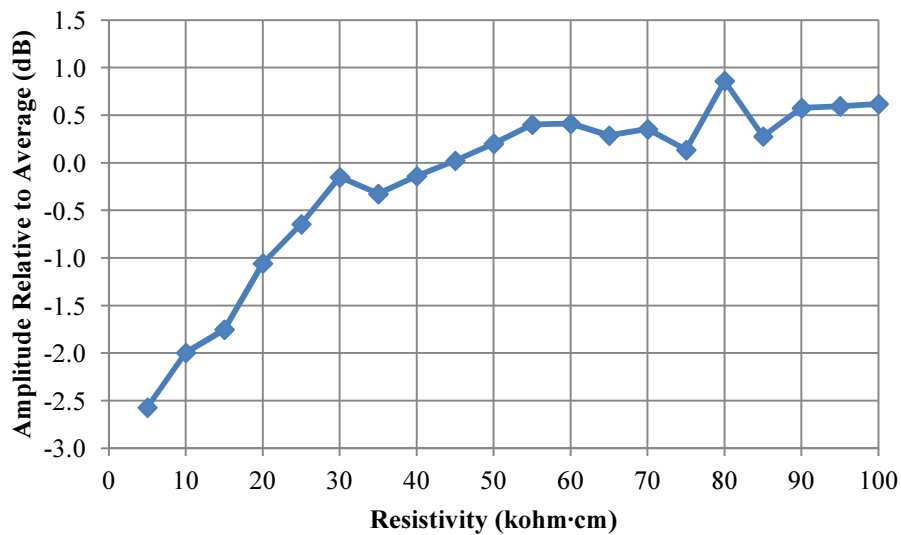


Figure 15: Comparison of average relative GPR amplitude to ER

A comparative analysis was also conducted between HCP and GPR data, using the relative average amplitude for the GPR measurements. Figure 16 provides the results of this comparison,

which indicates a near-linear relationship between the two measurements. Locations of high GPR attenuation are associated with highly negative potentials. As the potential increases, there is a near-linear increase in relative amplitude. In addition, the average amplitude is approximately associated with a potential of  $-350$  mV CSE, a potential value that is generally associated with the threshold value for active corrosion (14). These results indicate that when the amplitude at a location falls below the average, that location has a high probability of active corrosion.

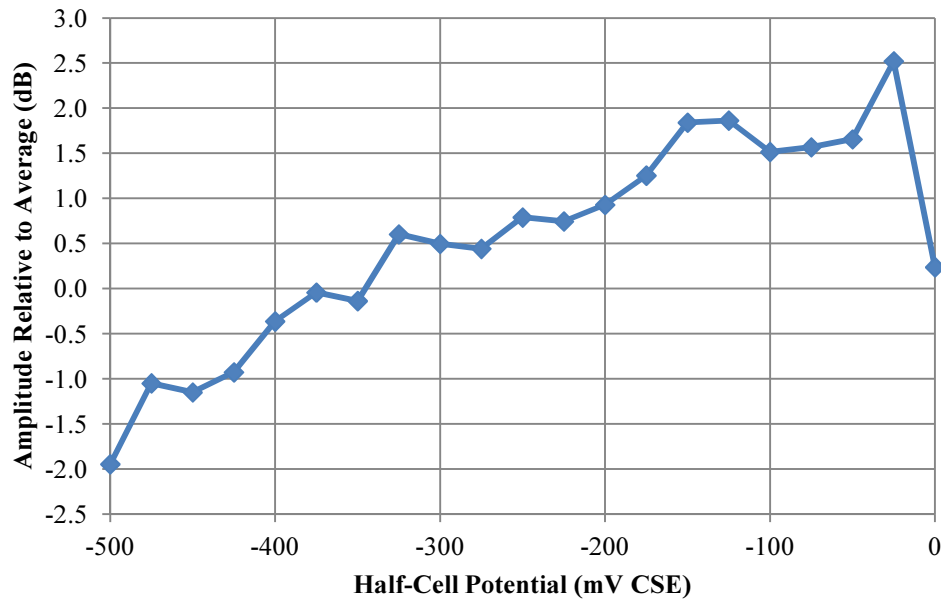


Figure 16: Comparison of average relative GPR amplitude to HCP

As an extension of the analysis conducted in Figure 16, the relative GPR amplitude was determined for the bridge in Haymarket, Virginia and overlaid on the HCP data (Figure 17). Using the linear relationship in Figure 16 to coordinate the color scale of the relative GPR amplitudes, a contour plot was developed. To assist in viewing the data, the passive region of the HCP data and relative amplitudes greater than zero were left out. The relative GPR amplitude contours are translucent to allow the viewing of the HCP and GPR data simultaneously. The areas of deterioration identified in both surveys are relatively similar. Also areas of extremely

low potentials are associated with areas of highly negative relative GPR amplitudes. Figure 16 and Figure 17 clearly show the strong relationship that exists between HCP and GPR data.

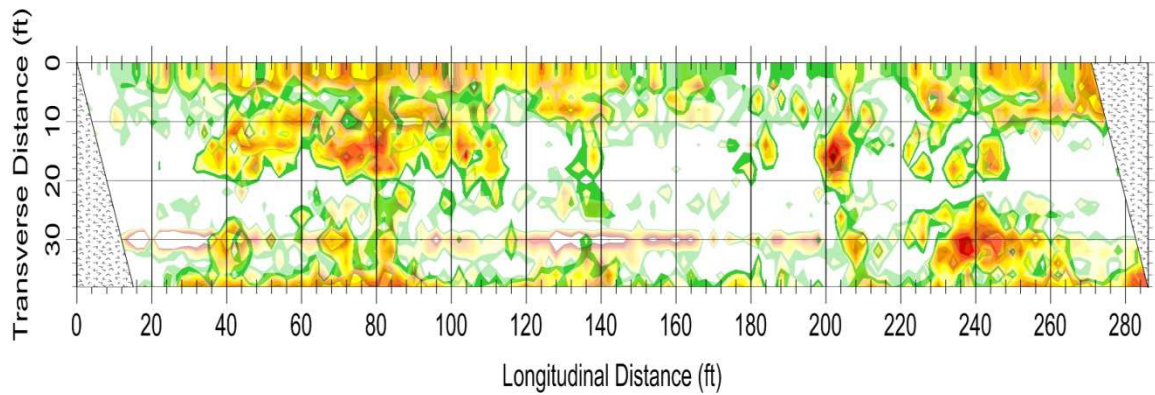


Figure 17: HCP overlaid with relative GPR amplitude (Haymarket, Virginia)

### *Impact Echo*

IE and CD are the two acoustic NDT methods in this study and an investigation of the relationships between them is of particular interest. Since they both aim to identify the location of delaminations, it is important to understand their level of agreement. CD can only identify severe delaminations, which are identified by IE as a signal rating of 4. IE, which is a more sensitive test method, can identify earlier stage delaminations and lateral cracking, classified as IE signal ratings 3 and 2. A CD measurement of 0 only means that there is not a severe delamination present and an IE rating of 1 indicates that no delamination or lateral cracking is present.

Table 9 provides the assessment of agreement and disagreement between the CD and IE measurements. Since CD can only identify severe delaminations, agreement and disagreement between these two methods must be defined. Disagreement would indicate that CD identified a severe delamination,  $CD=1$ , and IE had a signal rating of 1, 2 or 3. Disagreement would also occur if  $CD=0$  and IE had a signal rating of 4. Every other situation,  $CD=1/IE=4$ , and

CD=0/IE=1, 2, or 3, would indicate agreement. For the bridges in which IE data was collected, there was an average of 72.5% agreement and 27.5% disagreement between the CD and IE surveys. Overall, the agreement and disagreement between the two methods was relatively good.

Table 9: Agreement and disagreement between IE and CD results

<b>Structure</b>	<b>Percentage of Agreement</b>	<b>Percentage of Disagreement</b>
<b>VA 2009</b>	80.4	19.6
<b>VA 2011</b>	73.8	26.2
<b>MN</b>	79.7	20.3
<b>NY</b>	91.0	9.0
<b>NJ</b>	39.4	60.6
<b>O2</b>	70.4	29.6
<b>Average</b>	<b>72.5</b>	<b>27.5</b>

Based on this IE and CD comparison, a deeper look was taken at the data. Since severe delaminations are the only damage type that can be compared between IE and CD, a closer look was taken at the data when CD indicates a severe delamination (Table 10). When CD indicates a severe delamination, 22.4% of the time IE indicated a sound deck and 36.3% of the time IE disagreed about the severity of the delamination. Across all of the bridge decks, less than half (41.4%) of the locations that CD indicated as severe delamination were also indicated as severe by IE. This indicates a clear disparity regarding the identification and classification of delaminations.

Table 10: Comparison of severe delamination identification between CD and IE

Structure	CD=1 & IE=4	CD=1 & IE=3, or 2	CD=1 & IE=1	CD=1 & IE=3,2, or 1
VA 2009	36.9	19.2	43.9	63.1
VA 2011	48.8	24.7	26.6	51.3
MN	50.5	34.7	14.7	49.5
NY	15.2	69.7	15.2	84.8
NJ	66.7	33.3	0.0	33.3
O2	30.2	35.9	33.9	69.8
<b>Average</b>	<b>41.4</b>	<b>36.3</b>	<b>22.4</b>	<b>58.6</b>

An analysis was also conducted to establish if the IE data were correlated to the other NDT methods. Table 11 provides the results of an evaluation to determine how the average ER, HCP, and GPR measurements correlate to the IE signal rating. Relative HCP and GPR values were used in the analysis due to the strong variation of those measurements between bridges. The average NDT measurement for locations that have an IE signal rating of 4 showed a clear decrease when compared to the other signal ratings for that measurement device. The average resistivity for an IE=4 was 48.7 kohm·cm, which was less than the other ratings, which averaged to 59.9 kohm·cm. The average potential and GPR amplitude also showed a sharp decrease when IE=4, -43.8 mV CSE and -1.2 dB, when compared to the other IE signal ratings. The average measurements for IE signal ratings of 2 and 3, however, do not show a strong variation from each other or to the IE signal rating of 1, except in the case of HCP. The electrical potential for an IE signal rating of 3 does show a strong variation from the other IE signal ratings. This analysis shows there is a clear difference between IE signal rating of 4 with the other signal ratings. However, between signal ratings 1, 2, and 3, there is little difference. This could be due to the fact that identifying signal ratings 2 and 3 in the processing of IE data is very difficult. This difficulty in evaluating the IE signal may lead to a decrease in accuracy for these locations. It could also indicate that IE is identifying more mechanical damage in the deck. ER, HCP, and

GPR would show a decreased level of correlation to mechanical damage, because these methods primarily identify parameters related to chloride-induced corrosion.

Table 11: Average NDT measurement based on impact echo signal rating

IE Rating	ER (kohm·cm)	Relative HCP (mV CSE)	Relative GPR (dB)
1	60.3	10.7	0.2
2	61.6	13.9	0.4
3	57.9	2.2	0.2
4	48.7	-43.8	-1.2

As another way to look at the IE signal rating and how it compares with the other NDT methods, Figure 18, Figure 19, and Figure 20 were developed to look at the distribution of each measurement scale for each IE signal rating. Figure 18 provides the cumulative frequency distribution of resistivity for each of the IE signal ratings. Overall, there doesn't appear to be much difference between the resistivity distributions for each signal rating. IE signal rating of 4 does show some separation between the other signal ratings, while it's not a drastic change it is significant.

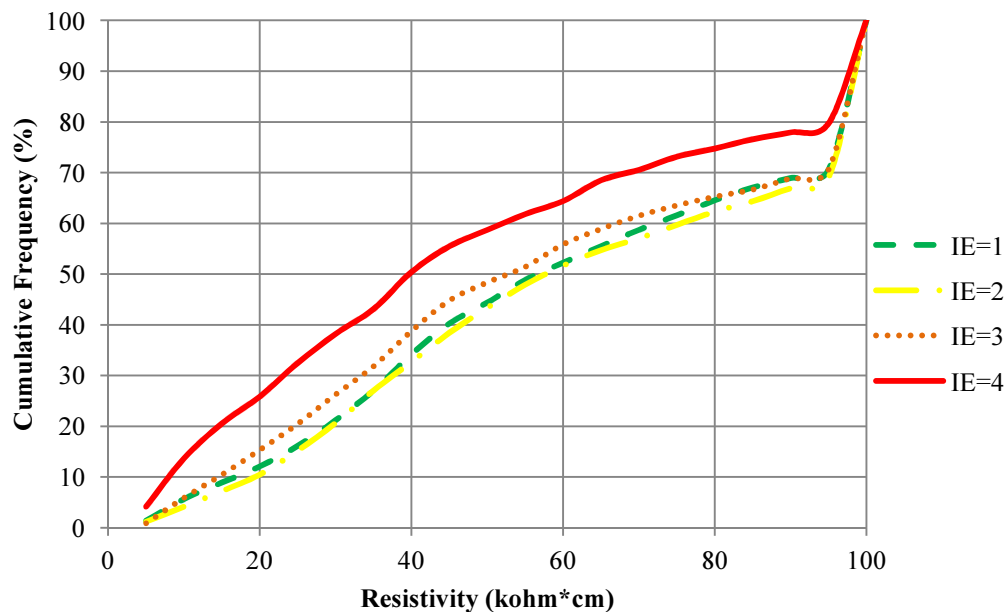


Figure 18: Cumulative frequency distribution of resistivity based on impact echo signal rating

Figure 19 provides the cumulative frequency distribution of potential values based on the IE signal rating. Similar to the distribution of resistivities, there is no difference in potential distribution for IE signal ratings of 1, 2, and 3. However, the IE signal rating of 4 does have a more negative distribution of potentials than the other signal ratings. There is approximately a 10% to 15% difference in IE signal rating 4 from the other signal ratings between the potentials  $-500$  mV CSE to  $-350$  mV CSE.

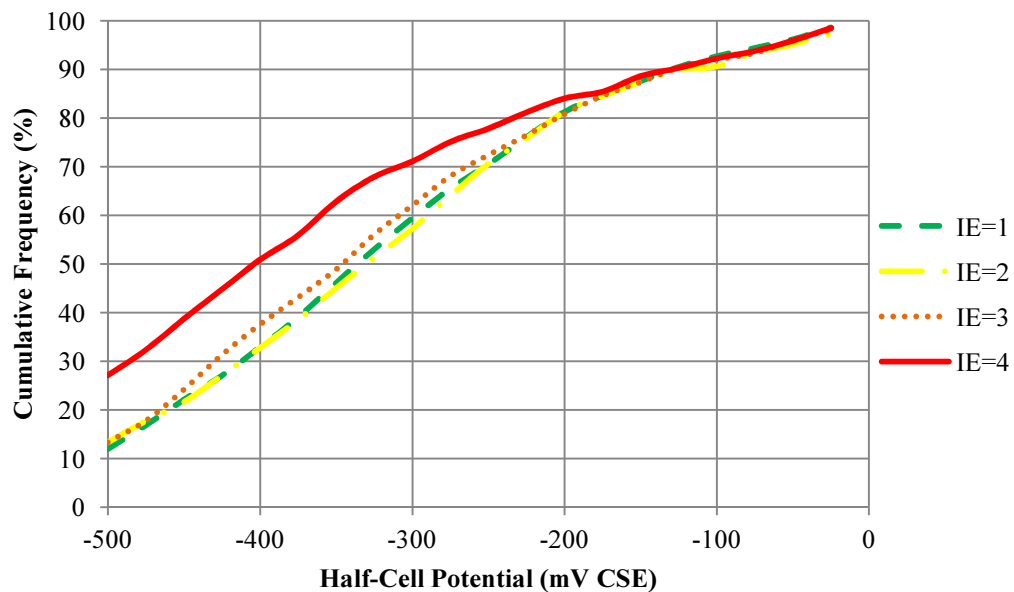


Figure 19: Cumulative frequency distribution of half-cell potential based on impact echo signal rating

Figure 20 provides the cumulative frequency distribution of the relative GPR amplitudes for each of the IE signal ratings. Again, like the previous three figures, IE signal ratings of 1, 2, and 3 do not show any significant variation. IE signal rating of 4, however, for GPR does show consistent variation in amplitude distribution over the whole spectrum of values. While this variation is not large, it is clear and significant.

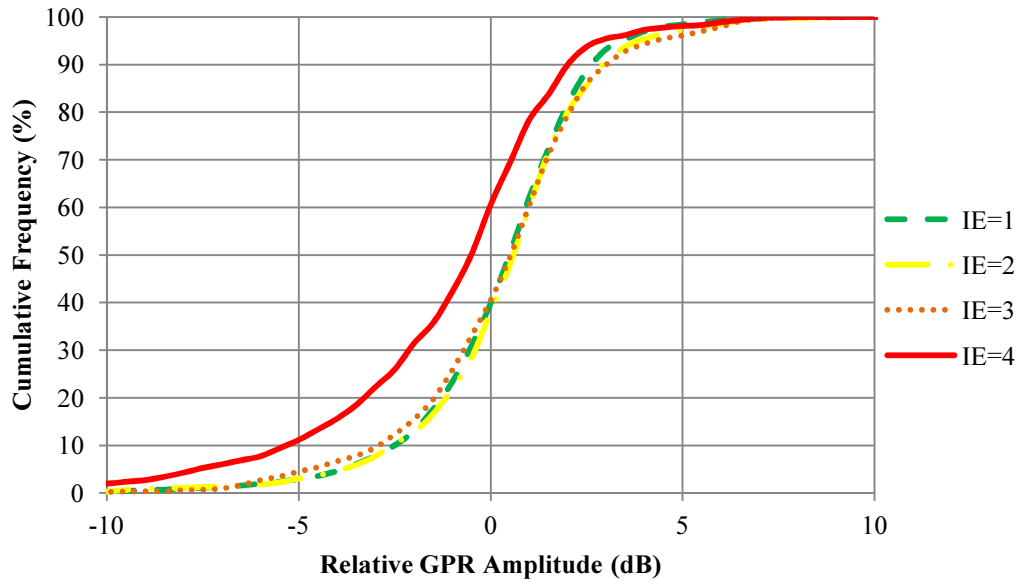


Figure 20: Cumulative frequency distribution of relative GPR amplitude based on impact echo signal rating

### *Cover Depth*

The cover depth for concrete reinforcement is an important factor in the service life of a structure. A shallow cover depth will allow for chlorides or carbonation to reach the reinforcement quicker, allowing for corrosion to initiate sooner. An analysis was conducted to evaluate the association cover depth has with deterioration on the 12 bridges in this study. Table 12 and Table 13 provide the average cover depth for each NDT method with respect to that method's threshold value or deck condition state. The first values of interest are the average cover depth for locations that were identified as CD=1 severely delaminated (2.57 in), CD=0 no delamination (2.73 in), and patched (2.17 in). Patch locations, which averaged the shallowest cover depth, are locations that in the past were delaminated and then repaired. The resulting shallow cover for these locations allowed for the initiation of corrosion activity and subsequent damage first, thus requiring these locations to be repaired. Current delaminated sections have the next shallowest cover, 2.57 in, and locations that are not delaminated are the deepest of the three at 2.73 in. This analysis indicates that deeper cover on average increases the time to concrete damage.

It is also interesting to compare the average cover depth of the locations above and below the various NDT threshold values. Locations that are below the HCP, ER, and GPR threshold values all have shallower cover on average than the locations above those respective thresholds.

However, this variation is small, approximately 0.1 in and thus is not statistically significant.

Table 13 provides the average cover depth for locations according to the IE signal rating and there appears to be no relationship between the IE signal ratings and cover depth. The IE signal ratings indicate the level of delamination or lateral cracking which was expected to provide similar cover depth results as the CD analysis. Unfortunately, a relationship between IE signal rating and cover depth did not exist.

Table 12: Average cover depth for various condition states

Condition State	HCP<= Thres	HCP>= Thres	ER<= Thres	ER> Thres	GPR<= Thres	GPR> Thres	CD=1	CD=0	Patch
<b>Average (in)</b>	2.62	2.74	2.66	2.70	2.66	2.71	2.57	2.73	2.17
<b>Standard Deviation (in)</b>	0.68	0.63	0.67	0.69	0.71	0.66	0.72	0.65	0.11

Table 13: Average cover depth for impact echo signal ratings

Impact Echo Signal Rating	1	2	3	4
<b>Average (in)</b>	2.69	2.64	2.77	2.69
<b>Standard Deviation (in)</b>	0.75	0.82	0.70	0.73

To investigate the relationship between cover depth and the NDT methods further, the average cover depth for the distribution of each of the NDT measurements was determined. Figure 21 provides the average cover depth for the distribution of potential values. While there is some variation in the curve, the general trend is that as cover depth increases the potential also increases. This result indicates that locations of lower cover are more likely to have active corrosion. This is in line with chloride penetration diffusion models in which chloride levels will reach the threshold sooner in shallower cover, thus initiating corrosion activity sooner. However,

it is also known that cover depth does have an effect on the measured potential. Shallow cover depth decreases potentials due to the decreased distance from the corrosion cell. However, based on the previous analyses regarding HCP, the confidence that low potentials are indicating active corrosion is high. The decreased potentials at locations of shallow cover are not purely a result of the cover depth. The results in Figure 21 are most likely depicting a combination of shallow cover decreasing potentials and shallow cover allowing for the early initiation of corrosion.

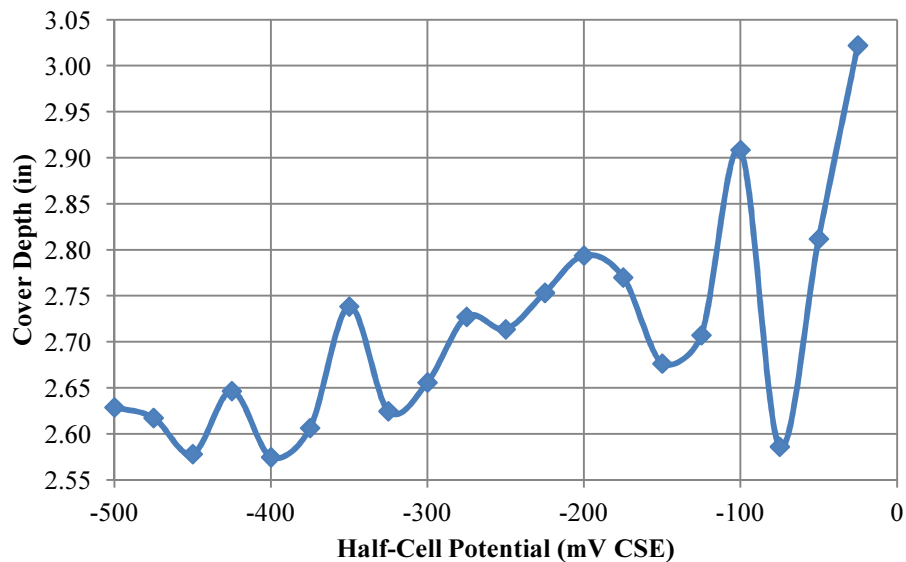


Figure 21: Average cover depth for distribution of half-cell potentials

Figure 22 provides the average cover depth for the distribution of relative GPR amplitudes. GPR amplitudes are affected by cover depth due to the travel distance of the electromagnetic wave. As the cover depth increases, the attenuation of the GPR signal will also increase. However, the cover depth effect is corrected in the post-processing of the GPR data. Review of the average cover depth for the distribution of relative amplitudes (Figure 22) indicates a trend in which higher attenuation is associated with lower cover depths. An association of low cover depths with high attenuation indicates that the correction for cover depth made in the GPR post-processing was adequate. If the post-processing correction was not adequate, highly attenuated signals

would be associated with deeper cover depth. This indicates the association low cover depth has with increased probability for deterioration. While the cover depth to relative amplitude curve is not perfectly straight, there is a general trend; as cover depth increases attenuation decreases. At each end of the curve, the data becomes highly variable; this is due to those points being a function of fewer data points. Very few bridges have GPR amplitudes that far from the average amplitude, making the average calculation highly variable.

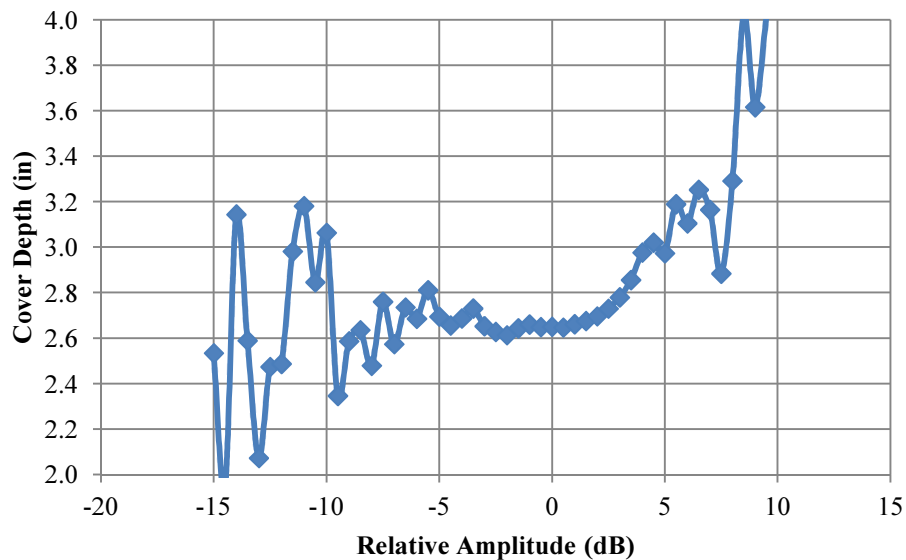


Figure 22: Average cover depth for distribution of relative amplitudes

Figure 23 provides the average cover depth for the distribution of resistivity values. Unlike HCP and GPR, there is no clear relationship between cover depth and ER over the distribution of values. However, at very low resistivities, less than 30 kohm·cm, there is a significant decrease in the cover depth as compared to the rest of the resistivity distribution. An exception would be at 5 kohm·cm, which actually has the highest cover of any of the resistivity values. This might be due to a statistical anomaly caused by the small number of locations that have a resistivity less than or equal to 5 kohm·cm. The standard deviation in cover depth for the 5 kohm·cm values is 1.32 in, while the standard deviation for the rest of the values averages 0.66 in. These

significantly lower cover depths at very low resistivities could indicate a significant build up of moisture and chlorides in these shallow covers. This result could also indicate that the resistivity is being affected by the near proximity of the reinforcement. Steel is a conductor, and if it is inside the resistivity measurement influence zone, it will lower the resistivity. However, the ER data has consistently shown a high level of association to areas of deterioration, therefore, the effect of steel influencing the resistivity measurement may be limited.

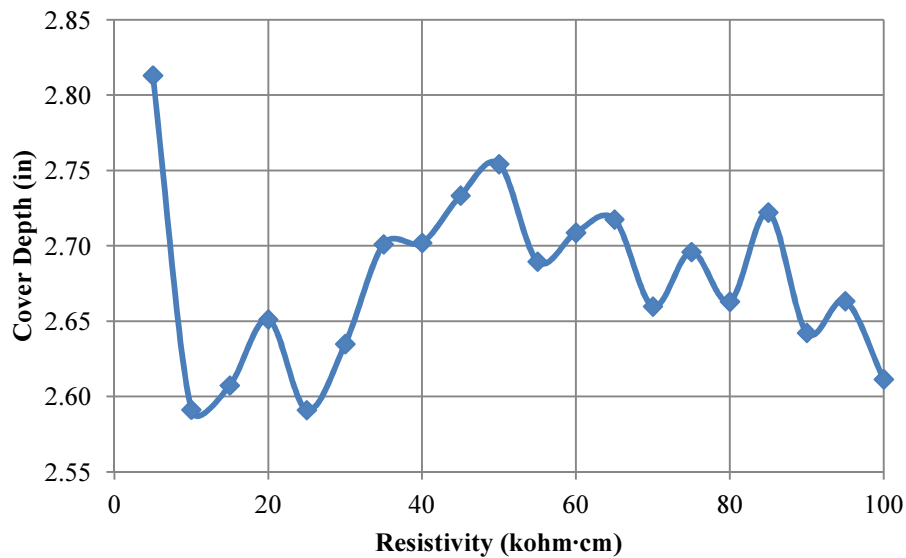


Figure 23: Average cover depth for distribution of resistivity

### *Spatial Comparisons*

The multi-modal NDT data was evaluated to determine how the measurements from each method related spatially. Figure 24 provides the areas of the 2009 Haymarket, Virginia survey which are below 40 kohm-cm for ER and below  $-350$  mV CSE for HCP. It can be seen that the two areas have a strong relationship, 74% of the locations that have a HCP  $\leq -350$  mV CSE have a resistivity  $\leq 40$  kohm-cm. Figure 24 shows that ER and HCP surveys complement each other quite well. Areas identified as a corrosive environment typically have potentials that indicate

active corrosion. This, along with previous research, further demonstrates how well ER and HCP complement each other.

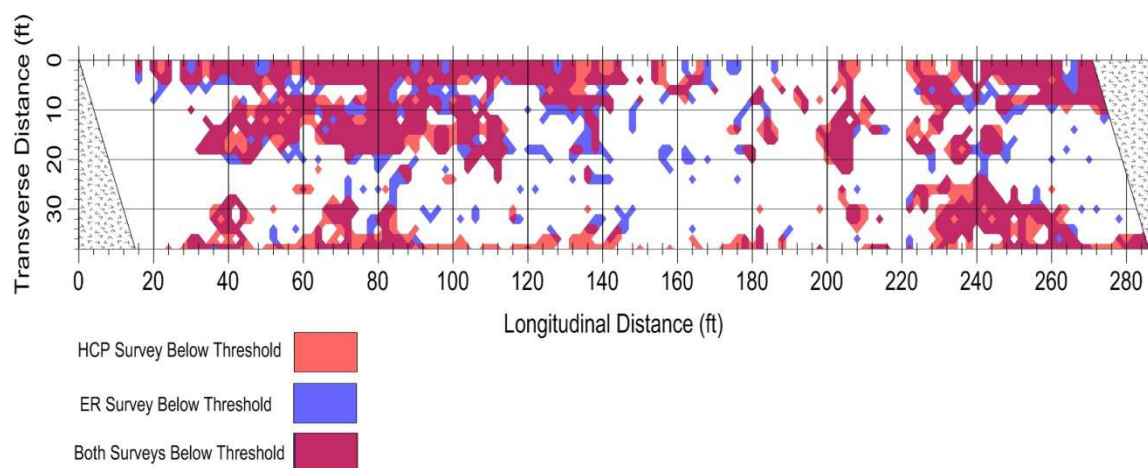


Figure 24: Areas of the 2009 ER and HCP surveys below 40 kohm·cm and -350 mV CSE (Haymarket, Virginia)

To expand on the analysis in Figure 24, an analysis was done to identify the amount of agreement between the various NDT methods on all 12 bridges. Agreement between the methods means that they both agree about some form of deterioration existing at a location and about no forms of deterioration existing at a location. For example, CD and ER would agree if CD=1 and resistivity was  $\leq 40$  kohm·cm, or if CD=0 and resistivity was  $> 40$  kohm·cm. At this initial phase in the research the thresholds for each bridge were assumed to be 40 kohm·cm for ER, -350 mV CSE for HCP,  $IE > 1$ , and CD=1. GPR is a relative measurement; therefore, the threshold values vary for each bridge. Due to the unique thresholds for each bridge, the GPR thresholds were taken from the identification methodology outlined in the Ground Penetrating Radar Threshold Analysis section ahead. The GPR thresholds are: Haymarket, VA -18.5 dB; Sandstone, MN -14.5 dB; Almond, NY -14.5 dB; Upper Freehold, NJ -13.5 dB; Sumner, IA -12.5 dB; and Conestoga, PA -14.5 dB. Table 14 is a matrix of the average deck area that is in agreement between the various methods. It is important to note that since HCP has two threshold values,

–350 mV CSE active and –200 mV CSE passive, that the whole deck area is not identified as deteriorated or un-deteriorated. On average, about 69% of the deck falls above or below the thresholds, while 31% of the deck is uncertain with regard to corrosion activity. As a way to correct for this, Table 15 provides the corrected percentages for the HCP comparison, in which the area above and below the active and passive thresholds is considered 100% of the deck area. Several values in Table 14 are highlighted because they show a high percentage of agreement between two NDT methods. These highly agreeable methods include CD/ ER, CD/GPR, and GPR/ER. When correcting for the amount of HCP area on the deck (Table 15), HCP/ER and HCP/CD also show a high level of spatial agreement. An important finding is that CD and ER both have high levels of agreement with the other NDT methods, excluding IE. ER, which identifies areas of high moisture and chloride concentrations, is highly related to locations of active corrosion (HCP) and decreased dielectric properties (GPR). CD, which identifies severe delaminations, shows similarities to HCP, ER, and GPR due to the nature of chloride-induced corrosion damage. Areas of low resistivity lead to active corrosion, which allows for the formation of corrosion product and eventual formation of delaminations. CD and GPR show strong similarities due to the scattering caused by the severe delaminations and also high concentrations of moisture and chlorides located at the delaminations.

IE shows consistently a low spatial agreement with all the other NDT methods. The lowest being with CD, which should be the highest, since they both identify delaminations. However, IE identifies much earlier stage delaminations; therefore, their complete agreement is not expected.

Table 14: Spatial agreement in condition between all methods, in percentage

	<b>ER</b>	<b>HCP</b>	<b>GPR</b>	<b>IE</b>	<b>CD</b>
<b>ER</b>	100	53.2	<b>64.4</b>	43.9	<b>71.2</b>
<b>HCP</b>	53.2	69	36.3	33.4	44.8
<b>GPR</b>	<b>64.4</b>	36.3	100	44.8	<b>66.0</b>
<b>IE</b>	43.9	33.4	44.8	100	40.4
<b>CD</b>	<b>71.2</b>	44.8	<b>66.0</b>	40.4	100

Table 15: Spatial agreement in condition between all methods, in percentage, HCP scaled to 100%,

	<b>ER</b>	<b>HCP</b>	<b>GPR</b>	<b>IE</b>	<b>CD</b>
<b>ER</b>	100	<b>77.0*</b>	<b>64.4</b>	43.9	<b>71.2</b>
<b>HCP</b>	<b>77.0*</b>	100*	55.7*	51.2*	<b>63.0*</b>
<b>GPR</b>	<b>64.4</b>	55.7*	100	44.8	<b>66.0</b>
<b>IE</b>	43.9	51.2*	44.8	100	40.4
<b>CD</b>	<b>71.2</b>	<b>63.0*</b>	<b>66.0</b>	40.4	100

\* Adjusted HCP percentage

The agreement percentages in Table 14 and Table 15 were established using the same generic thresholds for all of the bridges. An analysis was conducted to compare how those percentages would change when using the individual thresholds established by the threshold identification methodology. Table 16 presents the difference between using the generic thresholds and the individual threshold values for each NDT combination. A positive percentage in Table 16 indicates that the percentage increased when switching to the individual thresholds. Overall, the percentages remained relatively constant, with several of the combinations improving slightly. Only one of the combinations decreased, CD/ER, and then only by 2.0%.

Table 16: Change in percentage of agreement from general threshold to individual thresholds

	<b>ER</b>	<b>HCP</b>	<b>GPR</b>	<b>IE</b>	<b>CD</b>
<b>ER</b>	0	2.7	0.4	0.7	<b>-2.0</b>
<b>HCP</b>	2.7	0	7.4	0.2	3.9
<b>GPR</b>	0.4	7.4	0	0.0	0.0
<b>IE</b>	0.7	0.2	0.0	0	0.0
<b>CD</b>	<b>-2.0</b>	3.9	0.0	0.0	0

### *Comparisons with Time*

The bridge in Haymarket, Virginia was surveyed in September 2009 and again in August 2011. This allows for the unique ability to make data comparisons with time. Figure 25 shows the cumulative frequency distribution of the HCP values when they have been filtered according to

the resistivity measured at the same location. There were three data filters applied to the HCP data to identify its relationship with resistivity. The first two analyses looked to identify the distribution of potentials in 2009 and 2011 when the resistivity was above and below 40 kohm·cm for the same survey. The third analysis identified the distribution of potentials in 2011 based on whether the resistivity was above or below 40 kohm·cm in the 2009 survey. Locations in which the resistivity was below 40 kohm·cm in 2009 had potentials less than  $-350$  mV CSE 90% of the time in 2011, as compared to 75% of the time in 2009. This gives insight into the relationship between corrosive environment and active corrosion. Locations that have a corrosive environment are highly related to locations that become actively corroding in the future. There still remains a strong relationship between ER and HCP surveys conducted in the same year; however, there is an even stronger relationship between current HCP measurements and past ER measurements. Resistivity values that are low, typically  $\leq 40$  kohm·cm, create an environment in concrete that is a clear precursor to active corrosion.

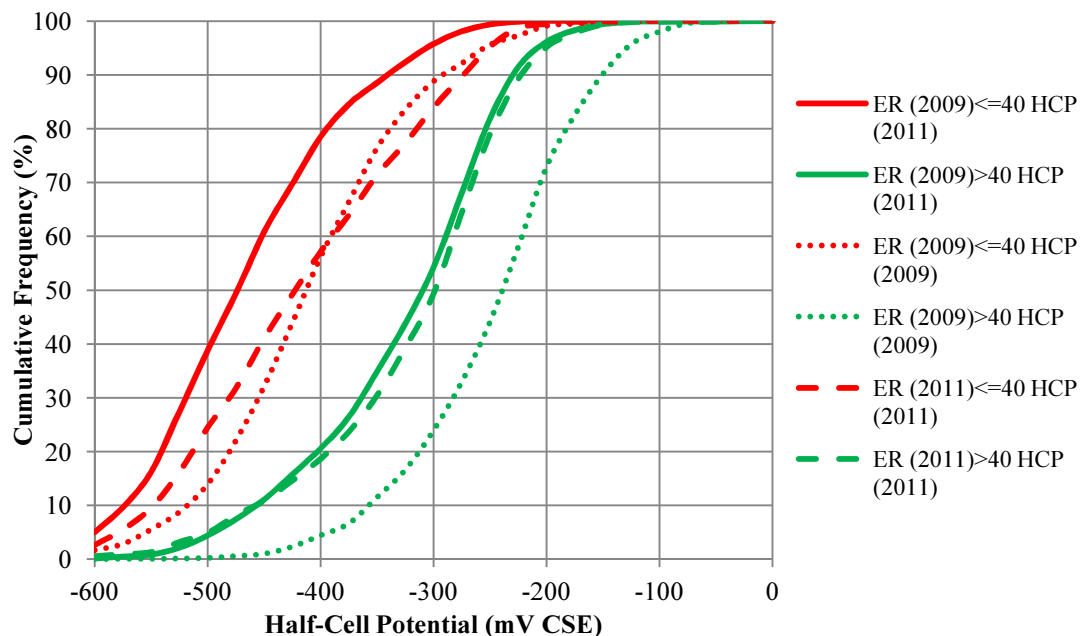


Figure 25: Distribution of half-cell potentials based on electrical resistivity for various years (Haymarket, Virginia)

Between the 2009 and 2011 surveys, the HCP at each location could have done one of six possible things in relation to the HCP thresholds (Table 17). An analysis was conducted using each of these six possibilities to determine if changes in the HCP also correlated to changes in the resistivity. Table 17 provides the average resistivity values in 2009 and 2011 based on the location's HCP and its relationship to the HCP threshold between the two surveys. The threshold values for the bridge in Haymarket, Virginia, HCP active  $-325$  mV CSE and HCP passive  $-250$  mV CSE, were identified using the threshold identification methodology outlined later in this research. Locations that were active in both 2009 and 2011 had the lowest average resistivity values, averaging well below  $40$  kohm·cm in both years. Locations that were shifting into the active region in 2011, transition-active and passive-active, had an average resistivity in 2011 near  $40$  kohm·cm. These results along with previous comparisons between ER and HCP indicate that when the concrete resistivity is near  $40$  kohm·cm, it provides an environment that is conducive to corrosion activity. Locations that were passive had a very high average resistivity, typically above  $80$  kohm·cm, and there were no locations that went from active to passive. Locations that had a HCP in the transition range typically had an average resistivity in the range of  $50$  to  $60$  kohm·cm. This analysis identifies a clear relationship between ER and HCP measurements.

Table 17: Average resistivity based on changing half-cell potential values (Haymarket, Virginia)

Half-Cell Potential		Number of Locations	Average Resistivity (kohm·cm)	
2009	2011		2009	2011
Active	Active	856	<b>32.3</b>	<b>26.5</b>
Active	Transition	212	54.1	40.7
Active	Passive	<b>0</b>	N/A	N/A
Transition	Active	212	67.7	<b>41.1</b>
Transition	Transition	341	68.2	50.4
Transition	Passive	2	99.0	64.5
Passive	Active	66	80.5	<b>43.6</b>
Passive	Transition	939	85.6	61.3
Passive	Passive	76	97.1	88.5

The NDT survey data from each of the 2009 and 2011 surveys were overlaid to provide insight

into the repeatability of each measurement and the progression of deterioration between the two years. Figure 26 provides the area of the bridge deck in Haymarket, Virginia that is  $\leq 40$  kohm·cm in the 2009 and 2011 ER surveys. In 2009, 3,104 ft<sup>2</sup> (29.8%) of the deck was  $\leq 40$  kohm·cm, and in 2011 that area increased to 5,192 ft<sup>2</sup> (49.8%). Of the locations in 2009 that were  $\leq 40$  kohm·cm, 75.8% of those locations were  $\leq 40$  kohm·cm in 2011. Figure 26 shows that there is a high level of repeatability in the ER measurements. Locations that were  $\leq 40$  kohm·cm in 2009 typically were still below 40 kohm·cm in 2011. Along with the repeatability of the measurements, there was also significant growth in the area that was  $\leq 40$  kohm·cm. These growth areas are an expansion from previous areas of corrosive environment. This indicates that future areas of corrosive environment are spatially related to current areas of corrosive environment. This result could be useful in the development of future life prediction models.

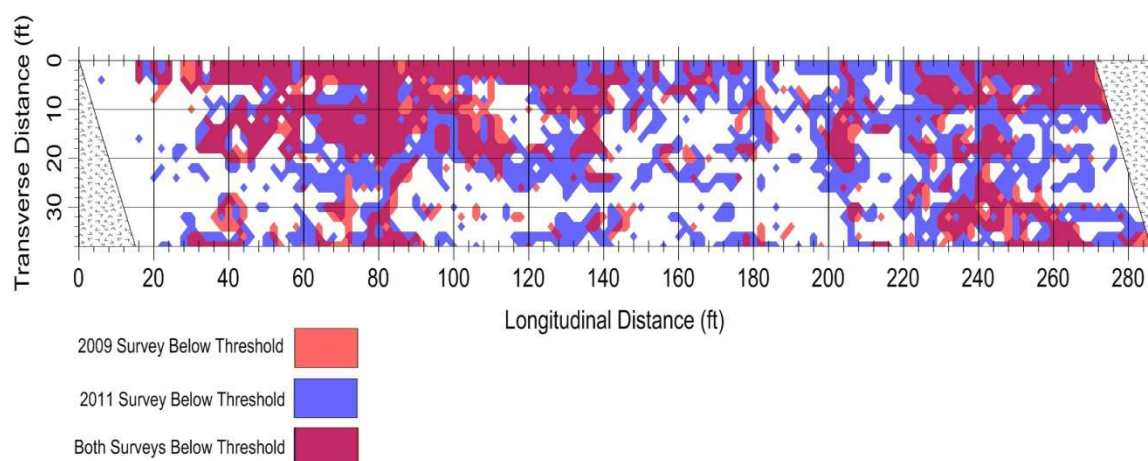


Figure 26: Areas of ER surveys in 2009 and 2011 below 40 kohm·cm (Haymarket, Virginia)

Figure 27 provides the area of the bridge deck in Haymarket, Virginia that is  $\leq -350$  mV CSE in the 2009 and 2011 HCP surveys. In 2009, 3,204 ft<sup>2</sup> (30.7%) of the deck was  $\leq -350$  mV CSE, and in 2011 that area increased to 5,272 ft<sup>2</sup> (50.5%). Of the locations in 2009 that were  $\leq -350$  mV CSE, 96.9% of those locations were  $\leq -350$  mV CSE in 2011. Like the ER measurements, HCP measurements show a high level of repeatability. This provides a high level of confidence

in the HCP measurements from both surveys. The growth of active corrosion from 2009 to 2011 shows a spatial relationship to the areas that were previously actively corroding. This indicates that future locations of corrosion activity could be predicted by knowing the current locations of active corrosion. Like the ER survey, this information could be useful in the calibration of life prediction models.

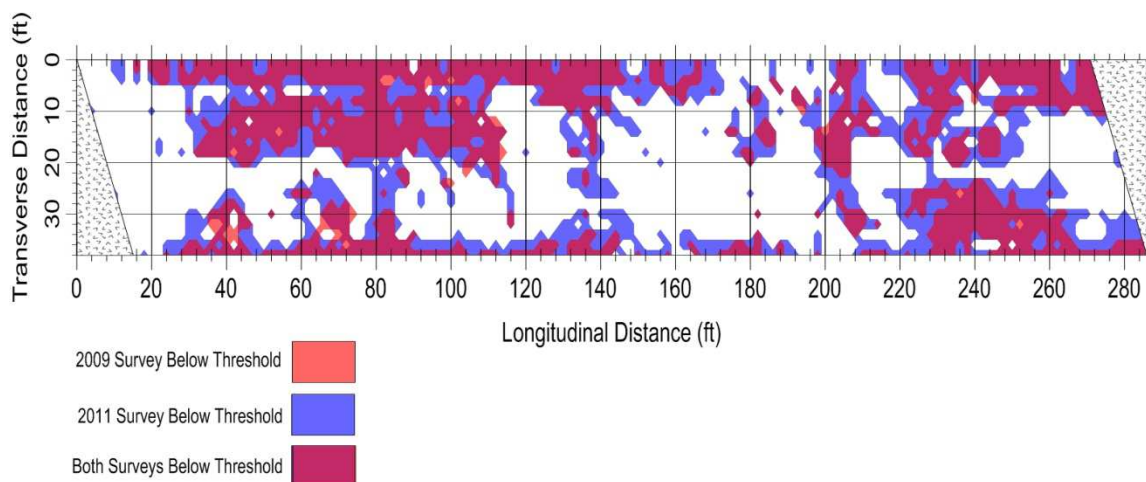


Figure 27: Areas of HCP surveys in 2009 and 2011 below  $-350$  mV CSE (Haymarket, Virginia)

Both the 2009 and 2011 surveys were conducted near the conclusion of summer, a time of the year in which corrosion activity is heightened due to increased temperatures. Corrosion activity and corrosion rate will fluxuate seasonally and if the Haymarket, Virginia Bridge is surveyed in the winter months, the areas of corrosive environment and active corrosion will be different. Understanding the seasonal effects on corrosion are important in the understanding a bridge deck's condition.

Figure 28 provides the area of the bridge deck in Haymarket, Virginia that is  $\leq -20$  dB in the 2009 and 2011 GPR surveys. In 2009,  $1,976 \text{ ft}^2$  (18.9%) of the deck was  $\leq -20$  dB, and in 2011 that area increased to  $3,660 \text{ ft}^2$  (35.1%). Of the locations in 2009 that were  $\leq -20$  dB, 79.9% of those locations were  $\leq -20$  dB in 2011. Like the previous NDT methods, GPR shows excellent

repeatability in the measurements. Areas that were indicated as deteriorated in 2009 were also deteriorated in 2011. There was also excellent spatial relationship between areas of deterioration growth and areas that were previously deteriorated. The results of the damage growth in the ER, HCP, and GPR surveys confirm that deterioration spreads from previously deteriorated regions.

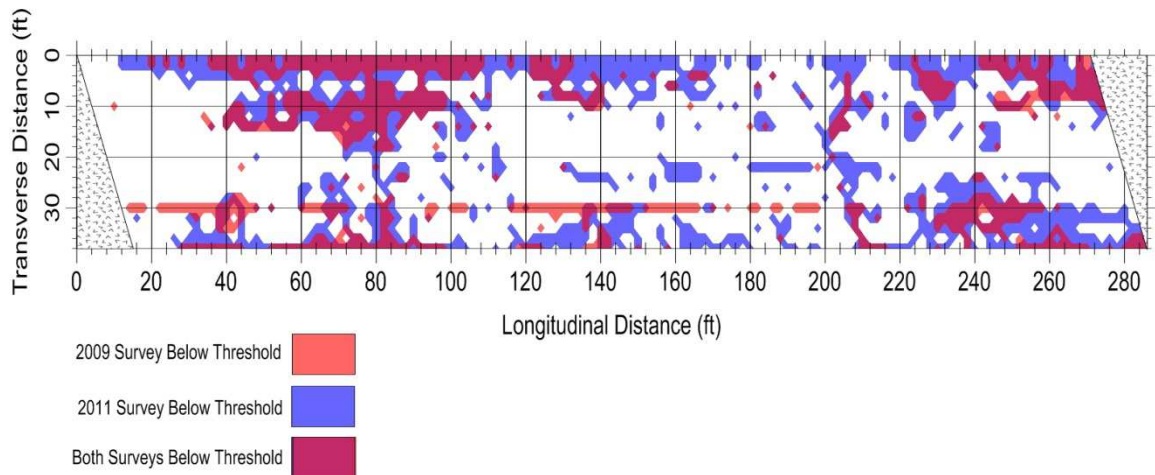


Figure 28: Areas of GPR surveys in 2009 and 2011 below  $-20$  dB (Haymarket, Virginia)

Figure 29 provides the results of the IE surveys conducted in 2009 and 2011 on the bridge in Haymarket, Virginia. Areas indicated as delaminated in this figure had an IE signal rating of 3 or 4. In 2009,  $2,052 \text{ ft}^2$  (19.7%) of the deck was indicated as delaminated. In 2011 that area increased to  $3,672 \text{ ft}^2$  (35.2%). Only 58.1% of the locations that were indicated as delaminated in 2009 were also indicated as delaminated in 2011. The repeatability in the IE data is poor when compared to the other NDT methods. It is also important to note that the placement of the IE probe for each test location between the two surveys is not exact and that this could account for some variation in the repeatability of the data. IE is an in-depth measurement of a delamination/cracking state and on small delaminations a subtle relocation of the probe could change the IE signal rating. For instance, on a small delamination, if the probe is placed at the center, an IE signal rating of 3 could be given. If the probe is placed a few inches away near the edge of the delamination, a signal rating of 2 could be given.

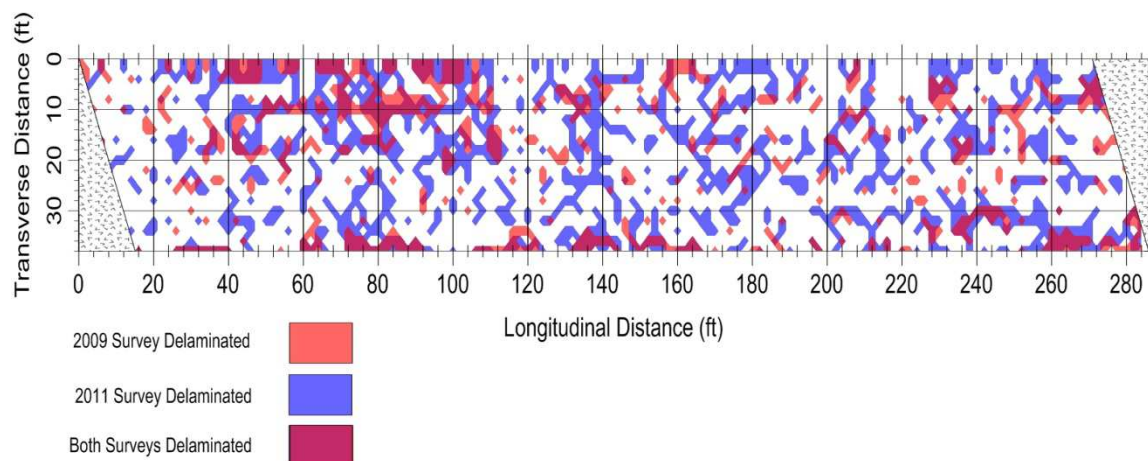


Figure 29: Areas of IE surveys in 2009 and 2011 with a signal rating of 3 or 4 (Haymarket, Virginia)

Figure 30 provides the areas of the bridge in Haymarket, Virginia in which CD identified severe delaminations. In 2009, the area of the deck severely delaminated was 1,972 ft<sup>2</sup> (18.9%), and that area increased to 2,636 ft<sup>2</sup> (25.3%) in 2011. Of the area that was identified as severely delaminated in 2009, 70.2% of that area was indicated as severely delaminated 2011. While 70.2% repeatability in the measurements is good, in reality it could have been much better because there was a slight change in CD data collection methodology between 2009 and 2011. Parsons Brinkerhoff, who collected the CD data, typically does CD to identify repair areas. When identifying areas of delamination for repair, if there are several delaminations near each other, there is no point in delineating each delamination, they are just indicated as one large delamination. However, since this work was for research purposes, in 2011 the methodology was changed and each delamination was carefully delineated. One area in particular in which this is evident in Figure 30 is 20 to 80 ft longitudinally and 0 to 4 ft transversely. That whole area was indicated as delaminated in 2009 and in 2011 smaller subsets of that area were indicated as delaminated. This is because the CD survey was done more precisely in 2011 to identify each delamination and its extent.

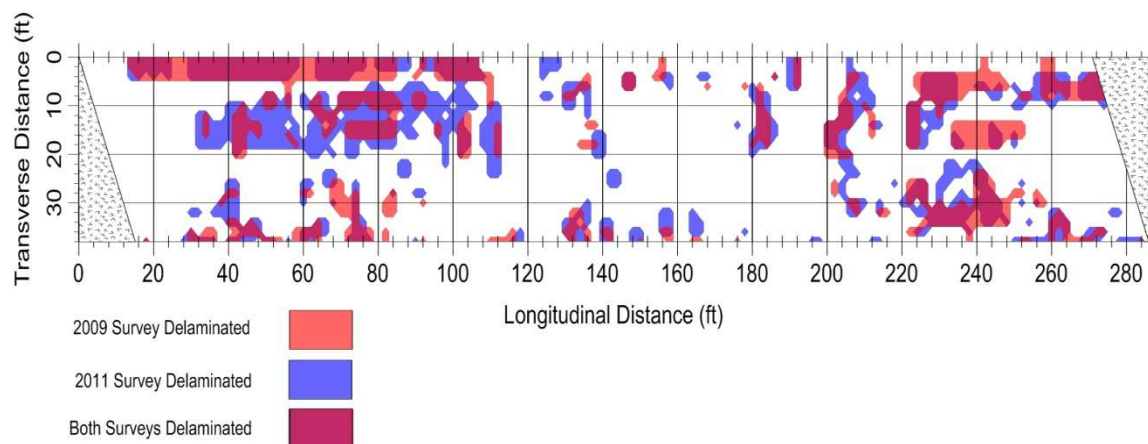


Figure 30: Areas of CD surveys in 2009 and 2011 with a severe delamination (Haymarket, Virginia)

An analysis was conducted to evaluate if the future condition of a test location is related to the current condition of surrounding test locations. The condition of each test location on the bridge in Haymarket, Virginia in 2009 was determined using the established condition states 0 through 4 (Table 3). Then, for each test location, the conditions of the locations immediately adjacent to that location were averaged. The averaged condition rating of the surrounding locations in 2009 was then compared to the test location's condition in 2011 (Figure 31). Figure 31 indicates that 90% of the locations in 2011 that had a condition of 0 had surrounding locations with a 2009 average condition less than 1.5. As the average condition of surrounding points increased in 2009, the condition of the central point in 2011 also increased. However, this is not the case for ratings 2 and 3, which seem to be in reverse order. The reason behind this might be due to the fact that condition rating 3 is based on the IE signal ratings 2 and 3. These ratings have shown consistently poor correlation with the other methods. The surrounding point of a location with a condition rating of 4, severe delamination, in 2011 had the highest average condition in 2009. The condition immediately surrounding a location has a clear influence on that location's future condition. Concrete degradation spreads; as a location deteriorates, that deterioration spreads to the surrounding locations.

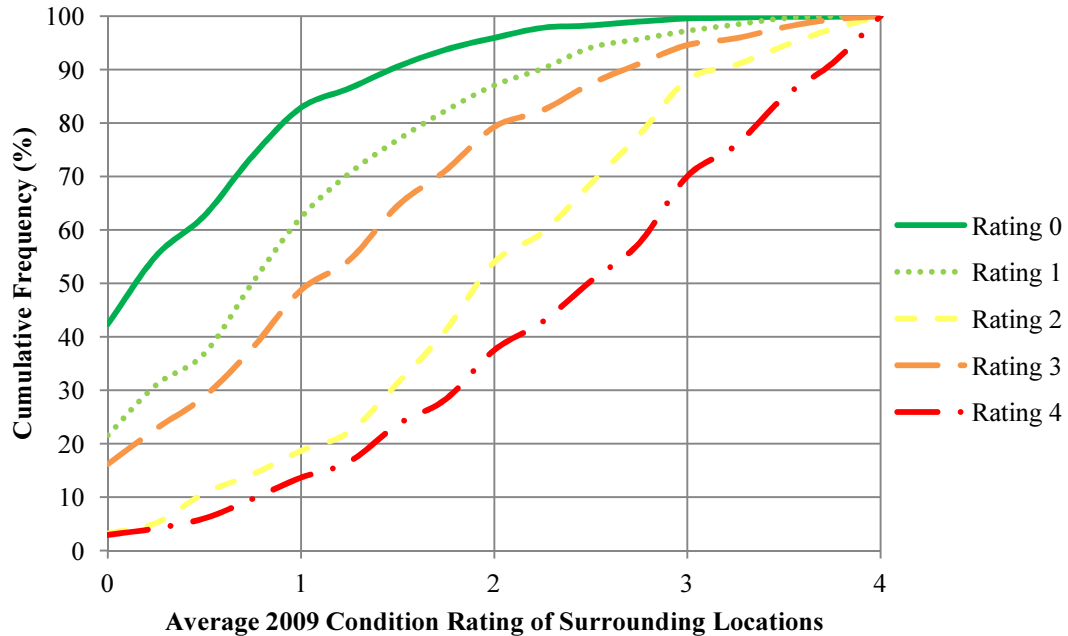


Figure 31: Influence of surrounding location's 2009 condition on the central test location's 2011 condition (Haymarket, Virginia)

### THRESHOLD ANALYSIS

Determination of the threshold values for ER, HCP, and GPR is an imperative step in the development of a damaged-based condition assessment program. The following sections describe the three threshold identification methods, their development, and the resulting analysis.

Appendix 2 – MATLAB Code for Multi-Modal Condition Assessment provides the source code for the automated condition assessment program, which includes the code for each NDT method's threshold identification.

The bridge in Haymarket, Virginia was the first bridge to be surveyed and was the primary data set used in the development of the threshold methodology. The rest of the structures in Table 2 were used to make the necessary adjustments to the threshold methods and to verify the applicability of the threshold methods to all of the structures. Note that all of the figures in sections Half-Cell Potential Threshold Analysis, Electrical Resistivity Threshold Analysis, and

Ground Penetrating Radar Threshold Analysis are from the bridge in Haymarket, Virginia. This is intended to provide a consistent presentation of the methodology throughout these sections. Selected figures from the analysis conducted on the other structures will be provided in the section, Application on Other Structures, along with the determined threshold values for each bridge in this study.

#### *Half-Cell Potential Threshold Analysis*

The fundamental principal of the HCP threshold identification is that when the resistivity of the concrete is very low, the probability that corrosion is active at that location is high. Similarly, when the resistivity is very high, the probability that corrosion is passive at that location is also high. Thereby, the HCP thresholds can be identified by looking at the potential distributions when the resistivity indicates a highly corrosive and highly non-corrosive environment. A location with a resistivity value  $\leq 30 \text{ kohm}\cdot\text{cm}$  typically provides an environment that is very favorable for corrosion activity. Analysis of the HCP values when the resistivity is  $\leq 30 \text{ kohm}\cdot\text{cm}$  provides insight into the potentials that occur when the probability of active corrosion is high. When the resistivity is  $\geq 70 \text{ kohm}\cdot\text{cm}$ , the probability that the steel is passive at these locations is quite high. Analysis of the potential distribution for these locations can provide insight into what potential values occur during a passive state.

The HCP threshold analysis begins by filtering the HCP data according to the resistivity value measured at the same location. The data is filtered according to low and high ER values in 5- $\text{kohm}\cdot\text{cm}$  increments. The low resistivity filtering identifies the distribution of potentials that have a resistivity less than or equal to each increment of 5, 10, 15 ... 30  $\text{kohm}\cdot\text{cm}$ . In the filtering, if a test location has a potential of  $-380 \text{ mV CSE}$  and a resistivity of 5  $\text{kohm}\cdot\text{cm}$ , this HCP measurement would be included in each low resistivity increment. A location with measurements of  $-410 \text{ mV CSE}$  and 12  $\text{kohm}\cdot\text{cm}$  would only be included in the increments 15 through 30  $\text{kohm}\cdot\text{cm}$ . The same procedure is used to filter the potentials at locations with a high

resistivity. The passive ER filtering identifies the distribution of the potentials that have a resistivity greater than or equal to each increment: 70, 75, 80... 95 kohm·cm. Figure 32 provides the cumulative frequency distribution of the HCP data filtered according to the measured ER. An interesting feature of Figure 32 is that each of the active and passive curves follows very similar trends. There is also significant spacing between the passive and active curves. Part of the reason the spacing is created is in how the data is filtered. The corrosive environment curves use a less than or equal filter, while the non-corrosive environment curves use a greater than or equal filter. This makes it so that the curves are representing two different ends of the data spectrum. There is clearly a very different distribution of potentials in a corrosive versus a non-corrosive environment.

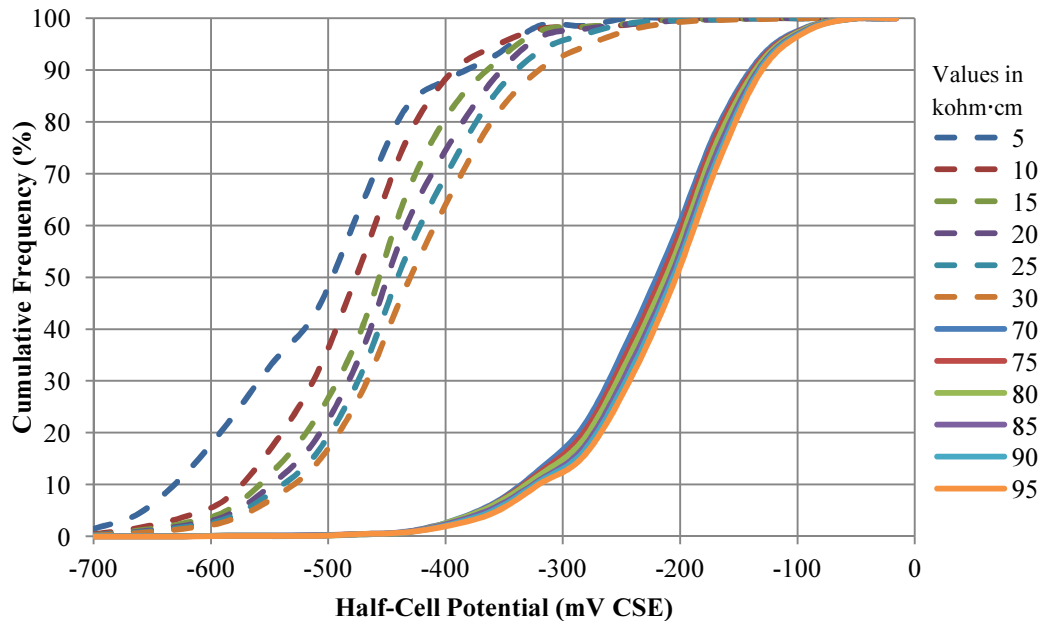


Figure 32: Cumulative frequency distribution of HCP data filtered according to resistivity (Haymarket, Virginia)

As a way to identify at which point in the potential distribution a transition from an active to passive condition occurs, the slope of the cumulative frequency curves is evaluated. The derivative of each curve is evaluated using the numerical method of centered finite-difference

(Equation (4)). Figure 33 depicts the derivative of each cumulative frequency curve provided in Figure 32. The location of the active threshold is the location at which the derivatives of the active and passive curves intersect. The potential at this intersection indicates a potential at which its occurrence in a corrosive environment is decreasing and its occurrence in a non-corrosive environment is increasing. There are six curves for both the active and passive filtering and every intersection is found between all of the active and passive curves, which results in 36 intersections. The potentials that occur at these 36 intersections are averaged and rounded to the nearest multiple of 25 mV CSE to determine the active threshold potential. The data presented in Figure 33 results in an active threshold of  $-325$  mV CSE.

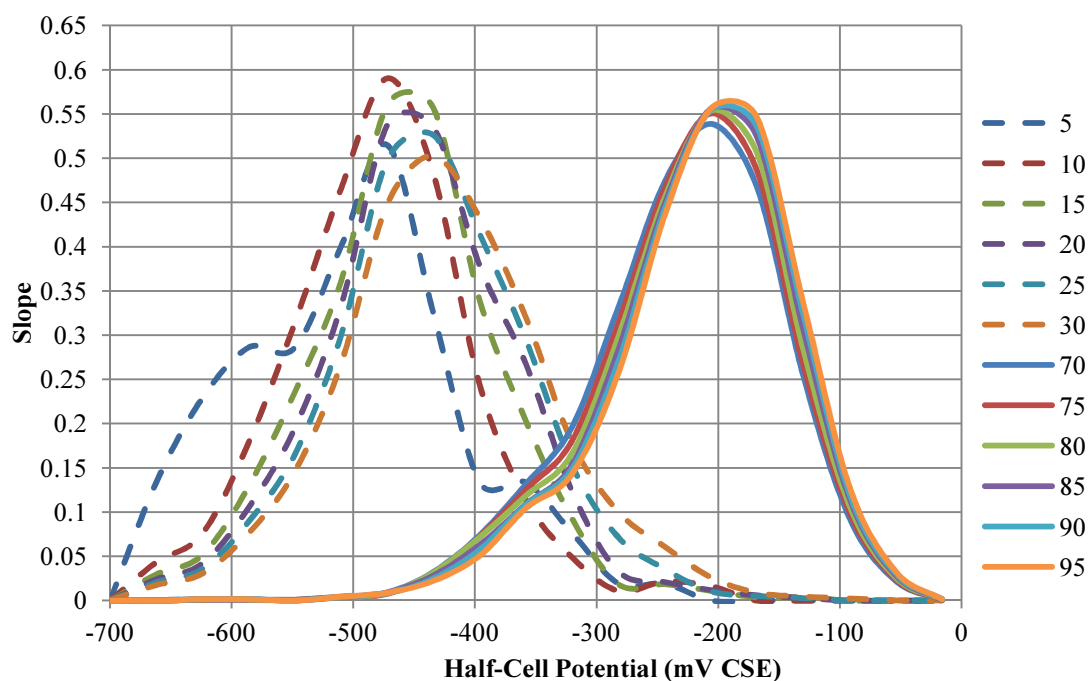


Figure 33: Slope of the cumulative frequency distribution of filtered HCP data (Haymarket, Virginia)

To identify the passive threshold, the objective is to identify potentials that occur in the non-corrosive environment, but no longer occur in a corrosive environment. The potential where the slopes of the active curves in Figure 33 start to approach zero indicates the potentials that

effectively don't occur in a corrosive environment. Therefore, the passive threshold is the potential at which the slope of the active cumulative frequency curve falls below 0.025. Potentials greater than the potential at that slope practically don't occur when the resistivity indicates a corrosive environment. The value of 0.025 was selected by reviewing how the active curves for each structure approached a zero slope. Empirically, 0.025 provided on average the best results for the bridges in this study. There are six active curves, so the potential at which the slope falls below 0.025 is determined for each of these curves. Then the six potentials are averaged and rounded to the nearest integer of 25 mV CSE to identify the passive threshold. The data presented in Figure 33 results in a passive threshold of -250 mV CSE.

$$f'(x_i) = \frac{f(x_{i+1}) - f(x_{i-1}))}{2h} \quad (4)$$

$f'(x_i)$  – Slope of  $i^{\text{th}}$  term

$f(x_{i+1})$  – Value of  $i+1$  term

$f(x_{i-1})$  – Value of  $i-1$  term

$h$  – Increment between  $i$  and  $i+1$  term

There are several checks in the HCP threshold identification to make sure that the proper thresholds are determined. When filtering the HCP data based on ER, the program checks to make sure that there are ER values  $\leq 30$  kohm·cm. Bridges which are in excellent condition may not have any locations with a corrosive environment. If that is the case, then the HCP threshold values are assigned the ASTM C876-09 (ASTM 2009) threshold values of -350 mV CSE active and -200 mV CSE passive. Another check in the methodology occurs because on some bridges, as will be shown in the section Application on Other Structures, there are some early inconsequential intersections of the slope curves. To remove these intersections from the active threshold identification, the program doesn't start looking for intersections along the curves until the slope has risen above 0.05 when moving from left to right along the active curves. In

addition, the program also only uses one intersection point between each active and passive curve in the threshold calculation. The program identifies every intersection of each curve, but if there are multiple intersections between two individual curves, then the program will select only one intersection. The program will select the intersection that is the closest to the average of all the intersections. There is also a check to make sure that the passive threshold is not abnormally high. If the passive threshold is greater than  $-100$  mV CSE, the program will rerun the passive threshold analysis using a slope of 0.05 as the limit.

#### *Electrical Resistivity Threshold Analysis*

After the HCP active and passive thresholds have been identified, the next step is to identify the ER threshold. The ER threshold indicates the resistivity below which the concrete provides an environment that is conducive to corrosion activity. The first step in ER threshold identification is to filter the ER data by the potential measured at the same location. The ER data is broken into two groups: locations with a potential that indicate active corrosion and locations that indicate passive reinforcement. The active and passive filtering is done according to the HCP thresholds that were defined by the HCP threshold methodology. Using the filtered ER data, a cumulative frequency curve is created for both the active and passive filtered data (Figure 34). The cumulative frequency calculation uses bin increments of  $5$  kohm·cm. Figure 34 depicts a strong difference in the distribution of resistivity measurements when filtered according to potentials that indicate active versus passive corrosion. It is of interest to compare Figure 34 with Figure 14, a plot of the cumulative frequency distribution of ER data based on HCP data for all of the bridges in this study. Both figures provide very similar results, which indicate the strong relationship between ER and HCP. It is also important to note the concavity of each curve. The active curve is concave down, while the passive curve is concave up. This means that for the active curve, as resistivity increases, the instances of active corrosion decrease and for the passive curve, as the resistivity increases, the instances of passive steel also increase.

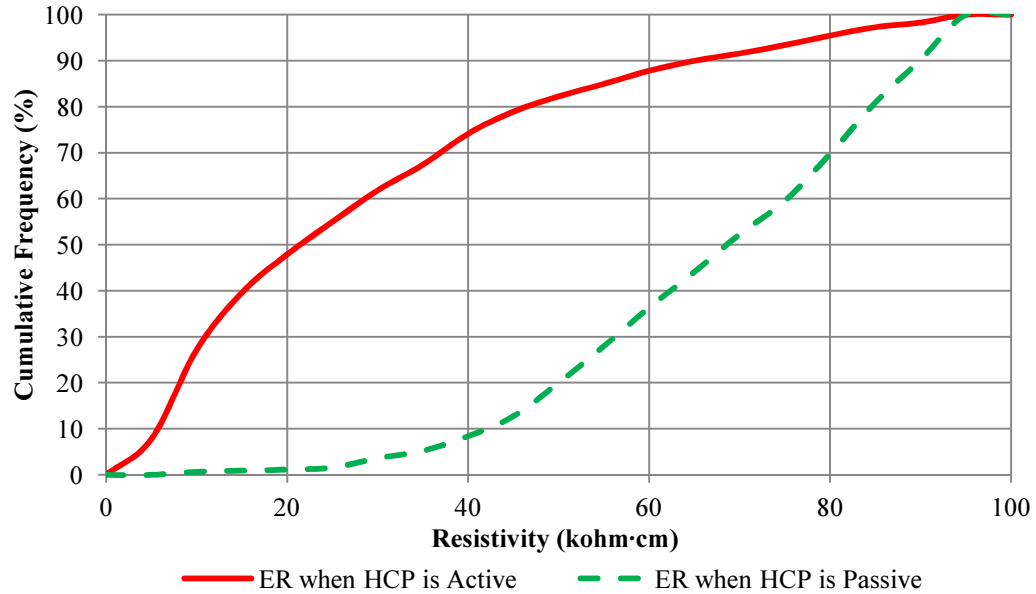


Figure 34: Cumulative frequency distribution of ER data filtered according to HCP data (Haymarket, Virginia)

The ER data collected for this research were primarily collected using an ER probe that can only measure up to 99 kohm-cm. If the concrete resistivity is above 99 kohm-cm, the probe indicates the concrete resistivity is 99 kohm-cm. This upper limit causes an abnormal jump in the data, since there is an abrupt increase in frequency due to the device's upper limit. This abrupt frequency increase does not allow for proper comparison between the potential and resistivity values when the resistivity is greater than 99 kohm-cm. The data that has an ER of 99 kohm-cm was trimmed for the ER threshold analysis in order to maintain a smooth curve.

Once the data has been filtered and the cumulative frequency calculated, the ER threshold is identified by evaluating the difference between the active and passive cumulative frequency curves (delta). The two curves have opposite concavity; therefore, the point at which the active curve levels off and the passive curve starts to increase is the threshold value. This identifies the resistivity value at which its occurrence at locations with active corrosion has started to become insignificant and its occurrence with a passive state starts to become significant. The ER

threshold is the resistivity at which delta is maximum. Figure 35 is a plot of delta, the difference between the active and passive cumulative frequency percent curves, for the bridge in Haymarket, Virginia. For this structure the ER threshold is identified as 45 kohm·cm. The curves don't always come out as smooth and symmetrical as Figure 35; therefore, the three highest delta values are selected and the corresponding resistivity values are averaged to the nearest whole number to determine the ER threshold.

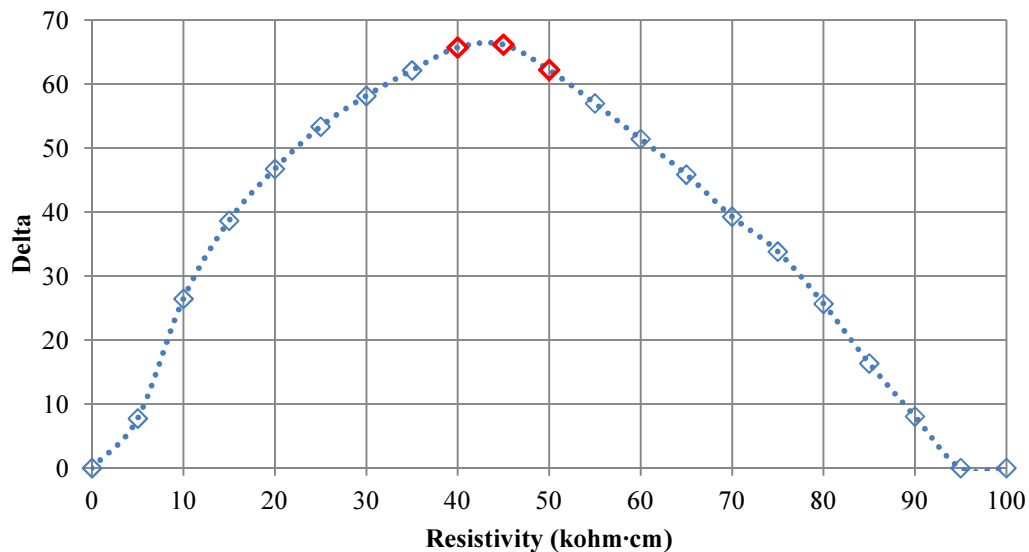


Figure 35: Delta curve of filtered ER cumulative frequency data (Haymarket, Virginia)

#### *Ground Penetrating Radar Threshold Analysis*

Threshold identification for the GPR data utilizes comparisons made between the GPR data and the ER, HCP, and CD data. GPR is a versatile NDT tool, in that it is capable of identifying several different types of reinforced concrete deterioration through signal analysis and identification of highly attenuated GPR waves. GPR amplitudes are affected by moisture, free ions, presence of corrosion product, and signal scattering due to significant cracking and delaminations. ER, HCP, and CD, which also detect some of the same factors, will indicate areas of deterioration that are similar to the areas of GPR attenuation. Using these similarities, the GPR

threshold can be identified by comparing the amplitude distribution in areas identified as distressed and un-distressed in ER, HCP, and CD surveys.

The GPR threshold identification involves three data comparisons to identify what GPR amplitudes occur at locations of deterioration and sound concrete. The three comparisons are: ER and HCP, ER and CD, and ER, HCP, and CD. These three filtering methods were selected for several reasons.

- ER, HCP, and CD show strong statistical correlation with GPR for areas of deterioration and non-deterioration,
- These combinations show the strongest variation in distribution of GPR data when compared to distressed and non-distressed areas,
- These filters show the strongest variation from the distribution of the unfiltered GPR data for each bridge, and
- These filters are consistently effective for all 12 bridges.

For each filtering combination, the distribution of GPR amplitudes is determined when the filtering measurements are above and below their respective threshold values. For CD, below or above the threshold would mean either there is or isn't a severe delamination present. For example, the ER and HCP comparison identifies the GPR amplitude distribution at locations where the potential and resistivity are both below and both above their respective threshold values. For simplicity, during the GPR threshold identification discussion when the measurements are below their thresholds this will be indicated as "deteriorated" and above their respective thresholds will be indicated as "sound." Using a cumulative frequency plot, the GPR amplitude distributions for each of the three analysis combinations are presented in Figure 36, Figure 37, and Figure 38. In these figures the cumulative frequency distribution of the complete unfiltered GPR data for the Haymarket, Virginia Bridge was added to provide a sense of scale.

Depicting the complete unfiltered GPR data curve provides an indication as to how much the distribution of the GPR amplitudes varies for deteriorated and sound states.

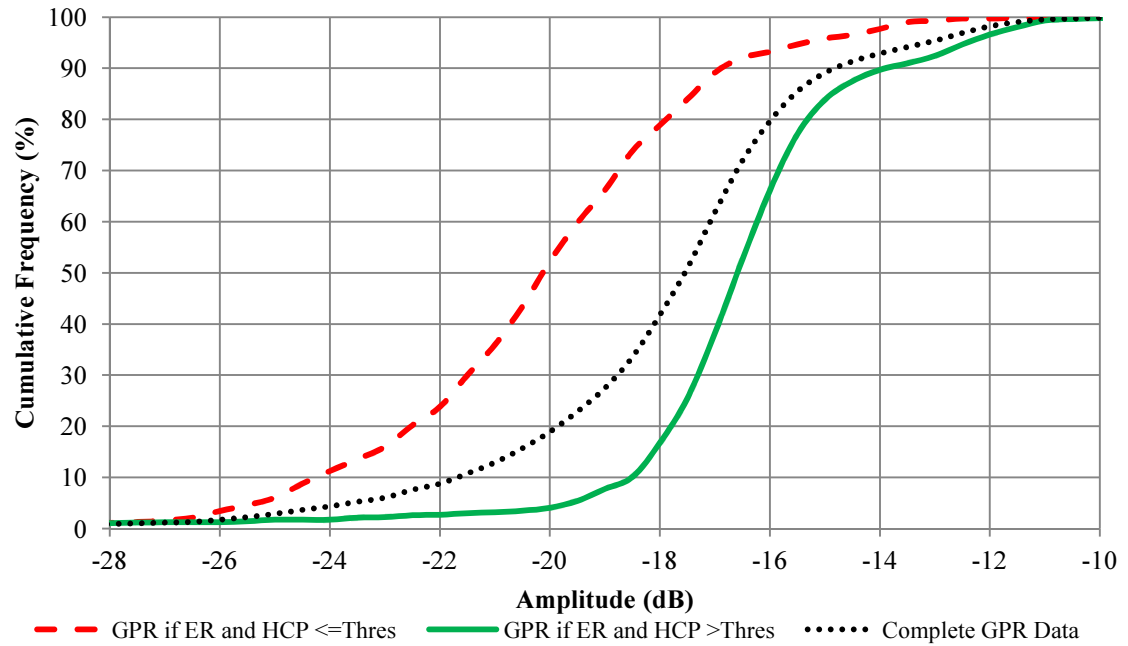


Figure 36: Cumulative frequency distribution of GPR amplitude filtered by ER and HCP data (Haymarket, Virginia)

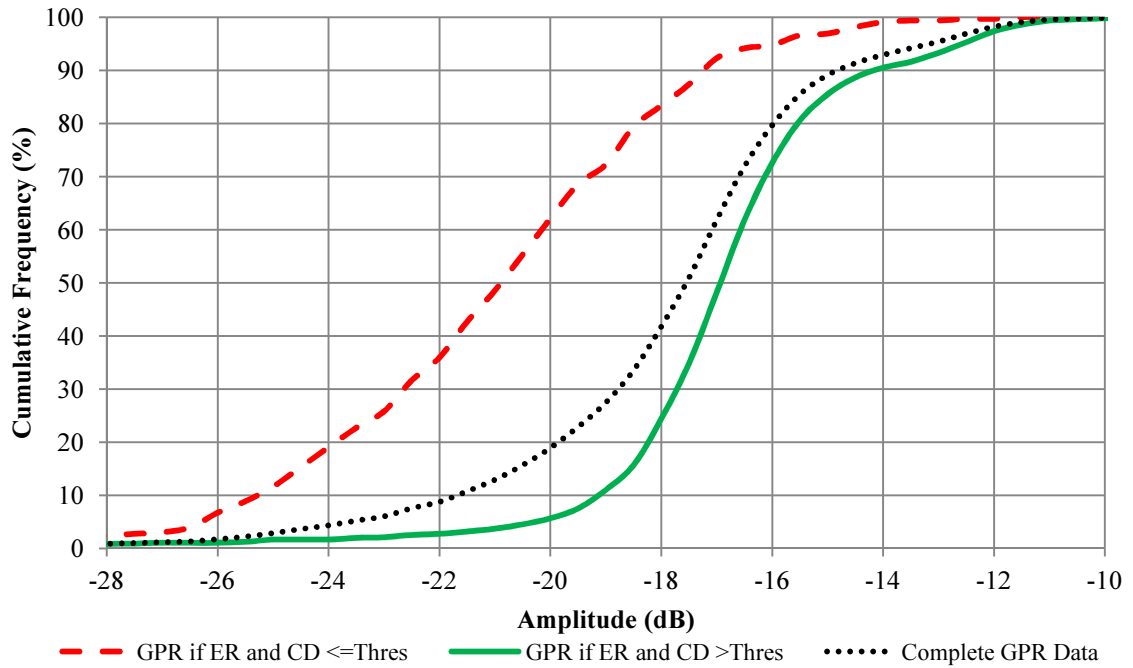


Figure 37: Cumulative frequency distribution of GPR amplitude filtered by ER and CD data (Haymarket, Virginia)

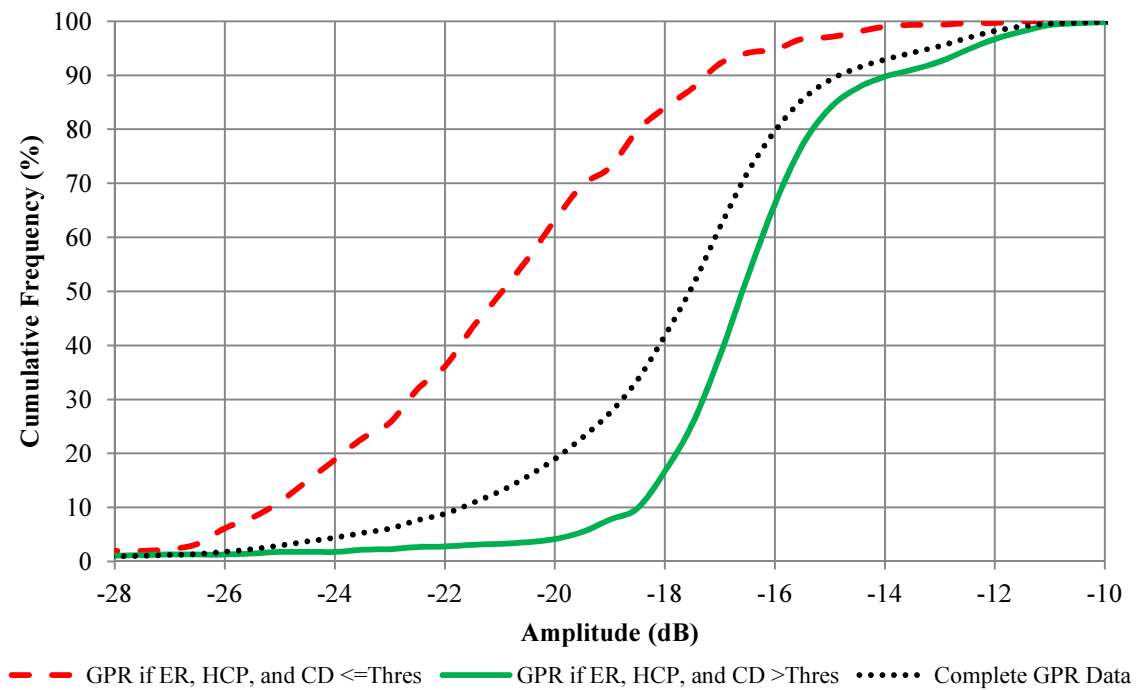


Figure 38: Cumulative frequency distribution of GPR amplitude filtered by ER, HCP, and CD data (Haymarket, Virginia)

Once the amplitudes have been filtered and cumulative frequency curves developed, the difference between the deteriorated and sound curves is calculated (delta). The maximum delta value indicates the amplitude at which its occurrence with deterioration is becoming insignificant and its occurrence with a sound condition is becoming significant. For each filtering method, the amplitudes of the three maximum delta values are averaged. The three average amplitude values from the three filtering methods are then averaged together to identify the GPR threshold, as rounded to the nearest 0.5 dB. Figure 39 provides the three delta curves for the GPR threshold analysis performed on the bridge in Haymarket, Virginia. The ER and HCP filtering yielded a value of  $-18.5$  dB, ER and CD filtering resulted in  $-19$  dB, and  $-18.5$  dB for the ER, HCP, and CD comparison. Averaging the three filtering results provides a GPR threshold amplitude of  $-18.5$  dB.

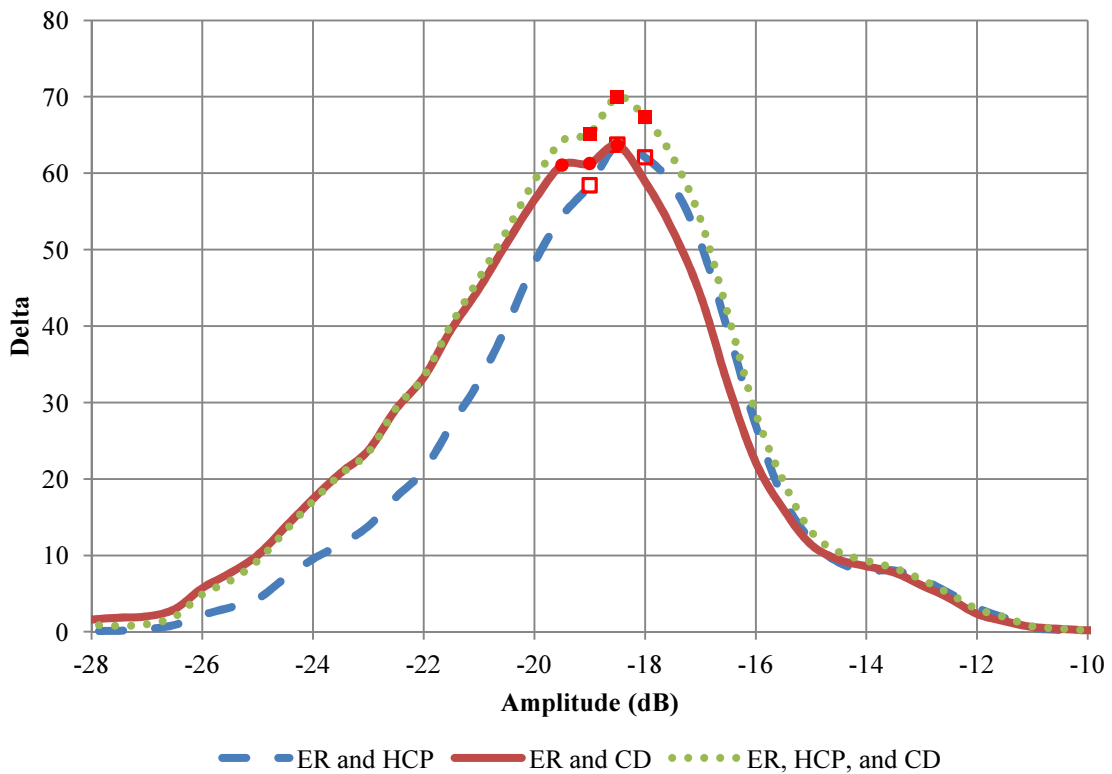


Figure 39: GPR threshold analysis delta curves (Haymarket, Virginia)

Some bridge decks do not have instances in which there is a severe delamination, active corrosion, and corrosive environment at the same location. This occurs on bridges that are in relatively good condition. If a structure does not have deteriorated and sound locations in one of the ER/HCP, ER/CD, or ER/HCP/CD filters, then that filter will be removed from the threshold analysis for that bridge. If the bridge is in such a condition that none of the filters have deteriorated and sound locations, then the threshold will be defined by the average GPR amplitude. Typically this will occur when a bridge is in very good condition and in which instances of severe delamination are limited or nonexistent. The reason that the average GPR amplitude is reserved as a fail-safe threshold identification method is that the calculated threshold values identified for the rest of the bridges are very similar to their average GPR (Table 18). They are typically within 0.5 dB of the average amplitude on that structure. Therefore, in situations when the other analysis methods are not applicable, the average GPR amplitude will be an initial threshold value.

Table 18: Comparison of GPR threshold values with average GPR amplitude

<b>Carries</b>	<b>Location</b>	<b>GPR Threshold (dB)</b>	<b>Average GPR Amplitude (dB)</b>
I-195 East	Upper Freehold Township, NJ	-13.5	-13.9
Pequea Boulevard	Conestoga, PA	-14.5	-14.5
State Route 123	Sandstone, MN	-14.5	-14.1
State Route 15	Haymarket, VA	-18.5	-18.0
State Route 21	Almond, NY	-14.5	-13.7
State Route 93	Sumner, IA	-12.5	-12.7

#### *Application on Other Structures*

The following section provides a sampling from the threshold analyses conducted on the other 11 bridges involved in this research. The objective of this section is to show how the data from the

other bridges was similar to and different from the bridge in Haymarket, Virginia, and how the threshold identification methodology was refined by using the 11 other data sets. Table 19 provides an overview of the threshold values identified using the developed threshold methodologies for the bridges in this study. The methods developed are robust statistical methods that work on a variety of structures. However, there still remains extensive work to validate the developed threshold methods by performing cores and autopsies to verify the accuracy of the identified thresholds. In Table 19, some of the structures do not have a GPR threshold because the GPR data for these structures were not available.

Table 19: Threshold analysis results

<b>Carries</b>	<b>Location</b>	<b>ER Threshold (kohm·cm)</b>	<b>HCP Active Threshold (mV CSE)</b>	<b>HCP Passive Threshold (mV CSE)</b>	<b>GPR Threshold (dB)</b>
I-495 South	Wilmington, DE	53	-350	-200	N/A
Interstate 195	Upper Freehold Township, NJ	35	-350	-200	-13.5
Pequea Boulevard	Conestoga, PA	30	-425	-300	-14.5
School House Road	Middletown, PA	40	-350	-200	N/A
State Route 123	Sandstone, MN	45	-400	-200	-14.5
State Route 15	Haymarket, VA	45	-325	-250	-18.5
State Route 18	Neptune, NJ	45	-275	-175	N/A
State Route 21	Almond, NY	42	-325	-250	-14.5
State Route 273	Elkton, MD	35	-350	-250	N/A
State Route 47	Deptford Township, NJ	47	-350	-200	N/A
State Route 93	Sumner, IA	35	-450	-375	-12.5
West Bangs Ave	Neptune, NJ	45	-250	-150	N/A

N/A – Data not available

Figure 40 is the slope of the filtered HCP data for the bridge in Sandstone, Minnesota. These data illustrate the importance of using several resistivity filter values and taking an average of the intersection points. The 5 kohm·cm filter has a significantly different intersection point with the passive curves than do the other active curves. This happens when the bridge is in a relatively good condition, meaning that there are very few locations of corrosive environment, resulting in very few resistivity measurements below 30 kohm·cm. This makes the cumulative distribution analysis dependent on fewer values, in turn making changes in slope more drastic.

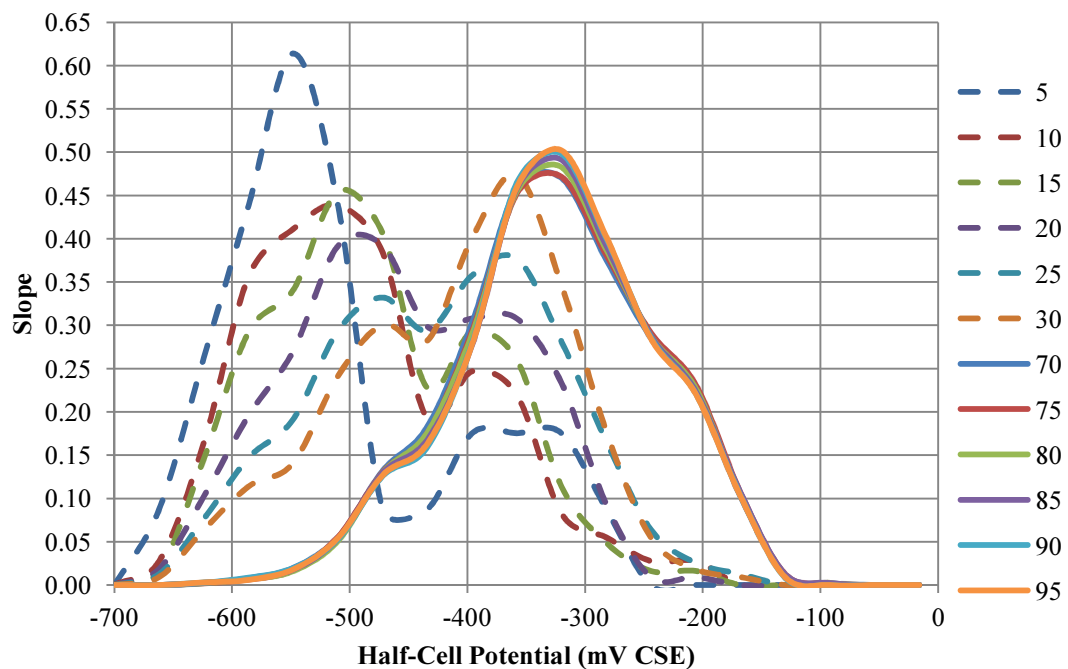


Figure 40: Slope of the cumulative frequency distribution of filtered HCP data (Sandstone, Minnesota)

Figure 41 depicts the slope of the filtered data for the HCP threshold analysis on the bridge in Elkton, Maryland. This data set provides tight curves for both passive and active data; however, the passive curves rise ever so slightly before the active curves causing an intersection with the active curves near  $-600$  mV CSE. Clearly, these intersections are inconsequential to the threshold and should not be included in the threshold identification. That is the reason the

program only starts to look for intersections after the slope has risen past a value of 0.05, and that only one intersection between each curve is selected.

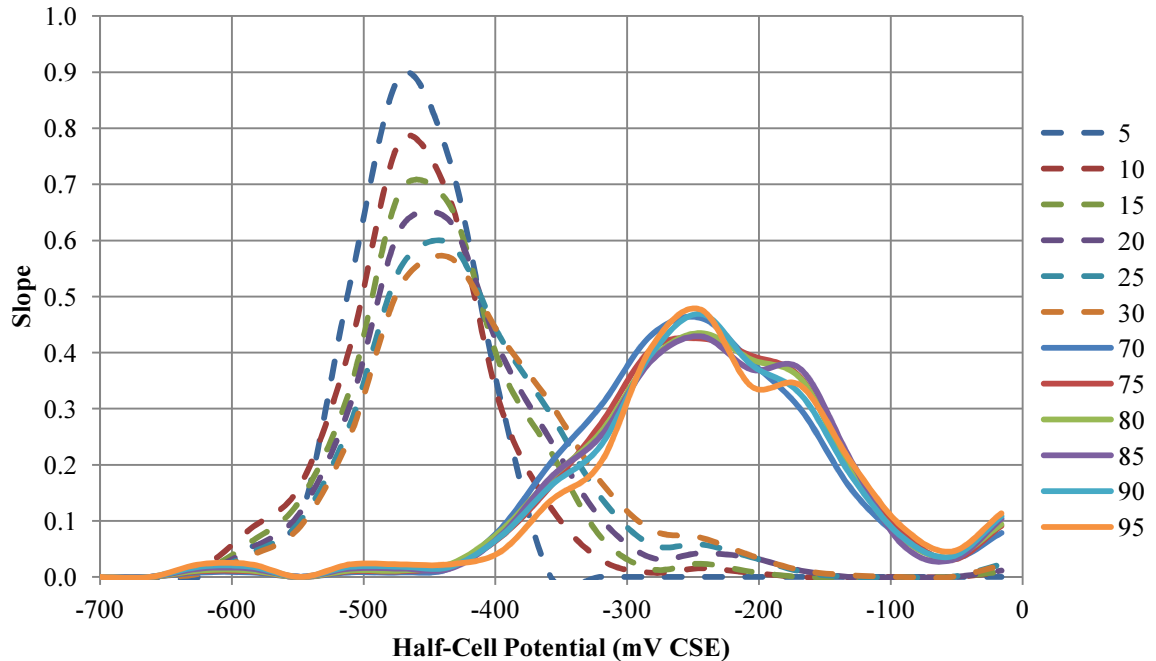


Figure 41: Slope of the cumulative frequency distribution of HCP data filtered according to resistivity (Elkton, Maryland)

Figure 42 provides an example of why it is important to take the three maximum delta values when performing the ER threshold analysis. The difference between the distributions of resistivity for active and passive potential filtering is relatively small for the bridge in Almond, New York. Therefore, in order to make sure the proper peak is picked and that one point is not overly affecting the results, an average resistivity is calculated from the three highest delta values. The three delta values are indicated in Figure 42 by the diamond markers. For this structure, the threshold is 42 kohm·cm, which is very close to the resistivity at the absolute maximum delta value of 40 kohm·cm.

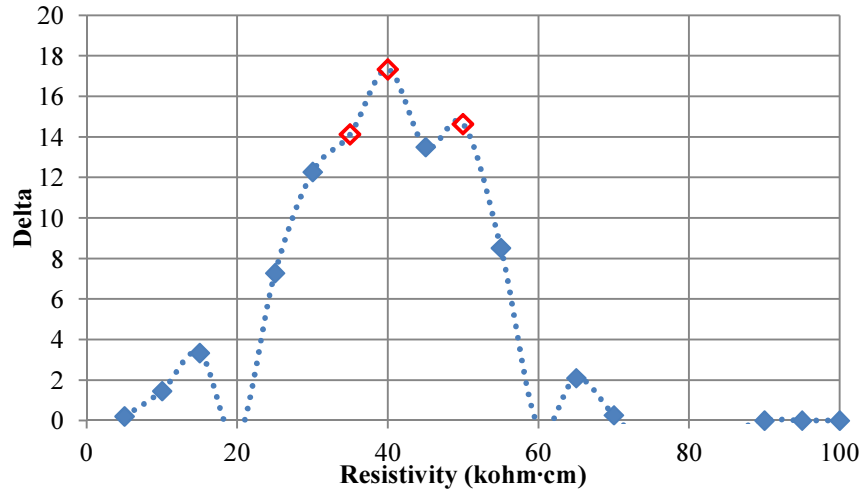


Figure 42: Delta curve of filtered ER cumulative frequency data (Almond, New York)

Figure 43 presents the delta plot for the GPR analysis of the bridge in Sandstone, Minnesota. This structure depicts the importance of using all three filtering methods, ER/HCP, ER/CD, and ER/HCP/CD. There is much more variation between the three filtering methods for this bridge than compared to the other bridges. By averaging the results of the three filtering methods, a more accurate GPR threshold is identified; making sure that one filtering method is not disproportionately affecting the results.

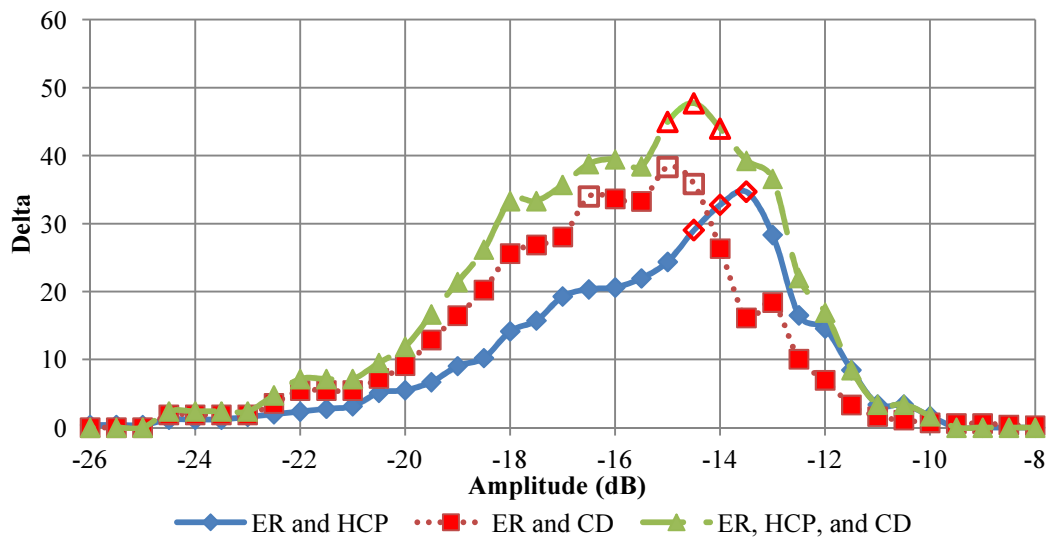


Figure 43: GPR threshold analysis delta curves (Sandstone, Minnesota)

The bridge in Upper Freehold, New Jersey has a limited amount of severe delaminations identified by CD. Due to the limited amount of severe delaminations, the ER/CD and ER/HCP/CD filters in the GPR threshold analysis do not provide any information (Figure 44). Therefore, the GPR threshold for the bridge in Upper Freehold, New Jersey is based only on the analysis of GPR amplitudes according to the ER/HCP filtering. This structure identifies the importance of applying all three filtering methods in the GPR threshold analysis.

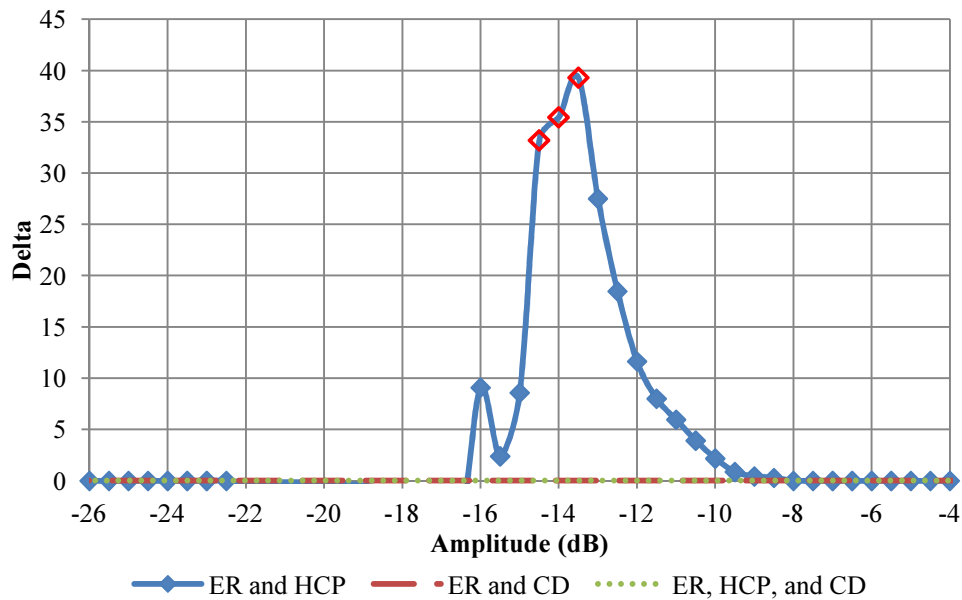


Figure 44: GPR threshold analysis delta curves (Upper Freehold Township, New Jersey)

## CONDITION ASSESSMENT

Once the threshold values for each structure have been identified a damage-oriented condition assessment of each structure can be developed. Figure 45 provides the condition assessment of the bridge deck in Haymarket, Virginia. According to the CD and IE surveys, 22.5% of the deck is severely delaminated and 11.5% is delaminated/lateral cracking. Thus, there is a significant portion of the deck, 34.0%, that is experiencing physical damage in the form of delamination. Of

the remaining deck area, 11.8% is actively corroding and 7.2% has a corrosive environment. The remaining 47.0% of the deck is not experiencing any form of deterioration. Table 20 and Table 21 provide the amount of deck area in each damage state for each bridge. The bold values in Table 20 and Table 21 are based on a complete multi-modal NDT analysis. For some of the bridges, the IE and GPR data could not be gathered; therefore, the analysis could not be completed for these bridges. A limited condition assessment using the available data was undertaken for these structures and the results of those analyses are presented. The results not in bold should be taken as an indication of the condition, but not as a complete assessment.

Table 20 provides the nonduplicating condition quantities for each bridge deck. The nonduplicating area is a tabulation of the damage area when only the highest order of damage is identified at each test location. Table 21 provides the duplicating condition quantities for each structure. The duplicating area calculation counts the area of each damage type, regardless if that area has been also counted in the area of another damage state.

The plots of each bridge's condition assessment are located in Appendix 4 –Condition Plots of Evaluated Bridges.

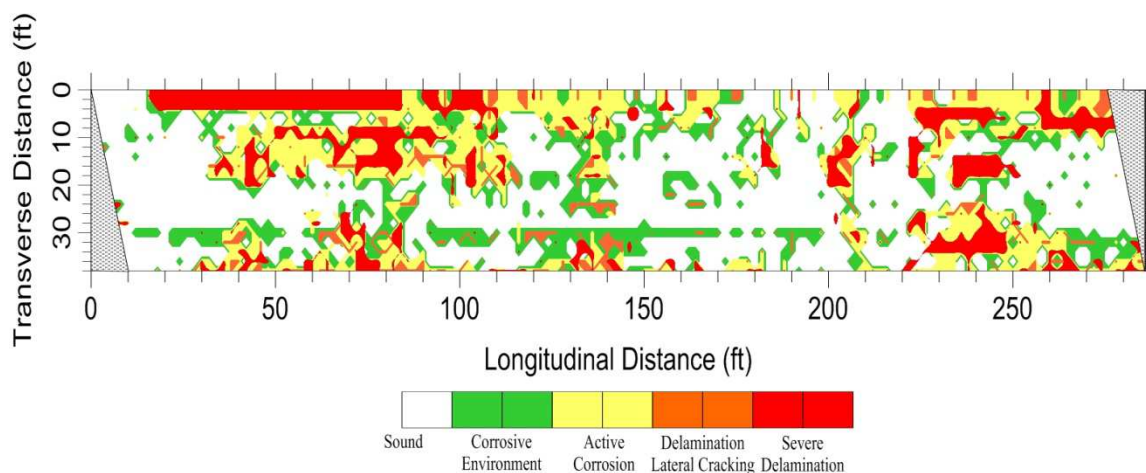


Figure 45: Condition assessment of Route 15 Bridge in Haymarket Virginia

Table 20: Nonduplicating condition quantities

Carries	Location	Sound		Corrosive Environment		Active Corrosion		Delamination/Lateral Cracking		Severe Delamination		Patches (Duplicate w/ Sound)	
		ft <sup>2</sup>	%	ft <sup>2</sup>	%	ft <sup>2</sup>	%	ft <sup>2</sup>	%	ft <sup>2</sup>	%	ft <sup>2</sup>	%
I-495 South	Wilmington, DE	11324	96.4	368	3.1	20	0.2	N/A	N/A	36	0.3	0	0.0
I-195 East	Upper Freehold Township, NJ	<b>1540</b>	<b>49.0</b>	<b>1136</b>	<b>36.2</b>	<b>24</b>	<b>0.8</b>	<b>132</b>	<b>4.2</b>	<b>308</b>	<b>9.8</b>	<b>0</b>	<b>0.0</b>
Pequea Boulevard	Conestoga, PA	3160	46.0	1088	15.9	1308	19.1	N/A	N/A	1308	19.1	116	1.7
School House Road	Middletown, PA	6920	66.6	3464	33.4	0	0.0	N/A	N/A	0	0.0	0	0.0
State Route 123	Sandstone, MN	<b>2180</b>	<b>33.9</b>	<b>736</b>	<b>11.4</b>	<b>496</b>	<b>7.7</b>	<b>1844</b>	<b>28.7</b>	<b>1176</b>	<b>18.3</b>	<b>0</b>	<b>0.0</b>
State Route 15	Haymarket, VA	<b>4884</b>	<b>47.0</b>	<b>748</b>	<b>7.2</b>	<b>1228</b>	<b>11.8</b>	<b>1192</b>	<b>11.5</b>	<b>2340</b>	<b>22.5</b>	<b>100</b>	<b>1.0</b>
State Route 18	Neptune, NJ	2764	55.0	1144	22.8	1080	21.5	N/A	N/A	36	0.7	52	1.0
State Route 21	Almond, NY	<b>160</b>	<b>3.3</b>	<b>120</b>	<b>2.4</b>	<b>1564</b>	<b>31.8</b>	<b>2592</b>	<b>52.8</b>	<b>476</b>	<b>9.7</b>	<b>0</b>	<b>0.0</b>
State Route 273	Elkton, MD	1640	41.0	380	9.5	1348	33.7	N/A	N/A	628	15.7	12	0.3
State Route 47	Deptford Township, NJ	8480	82.2	1748	16.9	80	0.8	N/A	N/A	8	0.1	0	0.0
State Route 93	Sumner, IA	<b>1000</b>	<b>34.0</b>	<b>140</b>	<b>4.8</b>	<b>364</b>	<b>12.4</b>	<b>312</b>	<b>10.6</b>	<b>1128</b>	<b>38.3</b>	<b>0</b>	<b>0.0</b>
West Bangs Ave	Neptune, NJ	3888	65.9	1392	23.6	436	7.4	N/A	N/A	188	3.2	60	1.0

N/A – Data not available

Table 21: Duplicating damage quantities

Carries	Location	Sound		Corrosive Environment		Active Corrosion		Delamination/Lateral Cracking		Severe Delamination		Patches	
		ft <sup>2</sup>	%	ft <sup>2</sup>	%	ft <sup>2</sup>	%	ft <sup>2</sup>	%	ft <sup>2</sup>	%	ft <sup>2</sup>	%
I-495 South	Wilmington, DE	11324	96.4	376	3.2	20	0.2	N/A	N/A	36	0.3	0	0.0
I-195 East	Upper Freehold Township, NJ	<b>1540</b>	<b>49.0</b>	<b>1588</b>	<b>50.6</b>	<b>48</b>	<b>1.5</b>	<b>132</b>	<b>4.2</b>	<b>308</b>	<b>9.8</b>	<b>0</b>	<b>0.0</b>
Pequea Boulevard	Conestoga, PA	3160	46.0	3212	46.8	2028	29.5	N/A	N/A	1308	19.1	620	9.0
School House Road	Middletown, PA	6920	66.6	3464	33.4	0	0.0	N/A	N/A	0	0.0	0	0.0
State Route 123	Sandstone, MN	<b>2180</b>	<b>33.9</b>	<b>4568</b>	<b>71.0</b>	<b>1944</b>	<b>30.2</b>	<b>1944</b>	<b>30.2</b>	<b>1176</b>	<b>18.3</b>	<b>0</b>	<b>0.0</b>
State Route 15	Haymarket, VA	<b>4884</b>	<b>47.0</b>	<b>6964</b>	<b>67.0</b>	<b>3816</b>	<b>36.7</b>	<b>1476</b>	<b>14.2</b>	<b>2340</b>	<b>22.5</b>	<b>204</b>	<b>2.0</b>
State Route 18	Neptune, NJ	2764	55.0	1976	39.3	1100	21.9	N/A	N/A	36	0.7	448	8.9
State Route 21	Almond, NY	<b>160</b>	<b>3.3</b>	<b>4856</b>	<b>98.9</b>	<b>4428</b>	<b>90.1</b>	<b>2772</b>	<b>56.4</b>	<b>476</b>	<b>9.7</b>	<b>0</b>	<b>0.0</b>
State Route 273	Elkton, MD	1640	41.0	1996	49.9	1868	46.7	N/A	N/A	628	15.7	112	2.8
State Route 47	Deptford Township, NJ	8480	82.2	1772	17.2	80	0.8	N/A	N/A	8	0.1	0	0.0
State Route 93	Sumner, IA	<b>1000</b>	<b>34.0</b>	<b>2468</b>	<b>83.8</b>	<b>1476</b>	<b>50.1</b>	<b>632</b>	<b>21.5</b>	<b>1128</b>	<b>38.3</b>	<b>0</b>	<b>0.0</b>
West Bangs Ave	Neptune, NJ	3888	65.9	1812	30.7	568	9.6	N/A	N/A	188	3.2	416	7.0

N/A – Data not available

## CONDITION RATING

The NBIS and AASHTO condition ratings for the 12 bridge decks in this study are provided in Table 22 and Table 23. The most current NBIS rating, as determined by the last visual inspection of each bridge by the bridge owner or its consultants, is listed in Table 22 along with the NBIS rating as determined by the NDT data. Ratings with an asterisk were based on a limited analysis. These bridges did not have IE and GPR data; therefore, the rating is not a completely accurate representation of the deck condition or the entire multi-modal NDT algorithm. The NDT-determined NBIS rating for each completed bridge produced a rating that was consistently one value lower than reported NBIS ratings from most recent visual inspection. Of the ratings performed on the structures with complete data sets, the I-195 East, Route 123, and Route 21 structures initially had an NBIS rating the same as the visual inspection. This was based purely on the quantity of severe delaminations (CD & IE). However, these three bridges had large areas of delamination/lateral cracking, active corrosion, and corrosive environment, which decreased their rating by one due to the consideration of NDT inputs that reflect conditions that cannot be discerned by visual inspection. The results of the NBIS condition rating using NDT data indicates that there is more damage to these structures than was identified by visual inspection. That is an expected result, since NDT provides a more in-depth assessment. This is why these rating systems should incorporate NDT condition assessment, because they provide a more complete and in-depth condition assessment beyond that visible through conventional inspection.

Table 22: NBIS rating according to NDT analysis

<b>Carries</b>	<b>Location</b>	<b>NBIS from Visual Inspection</b>	<b>NBIS from Multi-Modal NDT</b>
I-495 South	Wilmington, DE	7	8*
I-195 East	Upper Freehold Township, NJ	7	6
Pequea Boulevard	Conestoga, PA	4	6*
School House Road	Middletown, PA	8	8*
State Route 123	Sandstone, MN	6	5
State Route 15	Haymarket, VA	6	5
State Route 18	Neptune, NJ	6	8*
State Route 21	Almond, NY	7	6
State Route 273	Elkton, MD	6	5*
State Route 47	Deptford Township, NJ	7	8*
State Route 93	Sumner, IA	6	5
West Bangs Ave	Neptune, NJ	7	7*

\* Rating based on incomplete data

Table 23 provides the results of the AASHTO Bridge Element rating for the twelve bridge decks. The values in Table 23 that are bold indicate results from a complete multi-modal NDT analysis. The bridges that are not bold are missing IE and GPR results; therefore, those results are only a partial depiction of the deck condition. For each AASHTO rating, the square footage and percentage of the deck that fall into each category is provided. Since this method of deck rating is a new addition to the DOT bridge inspection methodology, there is no historical information that can be compared to these results. The AASHTO rating system does lend itself more easily to accept NDT data; however, it is not a seamless transition and still requires adjustments.

Table 23: AASHTO condition rating results

Carries	Location	Condition State 1 (ft <sup>2</sup> (%))	Condition State 2 (ft <sup>2</sup> (%))	Condition State 3 (ft <sup>2</sup> (%))	Condition State 4 (ft <sup>2</sup> (%))
I-495 South	Wilmington, DE	11692 (99.5)	20 (0.2)	36 (0.3)	0 (0)
I-195 East	Upper Freehold Township, NJ	<b>2736 (82.4)</b>	<b>320 (9.6)</b>	<b>264 (8.0)</b>	<b>0 (0)</b>
Pequea Boulevard	Conestoga, PA	4248 (61.9)	1308 (19.1)	1308 (19.1)	0 (0)
School House Road	Middletown, PA	10384 (100)	0 (0.0)	0 (0.0)	0 (0)
State Route 123	Sandstone, MN	<b>2916 (45.3)</b>	<b>2340 (36.4)</b>	<b>1176 (18.3)</b>	<b>0 (0)</b>
State Route 15	Haymarket, VA	<b>5632 (54.2)</b>	<b>2420 (23.3)</b>	<b>2340 (22.5)</b>	<b>0 (0)</b>
State Route 18	Neptune, NJ	3908 (77.8)	1080 (21.5)	36 (0.7)	0 (0)
State Route 21	Almond, NY	<b>280 (5.7)</b>	<b>4156 (84.6)</b>	<b>476 (9.7)</b>	<b>0 (0)</b>
State Route 273	Elkton, MD	2020 (50.5)	1348 (33.7)	628 (15.7)	0 (0)
State Route 47	Deptford Township, NJ	10228 (99.1)	80 (0.8)	8 (0.1)	0 (0)
State Route 93	Sumner, IA	<b>1140 (38.7)</b>	<b>676 (23.0)</b>	<b>1128 (38.3)</b>	<b>0 (0)</b>
West Bangs Ave	Neptune, NJ	5280 (89.5)	436 (7.4)	188 (3.2)	0 (0)

A major benefit of approaching condition rating qualitatively with NDT methods is that it will establish more consistent condition ratings. Visual inspection is very subjective; therefore, a bridge surveyed by five different inspectors will yield slightly different results. However, with NDT and its conversion to an NBIS and AASHTO rating system there is very limited subjectivity in the data collection and analysis. This will improve constancy in bridge deck evaluations and allow for better comparisons to be made between different bridge types and bridges owned by different agencies.

#### DATA AGREEMENT RATING

The data agreement rating and the percentage of complete agreement for each bridge is provided in Table 24. While complete agreement between all of the NDT methods is not expected, a level

of agreement is important, since some of the NDT methods measure related parameters. The percentage of complete agreement values that have an asterisk beside them are based on analyses conducted without IE and GPR data. The limited amount of data on these structures has artificially inflated the data agreement values. They were included for completeness; however, they do not reflect the true agreement for the deck. A data agreement rating was not produced for the structures missing IE and GPR. The data agreement rating cannot be calculated for structures that don't have each condition state identified.

Of the completed structures, the bridge in Haymarket, Virginia has by far the highest level of complete data agreement at 60.2% of the deck. It also received the highest data agreement rating at 90.5. It is important to review both the agreement rating and the complete agreement percentage, because a structure with a low percentage of complete agreement does not mean the multi-modal NDT data is incorrect. If there was always complete agreement between all the NDT methods, then the multi-modal NDT approach would not be necessary. These ratings show that each NDT method is related, however, they are still detecting different damage states. Most of the bridges have a data agreement rating of around 85 and a percentage of complete agreement at approximately 40%. The data agreement rating and percentage of deck in complete agreement can give an indication as to the cause of the identified deterioration. Since the methods utilized in this study are highly affected by corrosion-induced deterioration, if there is significant agreement between the methods, then that could indicate the primary cause of damage is due to corrosion. On the other hand, if the agreement levels are low, this could indicate that the cause of the damage is mechanical or some other type of deterioration mechanism.

Table 24: NDT data agreement rating and percentage of complete agreement

Carries	Location	Data Agreement Rating	Percentage of Deck in Complete Agreement
I-495 South	Wilmington, DE	N/A	99.6*
I-195 East	Upper Freehold Township, NJ	84.0	39.5
Pequea Boulevard	Conestoga, PA	N/A	67.9*
School House Road	Middletown, PA	N/A	100.0*
State Route 123	Sandstone, MN	84.6	41.9
State Route 15	Haymarket, VA	90.5	60.2
State Route 18	Neptune, NJ	N/A	94.3*
State Route 21	Almond, NY	82.9	23.5
State Route 273	Elkton, MD	N/A	89.6*
State Route 47	Deptford Township, NJ	N/A	99.4*
State Route 93	Sumner, IA	89.0	47.3
West Bangs Ave	Neptune, NJ	N/A	95.9*

N/A – Data not available

\* Based on limited NDT data

#### MULTI-MODAL CONDITION ASSESSMENT PROGRAM

As the final product of this research, a program was written to take processed multi-modal NDT data and produce a complete condition assessment. Appendix 2 – MATLAB Code for Multi-Modal Condition Assessment provides the MATLAB source code for the program. Appendix 3 – Sample Output from Condition Assessment Code provides a sample of the output for the analysis conducted on the bridge in Haymarket, Virginia.

The input file for the program is a tab-delimited text file that has the longitudinal and transverse coordinates, along with the HCP, ER, IE, CD, GPR amplitude, and GPR cover depth data (Table 25). A requirement of the input file is that every line of data must have an entry for each column; blank entries will cause an error. Figure 46 provides the input lines of code for the program.

Line 1 of the input code requires the location path for the data text file. The program takes the text file and enters that data into individual MATLAB vectors. It is important that the order of each data type in the text file match the first part of the input code, [long, tran, HCP, ER, IE, CD,

GPR, Cover], or an error will result. The data in the input text file should have the following units; long and tran in ft, ER in kohm·cm, HCP in mV CSE, GPR in dB, IE in 1/2/3/4 signal ratings, CD in 0/1, and Cover in inches. Line 2 of the input code recombines all the NDT data into a MATLAB matrix. Lines 3 through 6 of the input code are general identification information regarding the structure.

Table 25: Sample input file for the condition assessment program

4	1	-205	70	2	0	-17.0252	2.644
6	1	-180	58	4	1	-17.4291	2.385
8	1	-230	70	2	1	-16.9839	1.908
10	1	-225	53	2	0	-17.723	2.122
12	1	-235	59	1	0	-17.8039	1.908
14	1	-260	92	1	0	-17.6113	1.853

- 1) `[long, tran, HCP, ER, IE, CD, GPR, Cover]=textread('C:\Research\VA 2009 NDE DATA Tab Delimited.txt');`
- 2) `DATA=[long, tran, HCP, ER, IE, CD, GPR, Cover];`
- 3) `Carries='State Route 15';`
- 4) `Spans='Interstate 66';`
- 5) `State='Virginia';`
- 6) `City='Haymarket';`

Figure 46: Input information for the condition assessment code

Once the program accesses the input file, the first step the program takes is to identify each threshold, ER, HCP, and GPR, according to the predefined methodology. Once the thresholds have been identified, the program identifies the condition state of each location on the deck according to the predefined damage states (Table 3). While the highest order of damage is the most important, each damage state affecting each location is recorded. The program then produces plotting files for each condition state, which can be input into the program Surfer™ to produce the final condition plot. The program will then calculate the area of the deck, duplicating and nonduplicating, in each damage state. After the damage areas have been determined, then the deck is rated using the NBIS and AASHTO methodologies. The program also calculates the data

agreement rating and the percentage of complete agreement. The program takes all of this information and outputs it to a tab-delimited text file titled "ConditionAssessment.txt." The output text file is saved in the folder that is defined by MATLAB as the "current folder" during the program run. The program is very versatile and is capable of producing a complete condition assessment using multi-modal NDT data. The objective of this work is that as multi-modal NDT becomes more common, this code will be utilized and expanded on by the NDT community. This will greatly improve the effectiveness and accuracy of NDT condition assessment.

#### ALTERNATE GRID SPACING

An evaluation of grid spacing was conducted to establish whether NDT data collection could be more efficient. The first grid spacing analysis conducted was on a small area of the Rt. 18 Bridge in Neptune, New Jersey. Only ER and HCP measurements were made on this small grid. For each grid spacing that was evaluated, the average and standard deviation of the data collected were determined (Figure 47). The measured resistivity and potential values for each grid point remained relatively consistent over the various grid spacings. The average change in measured value from the 2 ft × 2 ft was 5.73 kohm·cm for ER and 39.4 mV CSE for HCP.

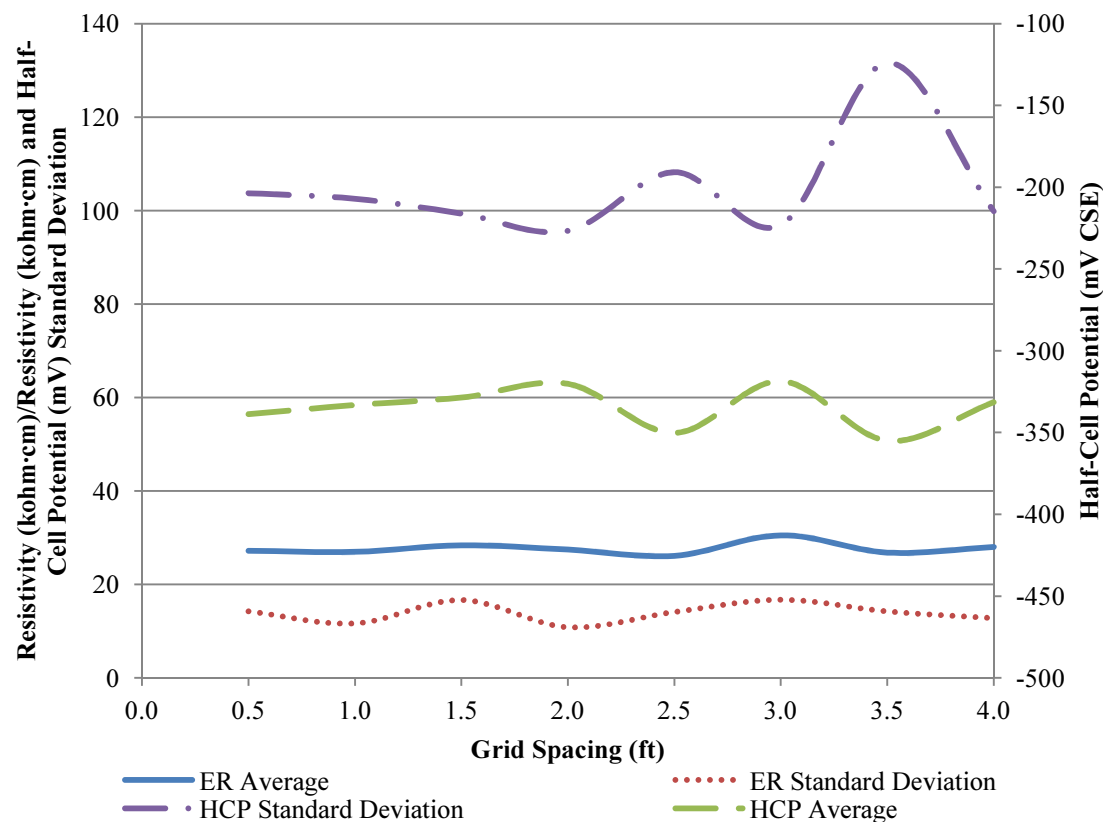


Figure 47: Analysis of ER and HCP measured values for changing survey grid spacing

An evaluation of the square footage of deck defined in each condition state according to each grid spacing was also conducted. The condition states were: corrosive environment and active corrosion as identified by ER and HCP. Based on the data collected on the bridge deck as a whole, the threshold values were determined to be 45 kohm-cm for ER, -275 mV CSE for active HCP, and -175 mV CSE for passive HCP. Using these threshold values, the area of the deck below and above each threshold was determined using the various grid spacings (Figure 48). The grid spacing had little effect on the amount of area that was in each condition category. The average variation in square footage for the resistivity was 2.29 ft<sup>2</sup> (2.4%) and the average variation in the square footage of active HCP was 4.27 ft<sup>2</sup> (6.2%). Overall the 2 ft × 2 ft grid provides an effective grid density to identify the condition of a reinforced concrete bridge deck when compared to a much smaller grid.

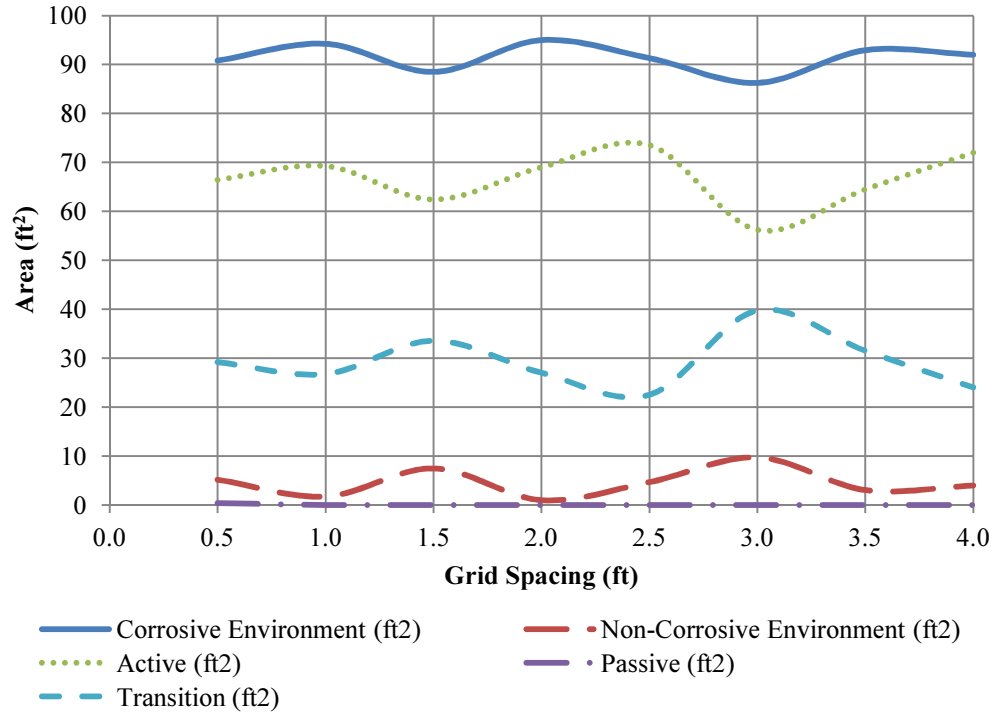


Figure 48: Quantities of damage area based on grid spacing

Figure 49 and Figure 50 provide the results of the ER and HCP surveys using various grid spacings. This helps to illustrate the effect that changing the grid spacing has on the NDT survey results. Grid spacings of 0.5 ft × 0.5, 1.0 ft × 1.0, 1.5 ft × 1.5, and 2 ft × 2 ft were plotted for each method. It is important to note that when plotting the information for the various grid spacings only the data at the set intervals was input into the software to plot. While there is a clear loss of detail as the grid spacings increase, the general evaluation of the deck area remains the same. There is a large area of corrosive environment and active corrosion in the center of both surveys. In the ER survey, the highly corrosive environment is surrounded by areas of still moderate corrosive environment. In the HCP survey, the active corrosion region in the center is surrounded by an area of uncretian corrosion activity. In all four plots, for both ER and HCP, the same general conclusions result from the four different grid spacings; there is a large area of deterioration in the center surrounded by an area that has a moderate corrosive environment,

however, corrosion activity has yet to initiate. This analysis shows that a 2 ft × 2 ft grid spacing is an adequate spacing to provide an effective assesment of a reinforced concrete bridge deck.

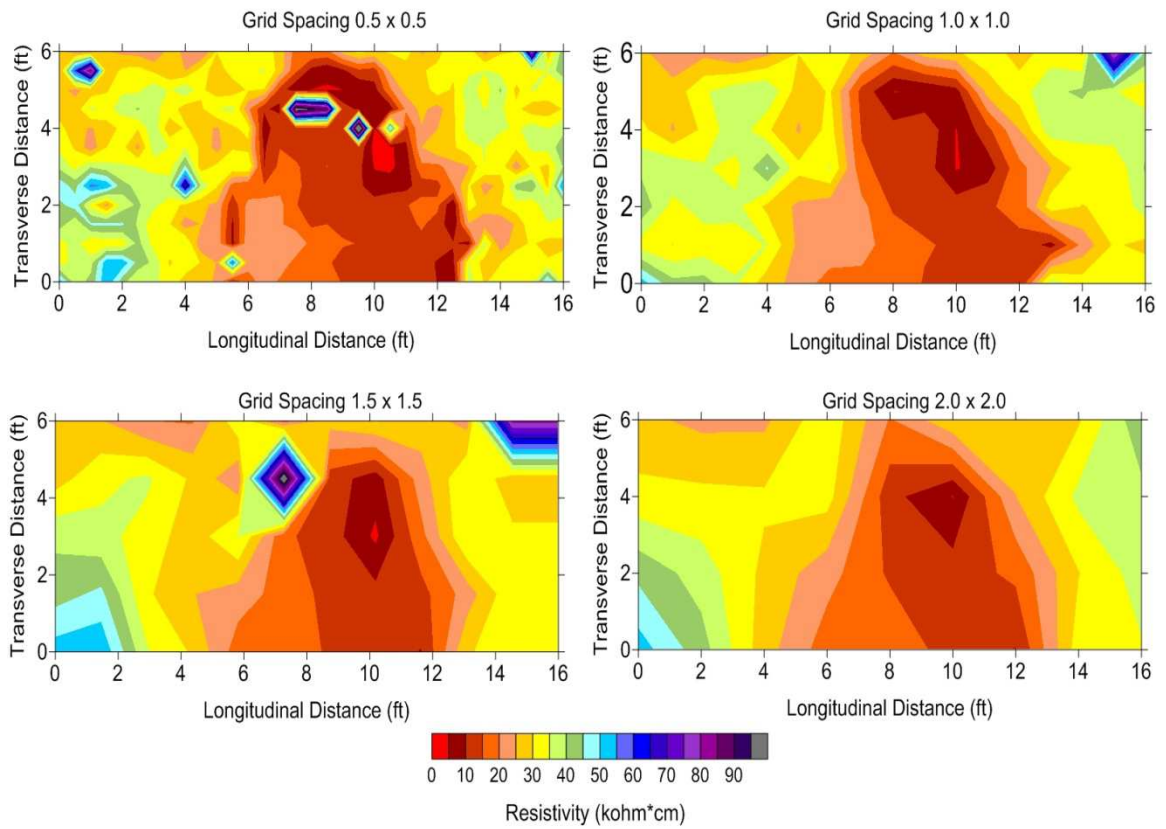


Figure 49: ER survey results using various grid spacings (Rt. 18 Neptune, New Jersey)

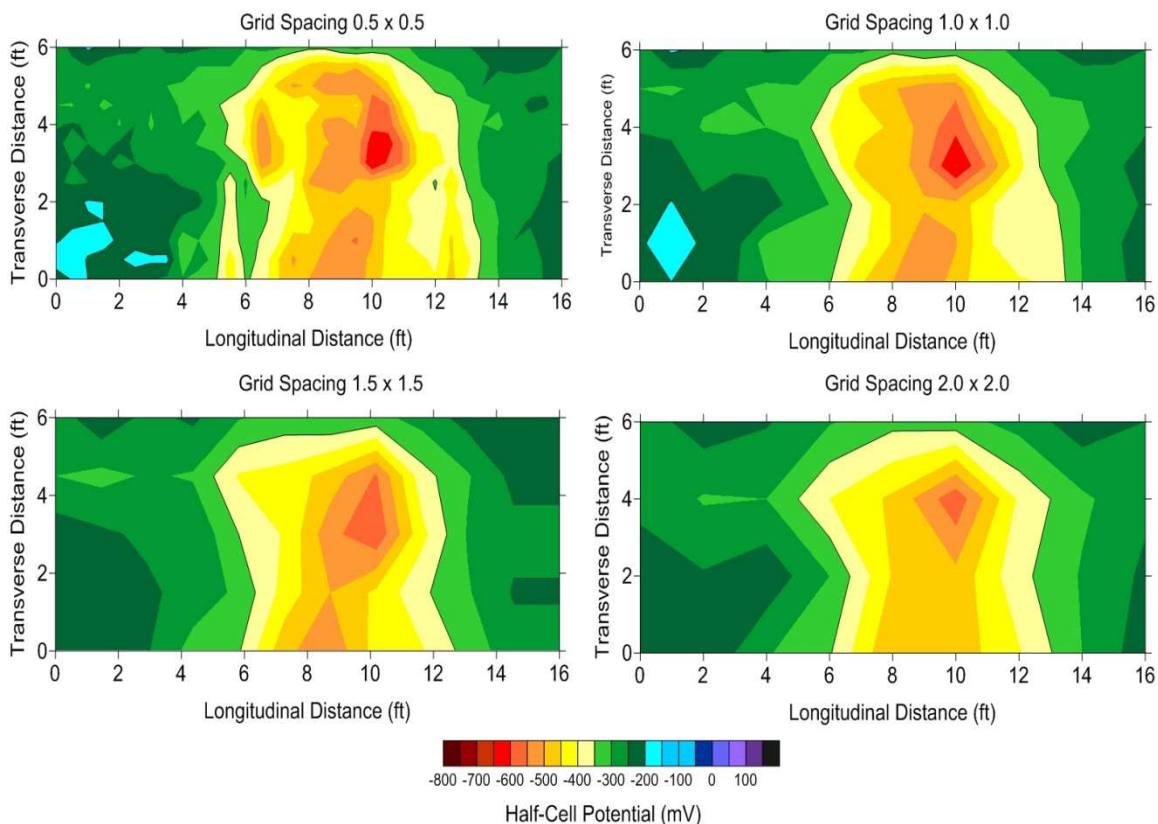


Figure 50: HCP survey results using various grid spacings (Rt. 18 Neptune, New Jersey)

An analysis was also conducted on the previously surveyed bridge decks to evaluate the effect of increasing the grid spacing past a 2 ft  $\times$  2 ft grid. For the 12 bridges that were a part of this analysis, the effect of changing the grid size was evaluated on each of the bridges and the results were averaged together. Figure 51 and Figure 52 plots the average change, compared to the 2 ft  $\times$  2 ft grid, in area identified above and below the threshold for ER, HCP, and GPR. The x-axis indicates the grid spacing increment; 2 ft  $\times$  2 ft is 2, 4 ft  $\times$  4 ft is 4, and so on. Figure 51 provides the results of the square spacing; the spacing increment is indicated on the x-axis. Figure 52 provides the results of using rectangular grid spacing. Figure 51 indicates a clear increasing trend in delta as the grid spacing increases. There is also a significant difference in the slope of areas below and above the threshold. The slopes of the areas below threshold are much steeper than the areas above threshold. This is due to the fact that areas of deterioration take up a smaller

proportion of most bridge decks, so when a change occurs in deteriorated area, it has a larger effect on the percentage; whereas, a change in sound area has little effect on its percentage, since it takes up a much larger percentage of the deck. In looking at the change in area identified as sound, using a rectangular grid spacing (Figure 52) with 2 or 4 ft in the transverse direction and up to 8 ft in the longitudinal direction has less than a 10% effect on the amount of area reported as sound. This indicates that a grid spacing of 4 ft × 8 ft could be used on a bridge deck and would still provide results that are within 10% of those of a 2 ft × 2 ft grid. If a larger 4 ft × 4 ft grid was used on the bridge deck in Haymarket, Virginia, there would be a 73.6% (720 points) reduction in test locations versus the 2 ft × 2 ft grid (2717 points).

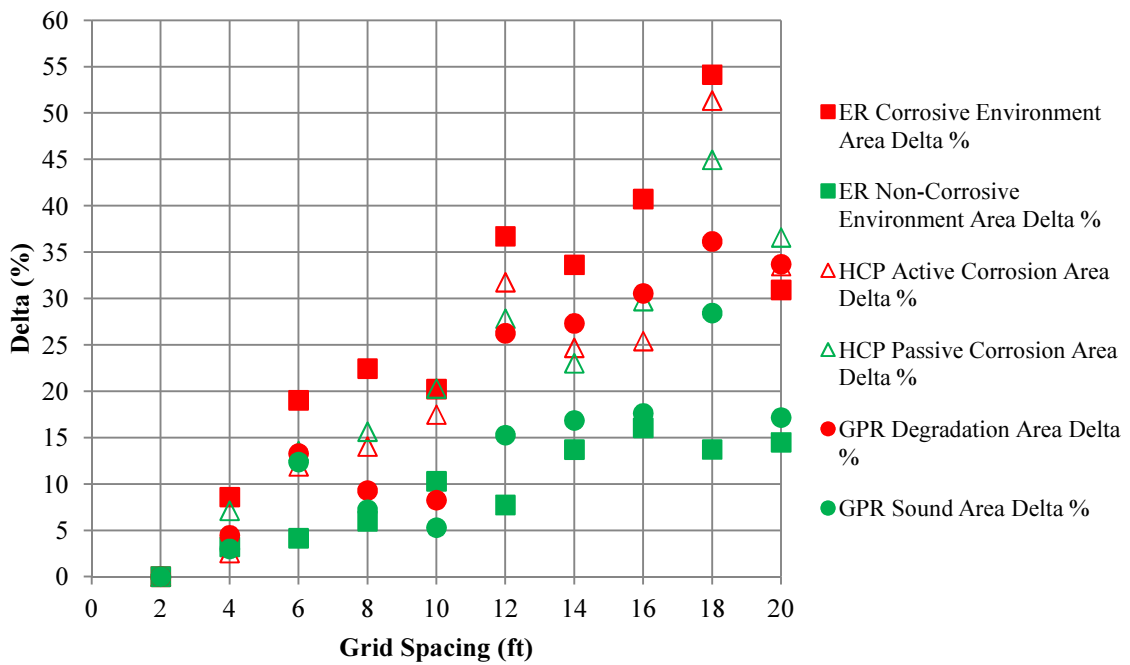


Figure 51: Percent change in detection area of electrical methods for various square grid spacings

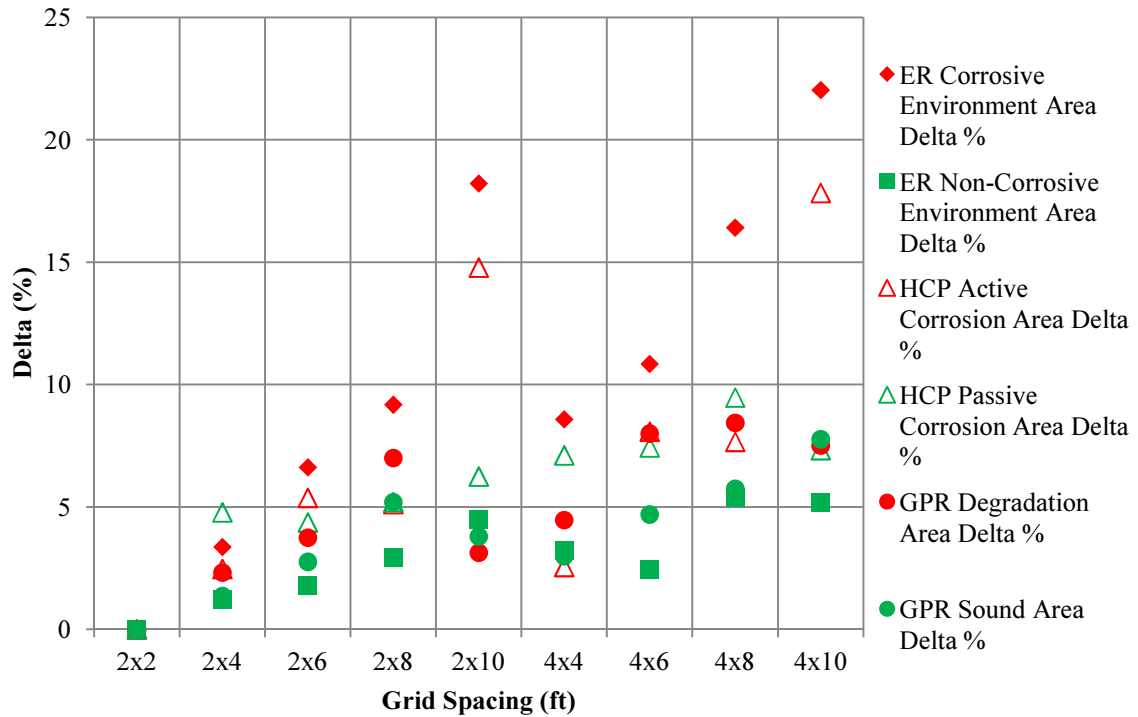


Figure 52: Percent change in detection area of electrical methods for various rectangular grid spacings

Figure 53 and Figure 54 provides the results of the analysis of areas identified as deteriorated and sound for the acoustic methods, IE and CD. Like the previous plot, the sound curves have a much shallower slope than the deteriorated curves. For the acoustic methods, the change in sound area stays below 5% for grid spacings as large as 4 ft × 8 ft and 6 ft × 6 ft. Due to the small areas of severe delaminations, the effect that changing the grid spacing has on the CD delaminated area is quite significant. The change in IE-identified areas of deterioration stays below 10% for spacings up to 4 ft × 8 ft.

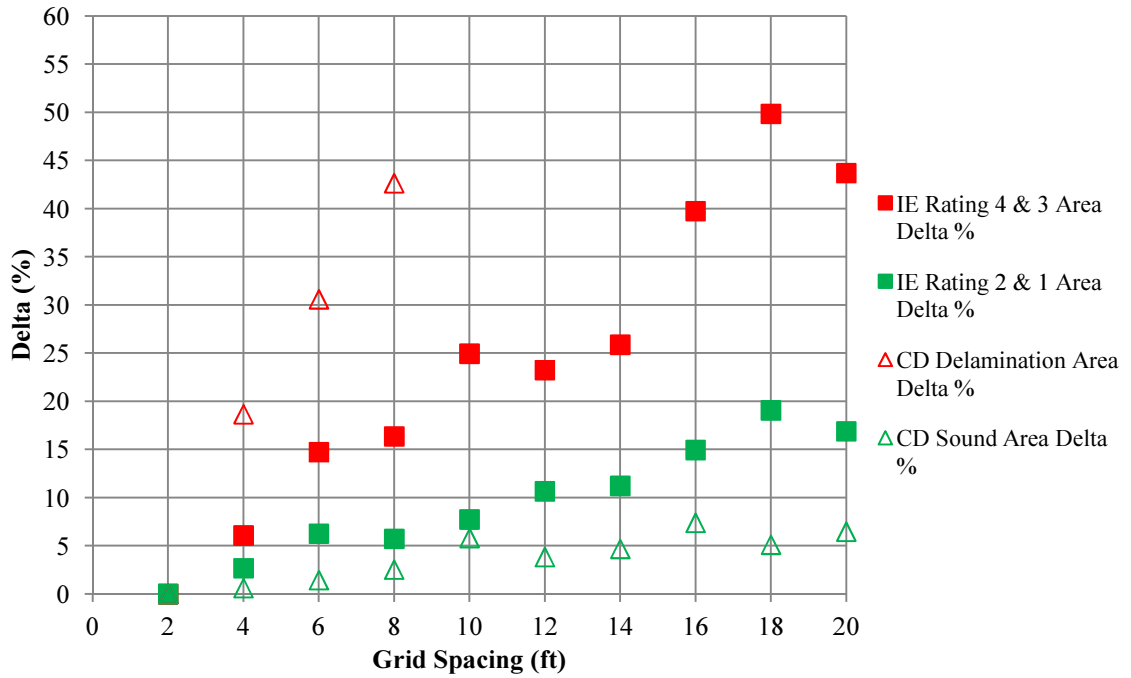


Figure 53: Percent change in detection area of acoustic methods for various square grid spacings

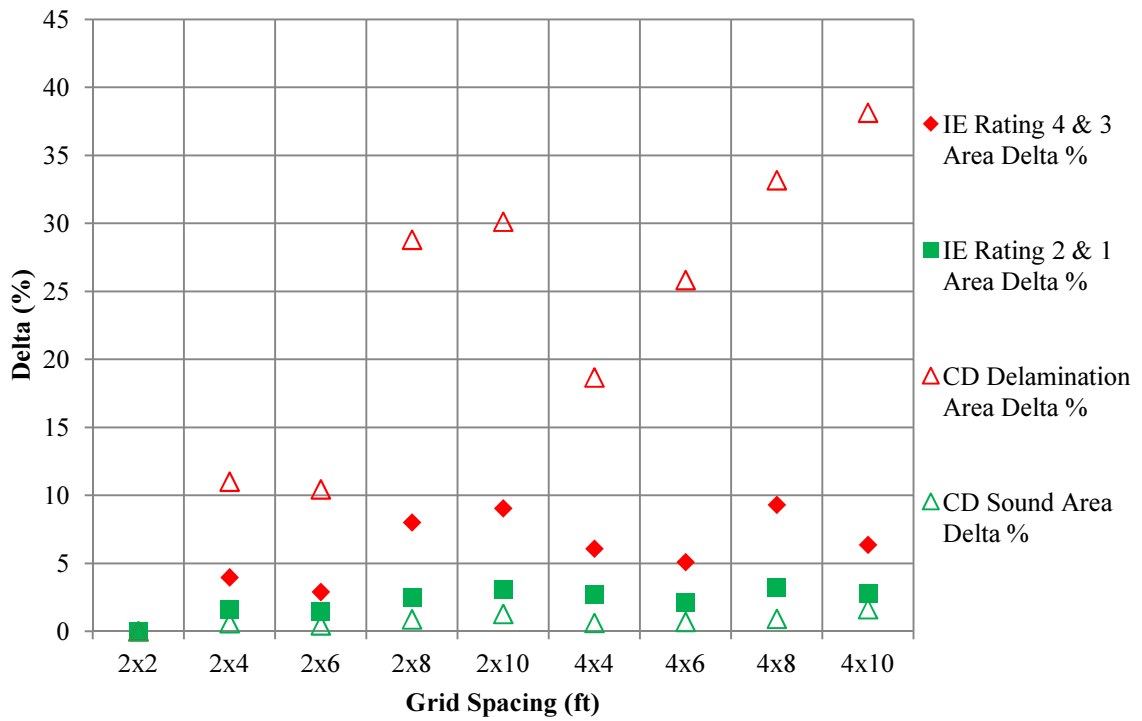


Figure 54: Percent change in detection area of acoustic methods for various rectangular grid spacings

Figure 55 provides the results of an analysis conducted to identify the effect that changing the grid spacing has on the average ER, HCP, and GPR measured values on the bridge deck. This figure includes both the square and rectangular grid spacings. Rectangular grid spacings are indicated by using a decimal for the longitudinal dimension. For example, 2 ft  $\times$  6 ft is indicated on the x-axis as 2.6. For grid spacings up to 4 ft  $\times$  8 ft there is less than 6% effect on the average measurement. Like the previous results, increasing the grid spacing slightly, especially in the longitudinal direction, has a limited effect on the results of the survey.

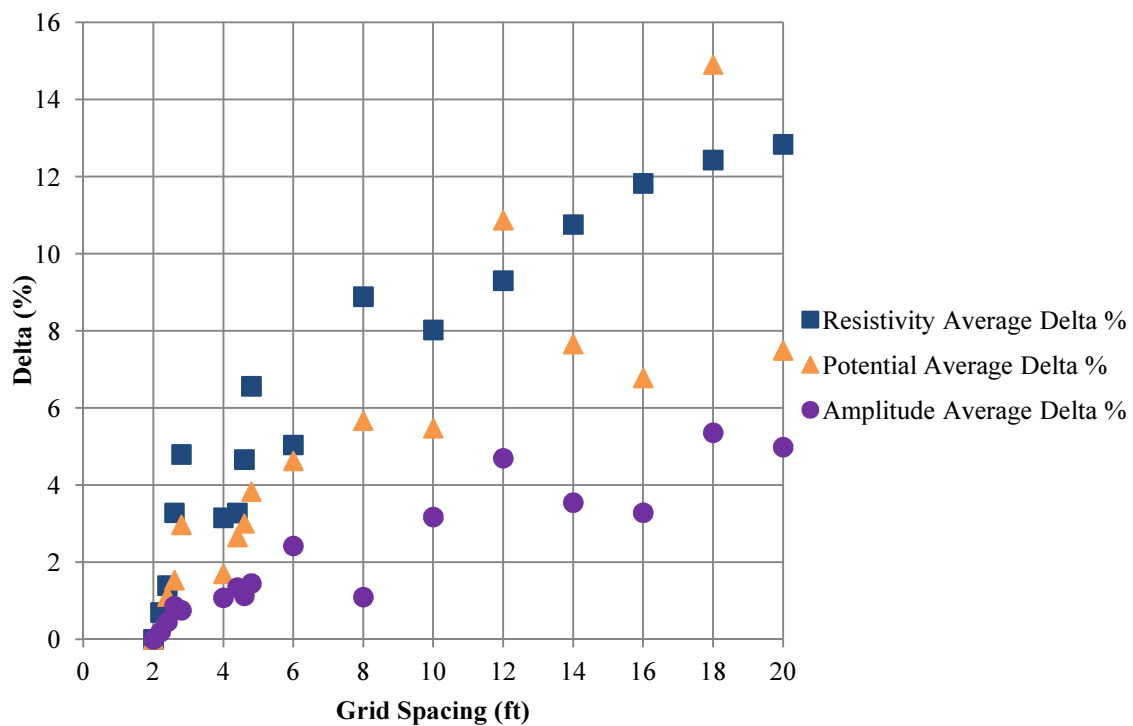


Figure 55: Percent change in average measurements due to various grid spacings

Figure 56 and Figure 57 provide a sampling of what the survey conducted on the Haymarket, Virginia Bridge would look like if a 2 ft  $\times$  6 or 4 ft  $\times$  8 ft grid spacing were used for the ER or HCP surveys. The most significant difference between the 2 ft  $\times$  2 ft grid spacing and the other two plots is that in the 2 ft  $\times$  6 ft and 4 ft  $\times$  8 ft plots, the results look more granular. Since each of these points must represent more of the deck in the longitudinal direction, they become

elongated. While the look of the plots may be strange, the information presented in all three plots for both technologies is very similar. The large areas of highly corrosive environment and active corrosion are very similar among all three grid spacings. Due to the nature of how the data is collected, there will clearly be areas of inflation and deflation relative to the true, however, the overall assessment of the deck is very similar for the larger grid spacings. If the survey was conducted using the 4 ft  $\times$  8 ft grid spacing, then the engineers would immediately know that this bridge is in serious condition. They would also know that the area from about 30 to 150 longitudinally was in need of further investigation. Using a much larger grid spacing provides a result that is similar enough to the much denser grid that a general condition assessment can still be provided.

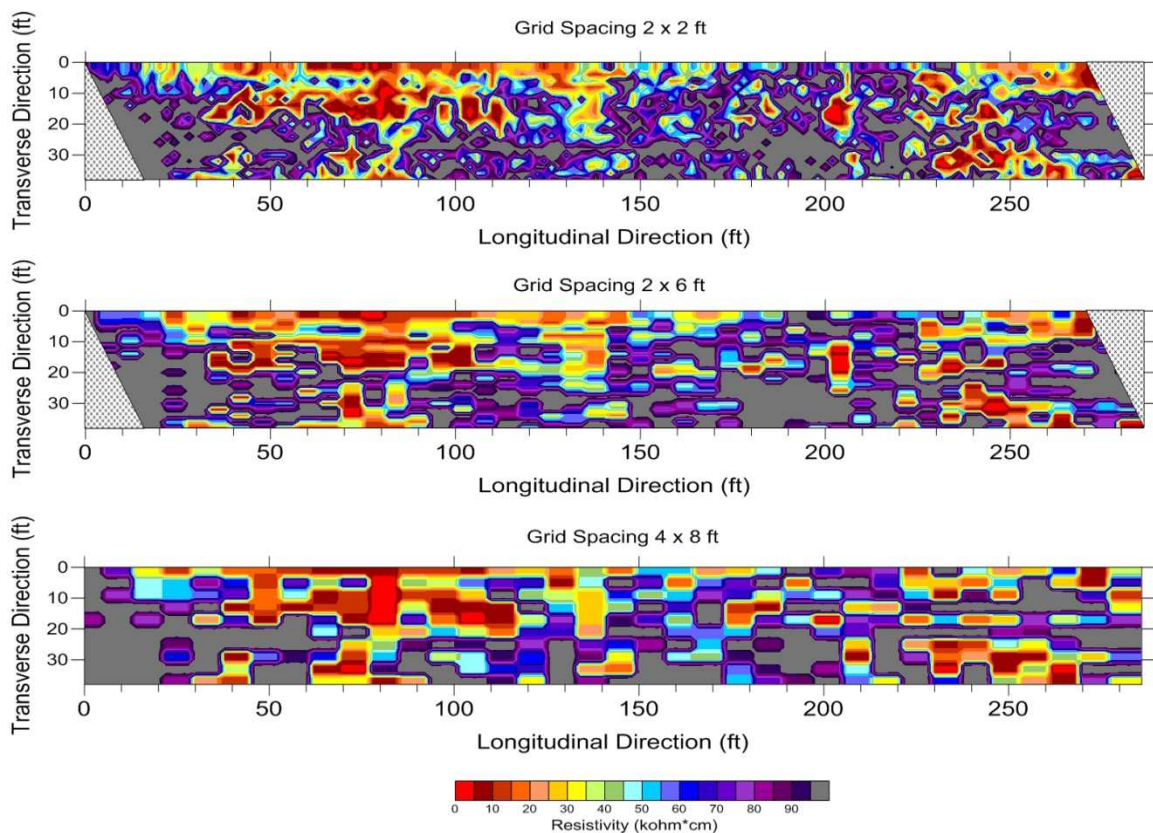


Figure 56: ER survey results using various grid spacings (Haymarket, Virginia)

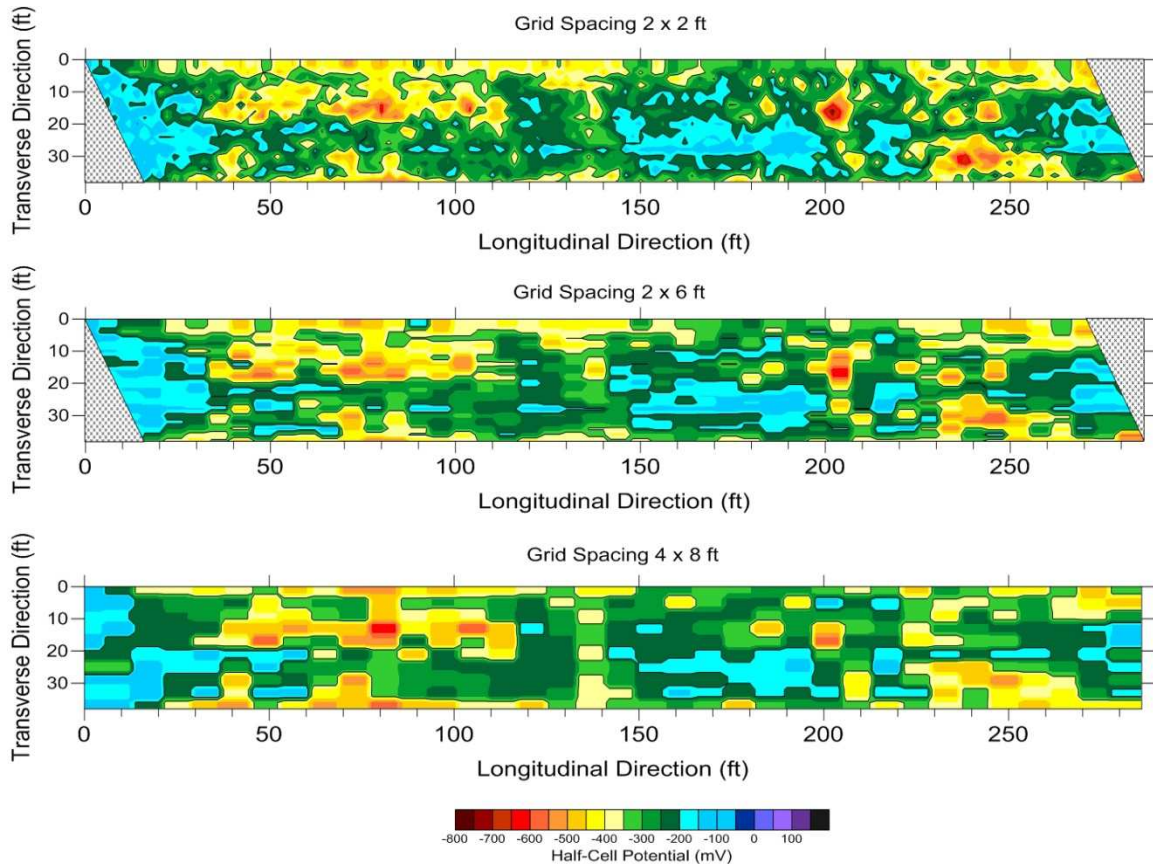


Figure 57: HCP survey results using various grid spacings (Haymarket, Virginia)

As the grid spacing increases, the variation in the results follows a fairly linear trend throughout the previous figures. However, the reductions in test locations for successively larger grid spacings follow an exponential trend (Table 26). Even a small increase in grid spacing, from  $2 \text{ ft} \times 2 \text{ ft}$  to  $2 \text{ ft} \times 4 \text{ ft}$ , causes a significant reduction in the amount of test locations, 49.8%. If such a large decrease in testing locations will only affect the results by a few percent, then this is a sizable benefit. A daytime lane closure for an NDT survey of a typical bridge deck is usually constrained within the hours of 9:30 am and 2:30 pm; 5 hours. Assuming that, in that 5-hour window, data is collected using a  $2 \text{ ft} \times 2 \text{ ft}$  grid, that same amount of area could be done by a  $4 \text{ ft} \times 4 \text{ ft}$  grid in 1.3 hours and a  $4 \text{ ft} \times 8 \text{ ft}$  grid in 0.65 hours. This is a very sizable reduction in testing time. This reduction in time would equate to considerable savings to the bridge owner.

Table 26: Percent reduction in amount of test points for various grids

Spacing	2×2	2×4	2×6	2×8	4×2	4×4	4×6	4×8
<b>Reduction in Test Points (%)</b>	0.0	49.8	66.3	74.6	48.7	74.3	82.7	87.0

The results of the grid analyses indicate that increasing the grid spacing can provide similar results to a much denser 2 ft × 2 ft grid while significantly decreasing the amount of time required for testing. The rectangular grid proved to be the most effective method at reducing the amount of test locations while still maintaining a high level of accuracy. These results could be applied to network level assessment of infrastructure, where quick evaluation of deck condition is necessary. A large evaluation grid would allow for the categorization of each bridge's deterioration level and allow for decisions to be made regarding what structures need to be evaluated more closely and what structures are in adequate condition.

## FINDINGS

The results of this research lead to several findings regarding multi-modal NDT. The following presents those findings.

- The areas of ER, HCP, and CD that indicated deterioration correlate well with areas of highly attenuated GPR signal.
- An IE signal rating of 4 was associated with a decrease in measured values for the ER, HCP, and GPR methods. When the IE signal rating was 1, 2, or 3, there was no clear deviation in measured values.
- Various NDT methods indicated strong spatial agreement between the areas above and below their respective thresholds. The methods that showed the strongest agreement were ER/HCP, ER/GPR, CD/ER, CD/HCP, and CD/GPR.

- ER, HCP, GPR, and CD showed a high level of repeatability in measurements collected on the same structure in different years. Areas of deterioration identified in the 2009 survey of the Haymarket, Virginia Bridge were also deteriorated in 2011.
- The correlations between ER, HCP, CD, and GPR can be used to identify threshold values in ER, HCP, and GPR.
- Each bridge had a different level of agreement between the multi-modal NDT data. A high level of data agreement is not necessary in understanding a bridge deck's condition; however, it did provide a higher confidence in the results. This form of analysis could be used to help identify the deterioration mechanism that is affecting the bridge deck. Corrosion-induced damage will have a high agreement rating, while damage caused from a structural issue will have lower agreement.

## CONCLUSIONS

This research was an in-depth analysis of multi-modal NDT condition assessment of bare reinforced concrete bridge decks. It produced a wide array of results and procedures that will aid in the further development of NDT condition assessment. The following presents the conclusions reached as a result of this research.

- Strong correlations exist between ER and HCP measurements made on reinforced concrete that suffers from chloride-induced corrosion. Areas that were indicated as having a corrosive environment typically also indicated active corrosion.
- IE and CD showed an overall agreement regarding the identification of delaminations. However, for strict comparison of CD indication of severe delamination, there was poor agreement with IE.

- The steel reinforcing cover depth is an important factor in the service life of a structure. Areas of low cover are more likely to experience deterioration sooner than areas of deeper cover.
- Patches typically had the shallowest cover on a bridge deck when compared to areas of severe delamination and sound concrete. Patch locations had delaminated in the past and were repaired, indicating that cover depth plays an important factor in time-to-damage for reinforced concrete.
- Areas of low resistivity lead to the future activation of corrosion. Locations with high concentrations of moisture and chloride provide an environment that is favorable to corrosion activity.
- According to the analyses conducted on the 12 bridge structures, resistivity less than 40 kohm·cm provides an environment that is favorable to corrosion activity.
- A location that is surrounded by highly deteriorated areas is more likely to become highly deteriorated in the future than a location that is surrounded by sound concrete. Reinforced concrete deterioration spreads over time to surrounding areas.
- A statistics-based approach to threshold identification provides a robust and versatile method to identify threshold values on various structures.
- Due to the nature of chloride-induced corrosion, the NDT methods ER, HCP, GPR, IE, and CD provide a detailed and complete assessment of reinforced concrete. These methods together provide insight into the various forms of deterioration that occur during the life of reinforced concrete.
- When providing a plot for condition assessment using contour plotting software, it is important to understand exactly what the software is doing to the data and image. Contouring software can create misleading information if done incorrectly and can create false transitions between data sets.

- Rating a bridge deck using just visual inspection is not an adequate method of evaluation. Significant deterioration may occur inside the concrete matrix that cannot be seen through a purely visual inspection.
- Condition assessment using a multi-modal NDT approach is a complex process, however, the developed software streamlines and automates a large portion of the process to help create a more versatile and effective result.
- A grid spacing larger than 2 ft × 2 ft can provide an overall condition assessment that is similar to a condition assessment provided by a 2 ft × 2 ft grid. Using a grid spacing of 2 ft × 6 ft or 4 ft × 8 ft significantly reduces the number of test locations and survey time, while still maintaining an effective general condition assessment. These large grid spacings can be used to quickly assess bridge conditions on a network level to identify what bridges are in need of an in-depth assessment and what bridges are in adequate condition.

## RECOMMENDATIONS

Based on the results and conclusions of this research, the following recommendations regarding bridge deck condition assessment and multi-modal NDT data collection have been made by the author.

- Whenever possible, use a multi-modal NDT approach when evaluating reinforced concrete. It is understood that not all the NDT methods utilized in this work can be applied to every condition assessment project due to cost effectiveness and field-work efficacy. However, it is important, when conducting a condition assessment, that more than one NDT method is utilized so as to identify as many deterioration states as possible. This will provide a more effective and complete condition assessment.

- It is recommended that when collecting, analyzing, and presenting ER, HCP, and GPR data, that care is taken when applying threshold values. Threshold values presented in literature are not absolutes; they shift based on many environmental factors. If the NDT practitioner doesn't have a firm understanding of the meaning of, and factors influencing, measured values, then an improper condition assessment will be produced.
- With the development of a condition based assessment the next step of this research should be to add the ability to forecast future damage. Predict the quantities of each deterioration state for various time increments using established deterioration rate research.
- NBIS and AASHTO Bridge Element ratings should adopt procedures to include NDT information as a part of the condition rating. Having these rating systems change to include NDT information is paramount for the future of bridge inspection and health monitoring.
- It is recommended that when a network level condition assessment of a bridge deck is required, that a rectangular grid spacing on the order of 2 ft × 6 ft or 4 ft × 8 ft be implemented. Increasing the grid spacing like this will provide a more cost-effective survey while still maintaining a reasonably effective condition assessment. A network level condition assessment using a large grid will provide a general condition assessment that will indicate if further evaluation action is needed on that structure.

## FUTURE WORK

While working on this research project, there were several additional research topics of importance and interest that became apparent. These ideas were not investigated as a part of this work, since they were outside the scope. The following is a list of these ideas and topics which merit further study.

- Autopsy of bridge deck samples to provide ground-truth verification for the threshold methodology - While the threshold analysis methods were developed using sound statistical analyses and known physical relationships, the inability to core into decks to verify results limits its widespread application. The bridge in Haymarket, Virginia is scheduled for replacement and would provide a great opportunity to collect ground-truth information. Also, any new bridges that are surveyed using the multi-modal NDT approach should be evaluated using this methodology to verify the methodology's applicability and provide any necessary adjustments.
- Further analysis into IE data and its relationship with the other NDT methods - The IE data showed consistently the least amount of data correlation to the other NDT methods. More work needs to be dedicated to understanding why.
- Evaluation of the deck condition surrounding patch locations - Ring anode effect is a problem that leads to increased corrosion activity around patch locations. An analysis of the condition data could provide insight into the seriousness of this problem and ways to identify it.
- Work closely with DOT bridge inspectors and bridge policy officials to further develop the NBIS and AASHTO deck ratings to gradually incorporate multi-modal NDT data - Condition assessment of bridge decks is moving ever more into the realm of NDT and these rating systems, which are federally mandated, should move towards adaptation of NDT data.
- The NDT survey should be distributed and the results analyzed - The survey was not completed due to difficulties in acquiring approval from the Rutgers Institutional Review Board (IRB) at the Office of Research and Sponsored Programs. The Office of Research and Sponsored Programs determined that the survey involved the collection of information from human subjects, which requires the Human Subjects Certification

Program (HSCP) to be completed by all researchers involved. Due to difficulties in this approval process, the survey was not approved in time to receive responses prior to the submission of this work. Therefore, the results of the survey were not presented as a part of this work and should be completed as future work.

## REFERENCES

- AASHTO. *AASHTO Guide Manual for Bridge Element Inspection*. 2011.
- ACI Committee 222. *Corrosion of Prestressing Steels*. American Concrete Institute, 2001.
- ACI Committee 222. *Protection of Metals in Concrete Against Corrosion*. American Concrete Institute, 2001.
- ASTM. *Standard Practice for Measuring Delaminations in Concrete Bridge Decks by Sounding*. ASTM, 1992.
- ASTM. *Standard Test Method for Corrosion Potentials of Uncoated Reinforcing Steel in Concrete*. ASTM, 2009.
- Broomfield, J. P. *Corrosion of Steel in Concrete*. Abingdon, Oxon: Taylor & Francis, 2007.
- Bungey, J. H. *Testing of Concrete in Structures*. 2. New York, New York: Chapman & Hall, 1989.
- Daniels, D. *Ground Penetrating Radar*. 2. London: The Institution of Engineering and Technology, 2004.
- Elkey, W., and E. J. Sellevold. *Electrical Resistivity of Concrete*. Oslo: Norwegian Road Research Laboratory, 1995.
- Elsener, B., C. Andrade, J. Gulikers, R. Polder, and M. Raupach. "Half-Cell Potential Measurements - Potential Mapping on Reinforced Concrete Structures." *Materials and Structures* 36 (August-September 2003): 461-471.
- Feliu, S., J. A. Gonzalez, and C. Andrade. "Electrochemical Methods for On-Site Determinations of Corrosion Rates of Rebars." In *Corrosion Activity of Steel Reinforced Concrete Structures*, by N. S. Berke, E. Escalante, C. K. Nmai and D. Whiting, 107-118. West Conshohocken, Pennsylvania: ASTM International, 1996.
- Funahashi, M. "Predicting Corrosion-Free Service Life of a Concrete Structure in a Chloride Environment." *Materials Journal (ACI)* 87, no. 6 (November 1990): 581-587.
- Gros, X. E., J. Bousigue, and K. Takahashi. "NDT data fusion at pixel level." (NDT&E International) 32 (1999): 283-292.
- Gu, P., and J. J. Beaudoin. "Obtaining Effective Half-Cell Potential Measurements in Reinforced Concrete Structures." *Construction Technology Update* (Institute for Research in Construction), July 1998: 1-4.
- Gucunski, N., et al. *Nondestructive Testing to Identify Concrete Bridge Deck Deterioration*. Washington, D.C.: Transportation Research Board, 2013.
- Gucunski, N., F. Romero, S. Kruschwitz, and R. Feldmann. "Comparative Study of Bridge Deck Deterioration Detection and Characterization by Multiple NDE Methods." Edinburgh: Structural Faults & Repair, 2010.
- Gucunski, N., F. Romero, S. Kruschwitz, R. Feldmann, A. Abu-Hawash, and M. Dunn. "Multiple Complementary Nondestructive Evaluation Technologies for Condition Assessment of Concrete

Bridge Decks." *Transportation Research Record: Journal of the Transportation Research Board* (Transportation Research Board of the National Academies), no. 2201 (December 2010): 34-44.

Gucunski, N., G. Slabaugh, Z. Wang, T. Fang, and A. Maher. "Visualization and Interpretation of Impact Echo Data from Bridge Deck Testing." *Journal of Transportation Research Board* (Transportation Research Board), 2007.

Gucunski, N., R. Feldmann, F. Romero, S. Kruschwitz, A. Abu-Hawash, and M. Dunn. "Multimodal condition assessment of bridge decks by NDE and its validation." *Mid-Continent Transportation Research Symposium*. Ames: Iowa State University, 2009.

Gucunski, N., R. Feldmann, F. Romero, S. Kruschwitz, and H. Parvardeh. "Comprehensive Condition Assessment of Bridge Decks by Multimodal NDE." *Nondestructive Characterization for Composite Materials, Aerospace Engineering, Civil Infrastructure, and Homeland Security*. San Diego, 2010.

Henderson, M. E., G. N. Dion, and R. D. Costley. "Acoustic Inspection of Concrete Bridge Decks." Newport Beach: Nondestructive Evaluation of Bridges and Highways III, 1999.

Horn, D. "Reliability Analysis Combining Multiple Inspection Techniques." Berlin: ECNDT, 2006.

Huston, D., J. Cui, D. Burns, and D. Hurley. "Concrete Bridge Deck Condition Assessment with Automated Multisensor Techniques." *Structure and Infrastructure Engineering*, 2010: 1-11.

Huston, D., P. Fuhr, K. Maser, and W. Weedon. "Nondestructive Testing of Reinforced Concrete Bridges Using Radar Imaging Techniques." *The New England Transportation Consortium Report*, 2002.

Kansas Department of Transportation Bureau of Local Projects Bridge Team. *Bridge Inspection Manual*. Topeka: Kansas Department of Transportation, 2012.

Kessler, R. J., R. G. Powers, E. Vivas, M. A. Paredes, and Y. P. Virmani. *Surface Resistivity as an Indicator of Concrete Chloride Penetration Resistance*. Skokie: Concrete Bridge Council, 2008.

Kohl, C., and D. Streicher. "Results of reconstructed and fused NDT-data measured in the laboratory and on-site at bridges." (*Cement & Concrete Composites*) 28 (2006).

Krauss, P. D., J. S. Lawler, and K. A. Steiner. *Guidelines for Selection of Bridge Deck Overlays, Sealers and Treatments*. National Cooperative Highway Research Program Transportation Research Board of The National Academies, 2008.

Maierhofer, C., G. Zacher, C. Kohl, and J. Wostmann. "Evaluation of Radar and Complementary Echo Methods for NDT of Concrete Elements." (*Journal of Nondestructive Evaluation*) 27 (2008).

Malhotra, V. M., and N. J. Carino. *Handbook on Nondestructive Testing of Concrete*. 2. West Cohshohocken, Pennsylvania: ASTM International, 2004.

McCafferty, E. *Introduction to Corrosion Science*. New York: Springer, 2010.

Morris, W., A. Vico, M. Vazquez, and S. R. de Sanchez. "Corrosion of Reinforcing Steel Evaluated by Means of Concrete Resistivity Measurements." *Corrosion Science* 44 (2002): 81-99.

New Jersey Department of Transportation. *Design Manual for Bridges and Structures*. 5th. Trenton: New Jersey Department of Transportation, 2009.

Parrillo, R., and R. Roberts. "Bridge Deck Condition Assessment Using Ground Penetrating Radar." *Ninth European Conference on NDT*. Berlin, 2006.

Poulsen, E., and L. Mejlbro. *Diffusion of Chloride in Concrete: Theory and Application*. New York, New York: Taylor & Francis, 2006.

Rapa, M., and W. H. Hartt. "Non-Destructive Evaluation of Jacketed Pre-Stressed Concrete Piles for Corrosion Damage." NACE, 1999.

Ryan, T., R. Hartle, J. Mann, and L. Danovich. *Bridge Inspector's Reference Manual*. Federal Highway Administration, U.S. Department of Transportation, 2006.

Virginia Department of Transportation. *Manuals of the Structure and Bridge Division*. Richmond: Virginia Department of Transportation, 2012.

Virginia Department of Transportation. *Element Data Collection Manual*. Richmond: Virginia Department of Transportation, 2007.

#### ACKNOWLEDGEMENT OF PREVIOUS PUBLICATION

Pailes, B.M., and Gucunski, N., "Statistical Correlation Method to Identify Half-Cell Potential and Electrical Resistivity Threshold Values," *Transportation Research Board 93<sup>rd</sup> Annual Meeting*, Washington, D.C., January 2014.

Pailes, B.M., Gucunski, N., and Brown, M.C., "Correlation of Non-Destructive Testing Results to Improve Assessment of Corrosion and Corrosion Damage of a Reinforced Concrete Deck," *Transportation Research Board 92<sup>nd</sup> Annual Meeting*, Washington, D.C., January 2013

APPENDICES

APPENDIX 1 – NON-DESTRUCTIVE TEST METHOD SURVEY

**Survey: Non-Destructive Evaluation of Bridges**

The following survey is intended to better understand how non-destructive evaluation (NDE) is viewed and utilized by people who are responsible for bridge maintenance and evaluation.  
**Note: Chain drag and hammer sounding are forms of NDE, however, unless specifically identified in the question they are not considered NDE in the context of this survey.**

**Respondent Information:** (All respondent information will be kept confidential)

Job Title \_\_\_\_\_ Organization \_\_\_\_\_ State \_\_\_\_\_

Question	Circle the appropriate answer			
	National	State	District	County
1	What level of infrastructure do you oversee?	Routinely	Occasionally	Never
2	Does your agency use or contract out NDE as a tool to evaluate the condition of its bridge inventory?	Yes	No	No
3	Did your agency regularly use or contract out NDE as a tool to evaluate the condition of its bridge inventory but has since stopped?	Yes	No	No
4	Does your agency have its own trained NDE personnel?	Yes	No	No
5	Does your agency use any NDE other than chain drag and hammer sounding to identify the condition of a bridge deck?	Yes	No	No
6	Does your agency use NDE to identify areas of damage in order to determine maintenance quantities?	Yes	No	No
7	Does your agency use NDE <i>only</i> to identify areas of damage in order to determine maintenance quantities?	Yes	No	No
8	Do you think NDE is an <i>effective</i> tool in the evaluation of a bridge's condition?	Yes	No	No
9	Do you think that NDE <i>accurately</i> identifies damage in a bridge structure?	Yes	No	No
10	Do you think NDE is an <i>efficient</i> tool in the evaluation of a bridge's condition?	Yes	No	No
11	Does your agency use NDE to identify areas for <i>preventative</i> maintenance?	Yes	No	No
12	Do you find that NDE helps you in making decisions regarding where, when, or how to do bridge maintenance?	Yes	No	No
13	Do you find that NDE helps you in making decisions regarding allocation of money for bridge maintenance?	Yes	No	No
14	Which of the following NDE methods are you familiar with? Check all that apply			
	Electrical Resistivity	Half-Cell Potential	Linear Polarization (3LP)	Acoustic Emission
	Ground Penetrating Radar	Infrared Thermography	Chain Drag/Hammer Sounding	Impulse Response
	Ultrasonic Surface Wave	Cross-Hole Sonic Logging	Eddy Current	Radiography
			Magnetic Flux Leakage	Other
15	What methods of NDE are your agencies personnel trained to carry out? Check all that apply			
	Electrical Resistivity	Half-Cell Potential	Linear Polarization (3LP)	Acoustic Emission
	Ground Penetrating Radar	Infrared Thermography	Chain Drag/Hammer Sounding	Impulse Response
	Ultrasonic Surface Wave	Cross-Hole Sonic Logging	Eddy Current	Radiography
			Magnetic Flux Leakage	Other
16	Which of the following NDE methods has your agency used or contracted out to evaluate the condition of a bridge deck? Check all that apply			
	Electrical Resistivity	Half-Cell Potential	Linear Polarization (3LP)	Acoustic Emission
	Ground Penetrating Radar	Infrared Thermography	Chain Drag/Hammer Sounding	Impulse Response
	Ultrasonic Surface Wave	Cross-Hole Sonic Logging	Eddy Current	Radiography
			Magnetic Flux Leakage	Other
17	Does your agency have a preferred method of NDE to evaluate a bridge deck? If yes identify the method	Yes	No	No
18	What parts of a bridge does your agency use NDE to assess the condition of? Check all that apply			
	Deck	Girders	Truss Members	Connections
			Exposed Substructure	Foundation
			Parapet	Other
19	Is there a specific part of the bridge that your agency uses NDE more on, like decks or piers? If yes identify the part	Yes	No	No
20	When performing a chain drag/hammer sounding survey to identify maintenance quantities do you increase the measured area by a factor for cost estim if yes, by how much?	Yes	No	No

The following questions refer to Figures 1 and 2

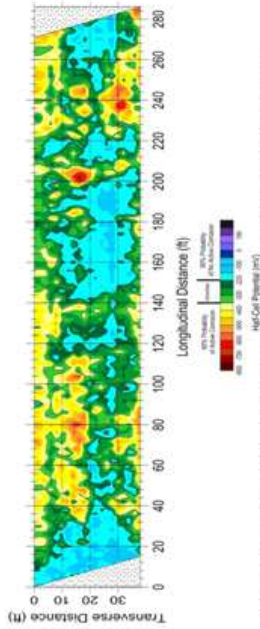
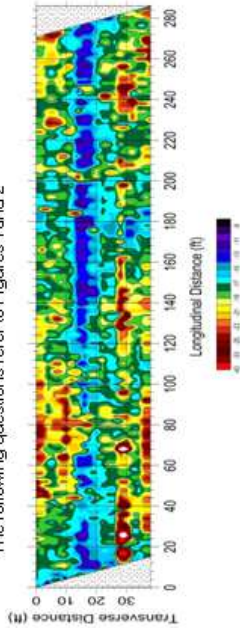


Figure 1: Ground Penetrating Radar Survey of a Reinforced Concrete Bridge Deck Figure 2: Half-Cell Potential Survey of a Reinforced Concrete Bridge Deck

- 21 FIGURE 1 - What condition state/damage type is identified by the **warm colors, red and yellow** ?  
 Sound Deck Corrosive Environment Active Corrosion Delamination Spall Unknown  
 Other Non-Corrosive Environment Passive Corrosion No Cracking No Delamination No Spall
- 22 FIGURE 1 - What condition state/damage type is identified by the **cold colors, green and blue** ?  
 Sound Deck Corrosive Environment Active Corrosion Delamination Spall Unknown  
 Other Non-Corrosive Environment Passive Corrosion No Cracking No Delamination No Spall
- 23 FIGURE 2 - What condition state/damage type is identified by the **warm colors, red and yellow** ?  
 Sound Deck Corrosive Environment Active Corrosion Delamination Spall Unknown  
 Other Non-Corrosive Environment Passive Corrosion No Cracking No Delamination No Spall
- 24 FIGURE 2 - What condition state/damage type is identified by the **cold colors, green and blue** ?  
 Sound Deck Corrosive Environment Active Corrosion Delamination Spall Unknown  
 Other Non-Corrosive Environment Passive Corrosion No Cracking No Delamination No Spall
- 25 Do you know why ground penetrating radar uses signal amplitude to evaluate a bridge deck?  
 Yes \_\_\_\_\_ No \_\_\_\_\_
- 26 Review of Figure 1 and Figure 2 reveals that the two contour maps indicate different areas of yellow and red colors. What does that mean to you?  
 Surveys are measuring two independent parameters \_\_\_\_\_ Surveys are identifying different types of concrete damage  
 Surveys are inaccurate regarding the condition of the deck \_\_\_\_\_ One survey is superior to the other in determining the deck condition  
 Other \_\_\_\_\_
- 27 Do you think that Figure 1 and Figure 2 should agree completely about the condition of the deck?  
 Yes \_\_\_\_\_ No \_\_\_\_\_
- 28 Identify what information with regards to a NDE survey would be of the highest interest to your agency for decision making? (1 being highest interest, 5 being least interest)  
 Location of Delaminations \_\_\_\_\_ Location of Cracking \_\_\_\_\_ Crack Size  
 Location of Corrosion \_\_\_\_\_ Location of Corrosive Environment \_\_\_\_\_
- 29 Rank the order of importance to your agency to identify the following condition states in reinforced concrete? (1 being most important, 6 being least important)  
 Sound Deck \_\_\_\_\_ Corrosive Environment \_\_\_\_\_ Active Corrosion \_\_\_\_\_  
 Cracking \_\_\_\_\_ Delamination \_\_\_\_\_ Spall \_\_\_\_\_
- 29 Rank what information with regards to a NDE survey would be of the highest interest to your agency for decision making? (1 being highest interest, 6 being least interest)  
 Current Condition State \_\_\_\_\_ Condition State in 5 years \_\_\_\_\_ Change in condition between surveys  
 Condition State in 3 years \_\_\_\_\_ Condition State in 10 years \_\_\_\_\_
- 30 What type of survey would you be more inclined to request on a bridge deck showing signs of deterioration?  
 Chain drag survey to identify delaminations (Cost - Low) \_\_\_\_\_  
 A GPR survey of a deck to identify areas of deterioration (Cost - Medium) \_\_\_\_\_  
 Multiple NDE method survey to identify the location of corrosion, reinforcement corrosion, cracking, and delamination (Cost - High) \_\_\_\_\_
- 31 Rank the most important factors when deciding whether or not to have a bridge deck surveyed for damage? (1 most important, 6 least important)  
 Cost of the survey \_\_\_\_\_ Importance of the bridge \_\_\_\_\_ Cost of the Bridge \_\_\_\_\_  
 Visually condition of the bridge \_\_\_\_\_ Bridge age \_\_\_\_\_ Federal/State bridge evaluation requirements \_\_\_\_\_

APPENDIX 2 – MATLAB CODE FOR MULTI-MODAL CONDITION ASSESSMENT

```

%-----Condition Assesment-----
---%

%Program by Brian M. Pailes 10/15/2013

%Inputs
%HCP - Values are in mV
%ER - Values are in kohm*cm
%GPR - Values are in dB
%CD - 1 for delamination 0 for no delamination

%Once thresholds have been identified convert it into plotable
condition data

%[HCP,ER, GPR]=textread('filename');
%DATA=[HCP,ER, GPR];

%Importing Data from research

%MN Pilot Bridge NDE data
%[long, tran, HCP, ER, IE, Cover, GPR, CD]=textread('C:\Users\Brian
Pailes\Documents\Brian Pailes\Rutgers University\Research\Data\LTBP\MN
LTBP Data\MN NDE DATA Tab Delimited.txt');
%DATA=[long, tran, HCP, ER, IE, CD, GPR, Cover];
%Carries='State Route 123';
%Spans='Kettle River';
%State='Minnesota';
%City='Sandstone';

%NY Pilot Bridge NDE Data
%[long, tran, HCP, ER, IE, Cover,GPR,PSPA,CD]=textread('C:\Users\Brian
Pailes\Documents\Brian Pailes\Rutgers University\Research\Data\LTBP\NY
LTBP Data\NY NDE DATA Tab Delimited.txt');
%DATA=[long, tran, HCP, ER, IE, CD, GPR, Cover];
%Carries='State Route 21';
%Spans='Karr Valley Creek';
%State='New York';
%City='Almond';

%NJ Pilot Bridge NDE Data
%[long, tran, HCP, ER,IE,Cover,GPR,PSPA,CD]=textread('C:\Users\Brian
Pailes\Documents\Brian Pailes\Rutgers University\Research\Data\LTBP\NJ
LTBP Data\NJ NDE DATA Tab Delimited.txt');
%DATA=[long, tran, HCP, ER, IE, CD, GPR, Cover];
%Carries='Interstate 195 East';
%Spans='Sharon Station Road';
%State='New Jersey';
%City='Upper Freehold Township';

%O2 Sumner Iowa Bridge NDE Data
%[long, tran, HCP, ER,IE,Cover,GPR,PSPA,CD]=textread('C:\Users\Brian
Pailes\Documents\Brian Pailes\Rutgers University\Research\Data\Iowa\O2
NDE DATA Tab Delimited.txt');

```

```
%DATA=[long, tran, HCP, ER, IE, CD, GPR, Cover];
%Carries='State Route 93';
%Spans='Natural Stream';
%State='Iowa';
%City='Sumner';

%O5 Indian Creek Iowa NO GPR DATA
%[long, tran, ER, HCP]=textread('C:\Users\Brian Pailes\Documents\Brian
Pailes\Rutgers University\Research\Data\Iowa\O5 NDE DATA Tab
Delimited.txt');
%DATA=[long, tran, HCP, ER, IE, CD, GPR, Cover];
%Carries='';
%Spans='';
%State='Iowa';
%City='';

%O6 Villisca Iowa NO GPR DATA
%[long, tran, ER, HCP]=textread('C:\Users\Brian Pailes\Documents\Brian
Pailes\Rutgers University\Research\Data\Iowa\O6 NDE DATA Tab
Delimited.txt');
%DATA=[long, tran, HCP, ER, IE, CD, GPR, Cover];
%Carries='';
%Spans='';
%State='Iowa';
%City='';

%I495 Wilmington DE
%[long, tran, HCP, ER]=textread('C:\Users\Brian Pailes\Documents\Brian
Pailes\Rutgers University\Research\Data\LTBP\I 495 South over Rt 13-
Wilmington DE\I495 NDE DATA Tab Delimited.txt');
%DATA=[long, tran, HCP, ER, IE, CD, GPR, Cover];
%Carries='Interstate 495 South';
%Spans='Route 13';
%State='Delaware';
%City='Wilmington';

%Pequea Blvd Conestoga PA
%[long, tran, HCP, ER]=textread('C:\Users\Brian Pailes\Documents\Brian
Pailes\Rutgers University\Research\Data\LTBP\Pequea Blvd over Pequea
Creek-Conestoga PA\Pequea Blvd NDE DATA Tab Delimited.txt');
%DATA=[long, tran, HCP, ER, IE, CD, GPR, Cover];
%Carries='Pequea Boulevard';
%Spans='Pequea Creek';
%State='Pennsylvania';
%City='Conestoga';

%Rt 18 Neptune NJ
%[long, tran, HCP, ER]=textread('C:\Users\Brian Pailes\Documents\Brian
Pailes\Rutgers University\Research\Data\LTBP\Rt 18 over Rt 66-Neptune
NJ\Rt 18 NDE DATA Tab Delimited.txt');
%DATA=[long, tran, HCP, ER, IE, CD, GPR, Cover];
%Carries='State Route 18';
%Spans='State Route 66';
%State='New Jersey';
%City='Neptune';
```

```

%Rt 47 Deptford Township NJ
%[long, tran, HCP, ER]=textread('C:\Users\Brian Pailes\Documents\Brian
Pailes\Rutgers University\Research\Data\LTBP\Rt 47 over Rt 55-Deptford
Township NJ\Rt 47 NDE DATA Tab Delimited.txt');
%DATA=[long, tran, HCP, ER, IE, CD, GPR, Cover];
%Carries='State Route 47';
%Spans='State Route 55';
%State='New Jersey';
%City='Deptford Township';

%Rt 273 Elkton MD
%[long, tran, HCP, ER]=textread('C:\Users\Brian Pailes\Documents\Brian
Pailes\Rutgers University\Research\Data\LTBP\Rt 273 over Little Elk
Creek-Elkton MD\Rt 273 NDE DATA Tab Delimited.txt');
%DATA=[long, tran, HCP, ER, IE, CD, GPR, Cover];
%Carries='State Route 273';
%Spans='Little Elk Creek';
%State='Maryland';
%City='Elkton';

%School House Rd Middletown PA
%[long, tran, HCP, ER]=textread('C:\Users\Brian Pailes\Documents\Brian
Pailes\Rutgers University\Research\Data\LTBP\School House Rd over Rt
283-Middletown PA\School House Rd NDE DATA Tab Delimited.txt');
%DATA=[long, tran, HCP, ER, IE, CD, GPR, Cover];
%Carries='School House Road';
%Spans='State Route 283';
%State='Pennsylvania';
%City='Middletown';

%West Bangs Neptune NJ
%[long, tran, HCP, ER]=textread('C:\Users\Brian Pailes\Documents\Brian
Pailes\Rutgers University\Research\Data\LTBP\West Bangs Ave over Rt 18-
Neptune NJ\West Bangs NDE DATA Tab Delimited.txt');
%DATA=[long, tran, HCP, ER, IE, CD, GPR, Cover];
%Carries='West Bangs Ave';
%Spans='State Route 18';
%State='New Jersey';
%City='Neptune';

%NOTE: when using VA pilot bridge data there are two years
%VA 2009 Pilot Bridge NDE Data
[long, tran, HCP, ER, IE, CD, GPR, Cover]=textread('C:\Users\Brian
Pailes\Documents\Brian Pailes\Rutgers University\Research\Data\LTBP\VA
LTBP Data\VA 2009 NDE DATA Tab Delimited.txt');
DATA=[long, tran, HCP, ER, IE, CD, GPR, Cover];
Carries='State Route 15';
Spans='Interstate 66';
State='Virginia';
City='Haymarket';

%VA 2011 Pilot Bridge NDE Data
%[long, tran, HCP, ER, IE, CD, GPR, Cover]=textread('C:\Users\Brian
Pailes\Documents\Brian Pailes\Rutgers University\Research\Data\LTBP\VA
LTBP Data\VA 2011 NDE DATA Tab Delimited.txt');
%DATA=[long, tran, HCP, ER, IE, CD, GPR, Cover];

```

```

%Carries='State Route 15';
%Spans='Interstate 66';
%State='Virginia';
%City='Haymarket';

%False Data used to check code
%[long, tran, HCP, ER,IE,Cover,GPR,PSPA,CD]=textread('C:\Users\Brian
Pailes\Documents\Brian Pailes\Rutgers University\Research\Data\FAKE
BRIDGE DECK DATA Tab Delimited.txt');
%DATA=[long, tran, HCP, ER,IE,Cover,GPR,PSPA,CD];

%determines number of data points
[AA,BB]=size(DATA);

%-----HCP Threshold Analysis-----
---%

%Filters HCP data based on the ER value at the same test location

    %Defines the "active" end of the ER scale
    k=1;
    ERlowlimit=30;
    ERlow=5;
    ERinc=5;
    ERnum=(ERlowlimit-ERlow)/ERinc)+1;

    %Filters out the HCP data based on the ER value and increments
    while(ERlow<=ERlowlimit)
        j=1;
        i=1;
        while(j<=AA)
            if(ER(j,1)<=ERlow)
                HCPActiveValues(i,k)=HCP(j,1);
                i=i+1;
            else
                i=i;
            end
            j=j+1;
        end
        istore(k,1)=i;
        ERlow=ERlow+ERinc;
        k=k+1;
    end

    %Defines the "passive" end of the ER scale

    [ii,kk]=size(HCPActiveValues);

    k=1+kk;
    ERhighlimit=95;
    ERhigh=70;
    ERinc=5;
    ERnum=(ERhighlimit-ERhigh)/ERinc)+1;
    while(ERhigh<=ERhighlimit)
        j=1;

```

```

    i=1;
    while(j<=AA)
        if(ER(j,1)>=ERhigh)
            HCPActiveValues(i,k)=HCP(j,1);
            i=i+1;
        else
            i=i;
        end
        j=j+1;
    end
    istore(k,1)=i;
    ERhigh=ERhigh+ERinc;
    k=k+1;
end

%Resets high and low limit on ER filtering
ERlow=5;
ERhigh=70;

%Replaces any zeros that are artificially entered into the matrix
with 99999
[ii,jj]=size(HCPActiveValues);

maxval=max(istore);
k=1;
while(k<=jj)
    i=istore(k,1);
    while(i<maxval)
        HCPActiveValues(i,k)=99999;
        i=i+1;
    end
    k=k+1;
end

%Creates the bins for the frequency analysis
i=1;
HCPBinHigh=60;
HCPBinLow=-700;
HCPBinInc=38;
HCPBinCorection=HCPBinInc/2;
while(HCPBinLow<=HCPBinHigh)
    HCPBins(i,1)=HCPBinLow-HCPBinCorection;
    HCPBinLow=HCPBinLow+HCPBinInc;
    i=i+1;
end
HCPBins(21,1)=90000;

%frequency analysis
HCPfreq=hist(HCPActiveValues,HCPBins);

%Removes the 99999 values entered earlier
[ii,jj]=size(HCPfreq);
k=1;
while(k<=jj)
    i=1;
    while(i<ii)

```

```

        HCPfreqreal(i,k)=HCPfreq(i,k);
        i=i+1;
    end
    k=k+1;
end

%Calculation of cumulative frequency
[ii,jj]=size(HCPfreqreal);
k=1;
while(k<=jj)
    i=1;
    while(i<=ii)
        j=i-1;
        if(i==1)
            HCPcummlative(i,k)=HCPfreqreal(i,k);
        else
            HCPcummlative(i,k)=HCPfreqreal(i,k)+HCPcummlative(j,k);
        end
        i=i+1;
    end
    k=k+1;
end

%Turning cummulative frequency into a percent
HCPsum=sum(HCPfreqreal);
[ii,jj]=size(HCPcummlative);
k=1;
while(k<=jj)
    i=1;
    while(i<=ii)
        HCPcummlativepercent(i,k)=(HCPcummlative(i,k)/HCPsum(1,k))*100;
        i=i+1;
    end
    k=k+1;
end

%Calculation of first derivative
[ii,jj]=size(HCPcummlativepercent);

k=1;
while(k<=jj)
    i=2;
    while(i<=ii)
        j=i+1;
        m=i-1;
        HCPFirstDerivative(i,k)=(HCPcummlativepercent(j,k)-
HCPcummlativepercent(m,k))/(2*HCPBinInc);
        i=i+1;
    end
    k=k+1;
end

%Creating a matrix for the ER's increments used in filtering

i=1;

```

```

ERvalue=ERlow;
while(ERvalue<=ERlowlimit)
    ERbinsforHCP(i,1)=ERvalue;
    ERvalue=ERinc+ERvalue;
    i=i+1;
end
ERvalue=ERhigh;
while(ERvalue<=ERhighlimit)
    ERbinsforHCP(i,1)=ERvalue;
    ERvalue=ERinc+ERvalue;
    i=i+1;
end

%Check to see if each ER filter has HCP values in it

[ii,jj]=size(HCPcummlative);
j=1;
while(j<=jj)
    aCheck=HCPcummlative(ii,j);
    if(aCheck>0)
        HCPcheck=1;
    else
        HCPcheck=0;
        j=jj;
    end
    j=j+1;
end

if(HCPcheck==1)

    %Determining where first derivative of the "active" ER filters
crosses      %"passive" ER filter

    ERnumlow=((ERlowlimit-ERlow)/ERinc)+1;
    ERnumhigh=((ERhighlimit-ERhigh)/ERinc)+1;

    %Locate location to start intersection identification
    [ii,jj]=size(HCPFirstDerivative);
    j=1;
    while(j<=6)
        i=1;
        while(i<=ii)
            Startvalue=HCPFirstDerivative(i,j);
            if(Startvalue>=.05)
                if(j==1)
                    Start5=i;
                elseif(j==2)
                    Start10=i;
                elseif(j==3)
                    Start15=i;
                elseif(j==4)
                    Start20=i;
                elseif(j==5)
                    Start25=i;
                else
                    Start30=i;
                end
            end
            i=i+1;
        end
        j=j+1;
    end
end

```



```

        xi=(a2-a1)/(b1-b2);
        yi=b1*xi+a1;

        check1=(x1-xi)*(xi-x2);
        check2=(u1-xi)*(xi-u2);

        if (check1>=0) && (check2>=0) && (abs(yi)>0)

HCPintersection(w,1)=HCPBins(i,1)+HCPBinCorection;

HCPintersection(w,2)=HCPFirstDerivative(i,k);

HCPintersection(w,3)=HCPBins(j,1)+HCPBinCorection;

HCPintersection(w,4)=HCPFirstDerivative(j,k);

HCPintersection(w,5)=HCPBins(n,1)+HCPBinCorection;

HCPintersection(w,6)=HCPFirstDerivative(n,m);

HCPintersection(w,7)=HCPBins(p,1)+HCPBinCorection;

HCPintersection(w,8)=HCPFirstDerivative(p,m);
                HCPintersection(w,9)=xi;
                HCPintersection(w,10)=yi;
                HCPintersection(w,11)=k;
                HCPintersection(w,12)=m;
                w=w+1;
        else
                i=i;
        end
    end
end
    end
        n=n+1;

        end
        i=i+1;
    end
        m=m+1;
end
    k=k+1;

end

    %If there are multiple intersections by one curve with another it
selects
    %only 1
    i=1;
    [ii,jj]=size(HCPintersection);
    while(i<ii)
        j=i+1;
        mean1=mean(HCPintersection);
        mean11=mean1(1,9);

```

```

if(HCPIntersection(i,11)==HCPIntersection(j,11))&&(HCPIntersection(i,12)
)==HCPIntersection(j,12))

    Delta1=abs(mean11-HCPIntersection(i,9));
    Delta2=abs(mean11-HCPIntersection(j,9));
    if(Delta1<Delta2)

HCPIntersection=HCPIntersection(setdiff(1:size(HCPIntersection,1),[j]),
:);

        else

HCPIntersection=HCPIntersection(setdiff(1:size(HCPIntersection,1),[i]),
:);

            end
            i=i;
            [ii,jj]=size(HCPIntersection);
        else
            i=i+1;
        end

    end

25 %Determines the active threshold rounded to the nearest integer of
sum11=0;
i=1;
[ii,jj]=size(HCPIntersection);
while(i<=ii)
    sum11=HCPIntersection(i,9)+sum11;
    i=i+1;
end

HCPActiveRAW=sum11/ii;
HCPRemainder=HCPActiveRAW/25;
HCPfactor=round(HCPRemainder);
HCPActive=HCPfactor*25;

%The method of finding the passive threshold will be when the slope
%of cumulative frequency plot for low ER values gets below 0.025.

%Primary method of passive threshold analysis
[ii,jj]=size(HCPFirstDerivative);
k=1;
while(k<=jj)
    [ii,jj]=size(HCPFirstDerivative);
    while(ii>1)
        if(abs(HCPFirstDerivative(ii,k))<0.025)
            ii=ii-1;
        else
            ii=ii+1;
            HCPSecondLimit(1,k)=HCPBins(ii,1)+HCPBinCorection;
            ii=1;
        end
    end
    k=k+1;
end

```

```

end

%Determine which method of passive threshold analysis to use

sum1=0;
i=1;

while(i<=ERnumlow)
    sum1=HCPSecondLimit(1,i)+sum1;
    i=i+1;
end

HCPPassiveRAW=sum1/ERnumlow;
HCPRemainder=HCPPassiveRAW/25;
HCPfactor=round(HCPRemainder);
HCPPassive=HCPfactor*25;

%If the passive threshold is abnormally low, then rechecking the
threshold
%using a slope of 0.05

if(HCPPassive>-100)
    [ii,jj]=size(HCPFirstDerivative);
    k=1;
    while(k<=jj)
        [ii,jj]=size(HCPFirstDerivative);
        while(ii>1)
            if(abs(HCPFirstDerivative(ii,k))<0.05)
                ii=ii-1;
            else
                ii=ii+1;
                HCPSecondLimit2(1,k)=HCPBins(ii,1)+HCPBinCorection;
                ii=1;
            end
        end
        k=k+1;
    end

sum2=0;
i=1;

while(i<=ERnumlow)
    sum2=HCPSecondLimit2(1,i)+sum2;
    i=i+1;
end
HCPPassiveRAW=sum2/ERnumlow;
HCPRemainder=HCPPassiveRAW/25;
HCPfactor=round(HCPRemainder);
HCPPassive=HCPfactor*25;
else
end

str1=sprintf('The threshold for active corrosion is %d mV',
HCPActive);

```

```

    str2=sprintf('The threshold for passive condition is %d mV',
HCPPassive);

    disp(str1);
    disp(str2);

    else
        HCPActive=-350;
        HCPPassive=-200;

        disp('The deck has ER values that indicate a deck in excellent
condition');
        disp('There are not enough low ER values to perform this
analysis');
        disp('The HCP threshold values will be set as default values');
        str1=sprintf('The threshold for active corrosion is %d mV',
HCPActive);
        str2=sprintf('The threshold for passive condition is %d mV',
HCPPassive);

        disp(str1);
        disp(str2);
    end

    %-----ER Threshold Analysis-----
    -----%

    [AA,BB]=size(DATA);

    %Creates the ER Bins for cumulative frequency
    ERlow=5;
    ERhigh=100;
    ERinc=5;
    ERbincor=ERinc/2;
    num= ((ERhigh-ERlow)/ERinc)+1;
    i=1;
    k=ERlow;
    while(i<=num)
        ERBins(i,1)=k-ERbincor;
        k=k+ERinc;
        i=i+1;
    end

    %Filters ER data if HCP is less than equal to active threshold
    indicatorER1=0;
    i=1;
    k=1;
    while(i<=AA)
        if(HCP(i,1)<=HCPActive)
            ERActive(k,1)=ER(i,1);
            k=k+1;
            i=i+1;
            indicatorER1=1;
        else
            i=i+1;
        end
    end

```

```

        end
    end

    %Filters ER data if HCP is greater than equal to passive threshold
    indicatorER2=0;
    i=1;
    k=1;
    while(i<=AA)
        if(HCP(i,1)>=HCPPassive)
            ERPassive(k,1)=ER(i,1);
            k=k+1;
            i=i+1;
            indicatorER2=1;
        else
            i=i+1;
        end
    end

    if(indicatorER1==1)&&(indicatorER2==1)
        FAILer=1;
        %Frequency analysis
        ERfreqactive=hist(ERActive,ERBins);
        ERfreqactive=transpose(ERfreqactive);
        ERfreqpassive=hist(ERPassive,ERBins);
        ERfreqpassive=transpose(ERfreqpassive);

        %Calculation of cumulative frequency
        %Note: analysis excludes last row, this is frequency of ER values
        over 99
        %which are statistically higher due to limits of ER device

        [ii,jj]=size(ERfreqactive);
        i=1;
        while(i<ii)
            if(i==1)
                ERcumulativeActive(i,1)=ERfreqactive(i,1);
            else
                j=i-1;
                ERcumulativeActive(i,1)=ERfreqactive(i,1)+ERcumulativeActive(j,1);
            end
            i=i+1;
        end

        [ii,jj]=size(ERfreqpassive);
        i=1;
        while(i<ii)
            if(i==1)
                ERcumulativePassive(i,1)=ERfreqpassive(i,1);
            else
                j=i-1;
                ERcumulativePassive(i,1)=ERfreqpassive(i,1)+ERcumulativePassive(j,1);
            end
            i=i+1;
        end
    end
end

```

```

%Turning cumulative frequency into a percent
[ii,jj]=size(ERfreqactive);
sumA=sum(ERfreqactive)-ERfreqactive(ii,jj);
[ii,jj]=size(ERCumulativeActive);
i=1;
while(i<=ii)

ERCumulativeActivePercent(i,1)=(ERCumulativeActive(i,1)/sumA)*100;
    i=i+1;
end

[ii,jj]=size(ERfreqpassive);
sumP=sum(ERfreqpassive)-ERfreqpassive(ii,jj);
[ii,jj]=size(ERCumulativePassive);
i=1;
while(i<=ii)

ERCumulativePassivePercent(i,1)=(ERCumulativePassive(i,1)/sumP)*100;
    i=i+1;
end

%The analysis method calculates the difference between the active
and
%passive cumulative frequency curves and locates the maximum value

[ii,jj]=size(ERCumulativeActive);
i=1;
while(i<=ii)
    ERdifference(i,1)=ERCumulativeActivePercent(i,1)-
ERCumulativePassivePercent(i,1);
    i=i+1;
end

%Finding the average of the maximum three values in difference
ERdiffsort=sort(ERdifference);
[ii,jj]=size(ERdiffsort);
iia=ii-1;
iib=ii-2;
a=ERdiffsort(ii,1);
b=ERdiffsort(iia,1);
c=ERdiffsort(iib,1);

i=1;
while(i<=ii)
    test=ERdifference(i,1);

    if(a==test)
        ERValue1=ERBins(i,1)+ERbincor;
        a=999999999;
    elseif(b==test)
        ERValue2=ERBins(i,1)+ERbincor;
        b=999999999;
    elseif(c==test)
        ERValue3=ERBins(i,1)+ERbincor;

```

```

        c=99999999;
    end
    i=i+1;
end

%Runs through a check to make sure that there are no outliers in
the
%averaging for the ER threshold

ERAverage3=(ERValue1+ERValue2+ERValue3)/3;
ERAverage2=(ERValue1+ERValue2)/2;
ERAverage1=ERValue1;

ERAverage3Check=abs(100-(ERAverage3/ERAverage1)*100);
ERAverage2Check=abs(100-(ERAverage2/ERAverage1)*100);

if(ERAverage3Check>=20)
    if(ERAverage2Check>=ERAverage3Check)
        ERThreshold=round(ERAverage3);
    else
        ERThreshold=round(ERAverage2);
    end
else
    ERThreshold=round(ERAverage3);
end

else
    FAILer=0;
end

    if(FAILer==1)
        str8=sprintf('The ER Threshold is %d kohm*cm',
ERThreshold);
        disp(str8);
    else
        disp('Due to no correlation between ER and HCP a default
value of');
        disp('40 kohm*cm will be used as the ER threshold')
        ERThreshold=40;
    end

%-----GPR Threshold Analysis-----
-----%

%determines number of data points
[AA, BB]=size(DATA);

%Creates the GPR Bins for cumulative frequency
GPRlow=-40;
GPRhigh=-0.5;
GPRinc=0.5;
GPRbincor=GPRinc/2;
num=((GPRhigh-GPRlow)/GPRinc)+1;
i=1;

```

```

k=GPRlow;
while(i<=num)
    GPRbins(i,1)=k-GPRbincor;
    k=k+GPRinc;
    i=i+1;
end

%Filters GPR data if HCP is less than equal to active threshold, ER
is less
%than or equal to threshold, and if CD=1
indicatorGPR1=0;
indicatorGPR2=0;
indicatorGPR3=0;

i=1;
k=1;
while(i<=AA)
    if(HCP(i,1)<=HCPActive)&&(ER(i,1)<=ERThreshold)&&(CD(i,1)==1)
        GPRactive(k,1)=GPR(i,1);
        k=k+1;
        i=i+1;
        indicatorGPR1=1;
    elseif(HCP(i,1)<=HCPActive)&&(ER(i,1)<=ERThreshold)&&(CD(i,1)==3)
        GPRactive(k,1)=GPR(i,1);
        k=k+1;
        i=i+1;
        indicatorGPR1=1;
    else
        i=i+1;
    end
end

%Filters Data if ER is less than threshold and CD=1
i=1;
k=1;
while(i<=AA)
    if(ER(i,1)<=ERThreshold)&&(CD(i,1)==1)
        GPRactive2(k,1)=GPR(i,1);
        k=k+1;
        i=i+1;
        indicatorGPR2=1;
    elseif(ER(i,1)<=ERThreshold)&&(CD(i,1)==3)
        GPRactive2(k,1)=GPR(i,1);
        k=k+1;
        i=i+1;
        indicatorGPR2=1;
    else
        i=i+1;
    end
end

%Filters data if ER and HCP are less than threshold
i=1;
k=1;
while(i<=AA)

```

```

        if(ER(i,1)<=ERThreshold)&&(HCP(i,1)<=HCPActive)
            GPRactive3(k,1)=GPR(i,1);
            k=k+1;
            i=i+1;
            indicatorGPR3=1;
        else
            i=i+1;
        end
    end
end

%Filters GPR data if HCP is greater than equal to passive
threshold, ER is
%greater than threshold, and CD=0
indicatorGPR4=0;
indicatorGPR5=0;
indicatorGPR6=0;

i=1;
k=1;
while(i<=AA)
    if(HCP(i,1)>=HCPPassive)&&(ER(i,1)>ERThreshold)&&(CD(i,1)==0)
        GPRpassive(k,1)=GPR(i,1);
        k=k+1;
        i=i+1;
        indicatorGPR4=1;
    elseif(HCP(i,1)>=HCPPassive)&&(ER(i,1)>ERThreshold)&&(CD(i,1)==2)
        GPRpassive(k,1)=GPR(i,1);
        k=k+1;
        i=i+1;
        indicatorGPR4=1;
    else
        i=i+1;
    end
end

%Filters Data if ER is greater than threshold and CD=0
i=1;
k=1;
while(i<=AA)
    if(ER(i,1)>ERThreshold)&&(CD(i,1)==0)
        GPRpassive2(k,1)=GPR(i,1);
        k=k+1;
        i=i+1;
        indicatorGPR5=1;
    elseif(ER(i,1)>ERThreshold)&&(CD(i,1)==2)
        GPRpassive2(k,1)=GPR(i,1);
        k=k+1;
        i=i+1;
        indicatorGPR5=1;
    else
        i=i+1;
    end
end

%Filters data if ER and HCP are greater than threshold

```

```

i=1;
k=1;
while(i<=AA)
    if(ER(i,1)>ERThreshold)&&(HCP(i,1)>=HCPPassive)
        GPRpassive3(k,1)=GPR(i,1);
        k=k+1;
        i=i+1;
        indicatorGPR6=1;
    else
        i=i+1;
    end
end

%The analysis has been separated for each of the three filtering
options

if(indicatorGPR1==1)&&(indicatorGPR4==1)
    FAIL1=1;
    %ER, HCP, and CD filter analysis

    %frequency analysis
    GPRfreqactive=hist(GPRactive,GPRbins);
    GPRfreqactive=transpose(GPRfreqactive);
    GPRfreqpassive=hist(GPRpassive,GPRbins);
    GPRfreqpassive=transpose(GPRfreqpassive);

    %calculation of cumulative frequency
    [ii,jj]=size(GPRfreqactive);
    i=1;
    while(i<ii)
        if(i==1)
            GPRcumulativeActive(i,1)=GPRfreqactive(i,1);
        else
            j=i-1;

GPRcumulativeActive(i,1)=GPRfreqactive(i,1)+GPRcumulativeActive(j,1);
            end
            i=i+1;
        end

        [ii,jj]=size(GPRfreqpassive);
        i=1;
        while(i<ii)
            if(i==1)
                GPRcumulativePassive(i,1)=GPRfreqpassive(i,1);
            else
                j=i-1;

GPRcumulativePassive(i,1)=GPRfreqpassive(i,1)+GPRcumulativePassive(j,1);
            end
            i=i+1;
        end

    %turning cumulative frequency into a percent
    sumAA=sum(GPRfreqactive);
    [ii,jj]=size(GPRcumulativeActive);

```

```

j=1;
i=1;
while(i<=ii)

GPRcumulativeActivePercent(i,j)=(GPRcumulativeActive(i,j)/sumAA)*100;
    i=i+1;
end

sumPP=sum(GPRfreqpassive);
[ii,jj]=size(GPRcumulativePassive);
j=1;
i=1;
while(i<=ii)

GPRcumulativePassivePercent(i,j)=(GPRcumulativePassive(i,j)/sumPP)*100;
    i=i+1;
end

%The analysis method calculates the difference between the
active and
%passive cumulative frequency curves and locates the maximum
value

[ii,jj]=size(GPRcumulativeActive);
j=1;
i=1;
while(i<=ii)
    GPRdifference(i,j)=GPRcumulativeActivePercent(i,j)-
GPRcumulativePassivePercent(i,j);
    i=i+1;
end

%finding the average of the maximum three values in difference
GPRdiffsort1=sort(GPRdifference(:,1));
[ii,jj]=size(GPRdiffsort1);
iia=ii-1;
iib=ii-2;
a=GPRdiffsort1(iia,1);
b=GPRdiffsort1(iib,1);
c=GPRdiffsort1(iib,1);

i=1;
while(i<=ii)
    test=GPRdifference(i,1);
    if(a==test)
        GPRValue11=GPRbins(i,1)+GPRbincor;
        a=9999999;
    elseif(b==test)
        GPRValue21=GPRbins(i,1)+GPRbincor;
        b=9999999;
    elseif(c==test)
        GPRValue31=GPRbins(i,1)+GPRbincor;
        c=9999999;
    end
    i=i+1;
end
end

```

```

        GPRAverage1=(GPRValue11+GPRValue21+GPRValue31)/3;
    else
        FAIL1=0;
    end

    if(indicatorGPR2==1)&&(indicatorGPR5==1)
        FAIL2=1;
        %ER and CD filter analysis

        %frequency analysis
        GPRfreqactive2=hist(GPRactive2,GPRbins);
        GPRfreqactive2=transpose(GPRfreqactive2);
        GPRfreqpassive2=hist(GPRpassive2,GPRbins);
        GPRfreqpassive2=transpose(GPRfreqpassive2);

        %calculation of cumulative frequency
        [ii,jj]=size(GPRfreqactive2);
        i=1;
        while(i<ii)
            if(i==1)
                GPRcumulativeActive(i,2)=GPRfreqactive2(i,1);
            else
                j=i-1;
            end
            GPRcumulativeActive(i,2)=GPRfreqactive2(i,1)+GPRcumulativeActive(j,2);
            i=i+1;
        end

        [ii,jj]=size(GPRfreqpassive2);
        i=1;
        while(i<ii)
            if(i==1)
                GPRcumulativePassive(i,2)=GPRfreqpassive2(i,1);
            else
                j=i-1;
            end
            GPRcumulativePassive(i,2)=GPRfreqpassive2(i,1)+GPRcumulativePassive(j,2);
            i=i+1;
        end

        %turning cumulative frequency into a percent
        sumAA2=sum(GPRfreqactive2);
        [ii,jj]=size(GPRcumulativeActive);
        j=2;
        i=1;
        while(i<=ii)
            GPRcumulativeActivePercent(i,j)=(GPRcumulativeActive(i,j)/sumAA2)*100;
            i=i+1;
        end
    end
end

```

```

sumPP2=sum(GPRfreqpassive2);
[ii,jj]=size(GPRcumulativePassive);
j=2;
i=1;
while(i<=ii)

GPRcumulativePassivePercent(i,j)=(GPRcumulativePassive(i,j)/sumPP2)*100;
    i=i+1;
end

    %The analysis method calculates the difference between the
active and
    %passive cumulative frequency curves and locates the maximum
value

    [ii,jj]=size(GPRcumulativeActive);
j=2;
i=1;
while(i<=ii)
    GPRdifference(i,j)=GPRcumulativeActivePercent(i,j)-
GPRcumulativePassivePercent(i,j);
    i=i+1;
end

    %finding the average of the maximum three values in difference
GPRdiffsort2=sort(GPRdifference(:,2));
[ii,jj]=size(GPRdiffsort2);
iia=ii-1;
iib=ii-2;
a2=GPRdiffsort2(ii,1);
b2=GPRdiffsort2(iia,1);
c2=GPRdiffsort2(iib,1);

i=1;
while(i<=ii)
    test=GPRdifference(i,2);
    if(a2==test)
        GPRValue12=GPRbins(i,1)+GPRbincor;
        a2=9999999;
    elseif(b2==test)
        GPRValue22=GPRbins(i,1)+GPRbincor;
        b2=9999999;
    elseif(c2==test)
        GPRValue32=GPRbins(i,1)+GPRbincor;
        c2=9999999;
    end
    i=i+1;
end

GPRAverage2=(GPRValue12+GPRValue22+GPRValue32)/3;
else
    FAIL2=0;
end

```

```

if(indicatorGPR3==1)&&(indicatorGPR6==1)
    FAIL3=1;
    %ER HCP filter analysis

    %frequency analysis
    GPRfreqactive3=hist(GPRactive3,GPRbins);
    GPRfreqactive3=transpose(GPRfreqactive3);
    GPRfreqpassive3=hist(GPRpassive3,GPRbins);
    GPRfreqpassive3=transpose(GPRfreqpassive3);

    %calculation of cumulative frequency
    [ii,jj]=size(GPRfreqactive3);
    i=1;
    while(i<ii)
        if(i==1)
            GPRcumulativeActive(i,3)=GPRfreqactive3(i,1);
        else
            j=i-1;

GPRcumulativeActive(i,3)=GPRfreqactive3(i,1)+GPRcumulativeActive(j,3);
            end
            i=i+1;
        end

        [ii,jj]=size(GPRfreqpassive3);
        i=1;
        while(i<ii)
            if(i==1)
                GPRcumulativePassive(i,3)=GPRfreqpassive3(i,1);
            else
                j=i-1;

GPRcumulativePassive(i,3)=GPRfreqpassive3(i,1)+GPRcumulativePassive(j,3);
            end
            i=i+1;
        end

        %turning cumulative frequency into a percent
        sumAA3=sum(GPRfreqactive3);
        [ii,jj]=size(GPRcumulativeActive);
        j=3;
        i=1;
        while(i<=ii)

GPRcumulativeActivePercent(i,j)=(GPRcumulativeActive(i,j)/sumAA3)*100;
            i=i+1;
        end

        sumPP3=sum(GPRfreqpassive3);
        [ii,jj]=size(GPRcumulativePassive);
        j=3;
        i=1;
        while(i<=ii)

GPRcumulativePassivePercent(i,j)=(GPRcumulativePassive(i,j)/sumPP3)*100;
            i=i+1;
        end
    end
end

```

```

end

    %The analysis method calculates the difference between the
active and
    %passive cumulative frequency curves and locates the maximum
value

    [ii,jj]=size(GPRcumulativeActive);
    j=3;
    i=1;
    while(i<=ii)
        GPRdifference(i,j)=GPRcumulativeActivePercent(i,j)-
GPRcumulativePassivePercent(i,j);
        i=i+1;
    end

    %finding the average of the maximum three values in difference
GPRdiffsort3=sort(GPRdifference(:,3));

    [ii,jj]=size(GPRdiffsort3);
    iia=ii-1;
    iib=ii-2;
    a3=GPRdiffsort3(ii,1);
    b3=GPRdiffsort3(iia,1);
    c3=GPRdiffsort3(iib,1);

    i=1;
    while(i<=ii)
        test=GPRdifference(i,3);
        if(a3==test)
            GPRValue13=GPRbins(i,1)+GPRbincor;
            a3=99999999;
        elseif(b3==test)
            GPRValue23=GPRbins(i,1)+GPRbincor;
            b3=99999999;
        elseif(c3==test)
            GPRValue33=GPRbins(i,1)+GPRbincor;
            c3=99999999;
        end
        i=i+1;
    end

    GPRAverage3=(GPRValue13+GPRValue23+GPRValue33)/3;
else
    FAIL3=0;
end

%Determines which values to average
counter=0;
if(FAIL1==0) && (FAIL2==0) && (FAIL3==0)
    if(indicatorGPR1==1)
        maxActive1=max(GPRactive);
        counter=counter+1;
    else
        maxActive1=0;
    end
end

```

```

end
if(indicatorGPR2==1)
    maxActive2=max(GPRactive2);
    counter=counter+1;
else
    maxActive2=0;
end
if(indicatorGPR3==1)
    maxActive3=max(GPRactive3);
    counter=counter+1;
else
    maxActive3=0;
end
if(indicatorGPR4==1)
    minPassive1=min(GPRpassive);
    counter=counter+1;
else
    minPassive1=0;
end
if(indicatorGPR5==1)
    minPassive2=min(GPRpassive2);
    counter=counter+1;
else
    minPassive2=0;
end
if(indicatorGPR6==1)
    minPassive3=min(GPRpassive3);
    counter=counter+1;
else
    minPassive3=0;
end

if(counter>0)

GPRAverage=(maxActive1+maxActive2+maxActive3+minPassive1+minPassive2+mi
nPassive3)/counter;
    disp('There are no locations that correlate between ER,
HCP, and CD');
    disp('The GPR threshold identified by the min and max GPR
values found in limited filtering');
    disp('If the min/max value is 0 then it has no instances on
this bridge and is not used in the average');
    str7=sprintf('Max Active HCP ER CD Filtering %g dB',
maxActive1);
    str8=sprintf('Max Active ER CD Filtering %g dB',
maxActive2);
    str9=sprintf('Max Active HCP ER Filtering %g dB',
maxActive3);
    str10=sprintf('Min Passive HCP ER CD Filtering %g dB',
minPassive1);
    str11=sprintf('Min Passive ER CD Filtering %g dB',
minPassive2);
    str12=sprintf('Min Passive HCP ER Filtering %g dB',
minPassive3);
    disp(str7);
    disp(str8);
    disp(str9);

```

```

        disp(str10);
        disp(str11);
        disp(str12);
    else
        GPRAverage=mean(GPR);
        disp('There are no locations that correlate between ER,
HCP, and CD');
        disp('GPR threshold will be the average GPR amplitude %g
dB');
    end

elseif(FAIL1==0) && (FAIL2==0)
    GPRAverage=(GPRAverage3);

    str4=sprintf('The GPR threshold identified by the ER and HCP
filter is %g dB', GPRAverage3);
    disp('There is no GPR threshold identified by the ER, HCP, and
CD filter');
    disp('There is no GPR threshold identified by the ER and CD
filter');
    disp(str4);

elseif(FAIL1==0) && (FAIL3==0)
    GPRAverage=(GPRAverage2);

    str3=sprintf('The GPR threshold identified by the ER and CD
filter is %g dB', GPRAverage2);
    disp('There is no GPR threshold identified by the ER, HCP, and
CD filter');
    disp(str3);
    disp('There is no GPR threshold identified by the ER and HCP
filter');

elseif(FAIL2==0) && (FAIL3==0)
    GPRAverage=(GPRAverage1);

    str2=sprintf('The GPR threshold identified by the ER, HCP, and
CD filter is %g dB', GPRAverage1);
    disp(str2);
    disp('There is no GPR threshold identified by the ER and CD
filter');
    disp('There is no GPR threshold identified by the ER and HCP
filter');

elseif(FAIL1==0)
    GPRAverage=(GPRAverage2+GPRAverage3)/2;

    str3=sprintf('The GPR threshold identified by the ER and CD
filter is %g dB', GPRAverage2);
    str4=sprintf('The GPR threshold identified by the ER and HCP
filter is %g dB', GPRAverage3);
    disp('There is no GPR threshold identified by the ER, HCP, and
CD filter');
    disp(str3);
    disp(str4);

```

```

elseif(FAIL2==0)
    GPRAverage=(GPRAverage1+GPRAverage3)/2;

    str2=sprintf('The GPR threshold identified by the ER, HCP, and
CD filter is %g dB', GPRAverage1);
    str4=sprintf('The GPR threshold identified by the ER and HCP
filter is %g dB', GPRAverage3);
    disp(str2);
    disp('There is no GPR threshold identified by the ER and CD
filter');
    disp(str4);

elseif(FAIL3==0)
    GPRAverage=(GPRAverage1+GPRAverage2)/2;

    str2=sprintf('The GPR threshold identified by the ER, HCP, and
CD filter is %g dB', GPRAverage1);
    str3=sprintf('The GPR threshold identified by the ER and CD
filter is %g dB', GPRAverage2);
    disp(str2);
    disp(str3);
    disp('There is no GPR threshold identified by the ER and HCP
filter');

else
    GPRAverage=(GPRAverage1+GPRAverage2+GPRAverage3)/3;

    str2=sprintf('The GPR threshold identified by the ER, HCP, and
CD filter is %g dB', GPRAverage1);
    str3=sprintf('The GPR threshold identified by the ER and CD
filter is %g dB', GPRAverage2);
    str4=sprintf('The GPR threshold identified by the ER and HCP
filter is %g dB', GPRAverage3);
    disp(str2);
    disp(str3);
    disp(str4);
end

GPRthreshold=round(GPRAverage/0.5)*0.5;

str1=sprintf('The GPR threshold is %g dB', GPRthreshold);
disp(str1);

%-----Define Patch Locations-----
---%
[ii,jj]=size(DATA);
%Duplication with Sound and Delamination Patch Locations
i=1;
while(i<=ii)
    if(DATA(i,6)>1)
        Patch(i,1)=DATA(i,1);
        Patch(i,2)=DATA(i,2);
        Patch(i,3)=1;
    else

```

```

        Patch(i,1)=DATA(i,1);
        Patch(i,2)=DATA(i,2);
        Patch(i,3)=0;
    end
    i=i+1;
end

%Duplication only with Sound Patch Locations, locations with delam and
%patch are coded with delamination only

i=1;
while(i<=ii)
    if(DATA(i,6)==2)
        PatchNONDUP(i,1)=DATA(i,1);
        PatchNONDUP(i,2)=DATA(i,2);
        PatchNONDUP(i,3)=1;
    else
        PatchNONDUP(i,1)=DATA(i,1);
        PatchNONDUP(i,2)=DATA(i,2);
        PatchNONDUP(i,3)=0;
    end
    i=i+1;
end

PatchsumNONDUP=sum(PatchNONDUP);
PatchNONDUPtotal=PatchsumNONDUP(1,3);

%-----Convert NDE Data into Conditions-----
---%

%Entering Longitudinal and Transverse info to condition
[ii,jj]=size(DATA);

i=1;
while(i<=ii)
    Condition(i,1)=long(i,1);
    Condition(i,2)=tran(i,1);
    i=i+1;
end

Delamcounter=0;
Crackcounter=0;
Corrosioncounter=0;
CorEnvcounter=0;
Goodcounter=0;

%Determines Condition based on hierarchy
i=1;
while(i<=ii)
    if(CD(i,1)==1)
        Condition(i,3)=4;
        Delamcounter=Delamcounter+1;
    elseif(CD(i,1)==3)
        Condition(i,3)=4;
        Delamcounter=Delamcounter+1;
    end
end

```

```

elseif(IE(i,1)==4) && (ER(i,1)<=ERThreshold)
    Condition(i,3)=4;
    Delamcounter=Delamcounter+1;
elseif(IE(i,1)==4) && (HCP(i,1)<=HCPActive)
    Condition(i,3)=4;
    Delamcounter=Delamcounter+1;
elseif(IE(i,1)==4) && (GPR(i,1)<=GPRthreshold)
    Condition(i,3)=4;
    Delamcounter=Delamcounter+1;
elseif(IE(i,1)==3) && (ER(i,1)<=ERThreshold)
    Condition(i,3)=3;
    Crackcounter=Crackcounter+1;
elseif(IE(i,1)==3) && (HCP(i,1)<=HCPActive)
    Condition(i,3)=3;
    Crackcounter=Crackcounter+1;
elseif(IE(i,1)==3) && (GPR(i,1)<=GPRthreshold)
    Condition(i,3)=3;
    Crackcounter=Crackcounter+1;
elseif(IE(i,1)==2) && (ER(i,1)<=ERThreshold)
    Condition(i,3)=3;
    Crackcounter=Crackcounter+1;
elseif(IE(i,1)==2) && (HCP(i,1)<=HCPActive)
    Condition(i,3)=3;
    Crackcounter=Crackcounter+1;
elseif(IE(i,1)==2) && (GPR(i,1)<=GPRthreshold)
    Condition(i,3)=3;
    Crackcounter=Crackcounter+1;
elseif(HCP(i,1)<=HCPActive)
    Condition(i,3)=2;
    Corrosioncounter=Corrosioncounter+1;
elseif(ER(i,1)<=ERThreshold)
    Condition(i,3)=1;
    CorEnvcounter=CorEnvcounter+1;
elseif(GPR(i,1)<=GPRthreshold)
    Condition(i,3)=1;
    CorEnvcounter=CorEnvcounter+1;
else
    Condition(i,3)=0;
    Goodcounter=Goodcounter+1;
end
i=i+1;
end

%For plotting purposes need to have the distribution of each damage
state
%regardless of damage priority

i=1;
while(i<=ii)
    if(CD(i,1)==1)
        Condition(i,4)=1;
    elseif(CD(i,1)==3)
        Condition(i,4)=1;
    else
        Condition(i,4)=0;
    end
end

```

```

if(IE(i,1)==4) && (ER(i,1)<=ERThreshold)
    Condition(i,5)=1;
elseif(IE(i,1)==4) && (HCP(i,1)<=HCPActive)
    Condition(i,5)=1;
elseif(IE(i,1)==4) && (GPR(i,1)<=GPRthreshold)
    Condition(i,5)=1;
else
    Condition(i,5)=0;
end

if(IE(i,1)==3) && (ER(i,1)<=ERThreshold)
    Condition(i,6)=1;
elseif(IE(i,1)==3) && (HCP(i,1)<=HCPActive)
    Condition(i,6)=1;
elseif(IE(i,1)==3) && (GPR(i,1)<=GPRthreshold)
    Condition(i,6)=1;
else
    Condition(i,6)=0;
end

if(IE(i,1)==2) && (ER(i,1)<=ERThreshold)
    Condition(i,7)=1;
elseif(IE(i,1)==2) && (HCP(i,1)<=HCPActive)
    Condition(i,7)=1;
elseif(IE(i,1)==2) && (GPR(i,1)<=GPRthreshold)
    Condition(i,7)=1;
else
    Condition(i,7)=0;
end

Condition(i,8)=Condition(i,6)+Condition(i,7);

if(HCP(i,1)<=HCPActive)
    Condition(i,9)=1;
else
    Condition(i,9)=0;
end

if(ER(i,1)<=ERThreshold)
    Condition(i,10)=1;
else
    Condition(i,10)=0;
end

if(GPR(i,1)<=GPRthreshold)
    Condition(i,11)=1;
else
    Condition(i,11)=0;
end

if(Condition(i,3)==0)
    Condition(i,12)=1;
else
    Condition(i,12)=0;
end

```

```

end

if(Patch(i,3)==1)
    Condition(i,13)=1;
else
    Condition(i,13)=0;
end

i=i+1;
end

%Creating individual plotting files for each condition
[ii,jj]=size(Condition);
i=1;
while(i<=ii)
    DelamPLOT(i,1)=Condition(i,1);
    DelamPLOT(i,2)=Condition(i,2);
    if(Condition(i,4)==1)
        DelamPLOT(i,3)=4;
    elseif(Condition(i,5)==1)
        DelamPLOT(i,3)=4;
    else
        DelamPLOT(i,3)=0;
    end

    CrackPLOT(i,1)=Condition(i,1);
    CrackPLOT(i,2)=Condition(i,2);
    if(Condition(i,8)==1)
        CrackPLOT(i,3)=3;
    else
        CrackPLOT(i,3)=0;
    end

    CorPLOT(i,1)=Condition(i,1);
    CorPLOT(i,2)=Condition(i,2);
    if(Condition(i,9)==1)
        CorPLOT(i,3)=2;
    else
        CorPLOT(i,3)=0;
    end

    CorEnPLOT(i,1)=Condition(i,1);
    CorEnPLOT(i,2)=Condition(i,2);
    if(Condition(i,10)==1)
        CorEnPLOT(i,3)=1;
    elseif(Condition(i,11)==1)
        CorEnPLOT(i,3)=1;
    else
        CorEnPLOT(i,3)=0;
    end

    PatchPLOT(i,1)=Condition(i,1);
    PatchPLOT(i,2)=Condition(i,2);
    if(Condition(i,13)==1)
        PatchPLOT(i,3)=5;

```

```

else
    PatchPLOT(i,3)=0;
end

ConditionPLOT(i,1)=Condition(i,1);
ConditionPLOT(i,2)=Condition(i,2);
ConditionPLOT(i,3)=Condition(i,3);

i=i+1;
end

csvwrite('DelamPLOT.txt',DelamPLOT);
csvwrite('CrackPLOT.txt',CrackPLOT);
csvwrite('CorPLOT.txt',CorPLOT);
csvwrite('CorEnPLOT.txt',CorEnPLOT);
csvwrite('PatchPLOT.txt',PatchPLOT);

%Condition Quantities (nonduplicating)
%Damage Area and Percentage Calculation

CorEnvArea=CorEnvcounter*4;
CorrosionArea=Corrosioncounter*4;
CrackArea=Crackcounter*4;
DelamArea=Delamcounter*4;
GoodArea=Goodcounter*4;
PatchNONDUPArea=PatchNONDUPtotal*4;

TotalArea=ii*4;

CorEnvAreaPercent=(CorEnvArea/TotalArea)*100;
CorrosionAreaPercent=(CorrosionArea/TotalArea)*100;
CrackAreaPercent=(CrackArea/TotalArea)*100;
DelamAreaPercent=(DelamArea/TotalArea)*100;
GoodAreaPercent=(GoodArea/TotalArea)*100;
PatchNONDUPAreaPercent=(PatchNONDUPArea/TotalArea)*100;

%Condition Quantities (duplicating)

duplicating=sum(Condition);
SoundDuplicating=duplicating(1,12)*4;
CorEnvDuplicating=(duplicating(1,11)+duplicating(1,10))*4;
CorrosionDuplicating=duplicating(1,9)*4;
CrackingDuplicating=duplicating(1,8)*4;
DelamDuplicating=Delamcounter*4;
PatchDuplicating=duplicating(1,13)*4;

CorEnvAreaPercentDuplicating=(CorEnvDuplicating/TotalArea)*100;
CorrosionAreaPercentDuplicating=(CorrosionDuplicating/TotalArea)*100;
CrackAreaPercentDuplicating=(CrackingDuplicating/TotalArea)*100;
DelamAreaPercentDuplicating=(DelamDuplicating/TotalArea)*100;
GoodAreaPercentDuplicating=(SoundDuplicating/TotalArea)*100;
PatchAreaPrecentDuplicating=(PatchDuplicating/TotalArea)*100;

%Confidence Level

```

```

TotalAgreementCounter=0;

[ii,jj]=size(Condition);
i=1;
while(i<=ii)
    Confidence(i,1)=Condition(i,1);
    Confidence(i,2)=Condition(i,2);

    if(Condition(i,3)==0)
        Confidence(i,3)=100;
        TotalAgreementCounter=TotalAgreementCounter+1;

elseif(Condition(i,3)==1)&&(Condition(i,10)==1)&&(Condition(i,11)==1)
    Confidence(i,3)=100;
    TotalAgreementCounter=TotalAgreementCounter+1;
elseif(Condition(i,3)==1)&&(Condition(i,11)==0)
    Confidence(i,3)=75;
elseif(Condition(i,3)==1)&&(Condition(i,10)==0)
    Confidence(i,3)=75;

elseif(Condition(i,3)==2)&&(Condition(i,10)==1)&&(Condition(i,11)==1)
    Confidence(i,3)=100;
    TotalAgreementCounter=TotalAgreementCounter+1;

elseif(Condition(i,3)==2)&&(Condition(i,10)==1)&&(Condition(i,11)==0)
    Confidence(i,3)=75;

elseif(Condition(i,3)==2)&&(Condition(i,10)==0)&&(Condition(i,11)==1)
    Confidence(i,3)=70;

elseif(Condition(i,3)==2)&&(Condition(i,10)==0)&&(Condition(i,11)==0)
    Confidence(i,3)=50;

elseif(Condition(i,3)==3)&&(Condition(i,9)==1)&&(Condition(i,10)==1)&&(
Condition(i,11)==1)
    Confidence(i,3)=100;
    TotalAgreementCounter=TotalAgreementCounter+1;

elseif(Condition(i,3)==3)&&(Condition(i,9)==1)&&(Condition(i,10)==0)&&(
Condition(i,11)==1)
    Confidence(i,3)=90;

elseif(Condition(i,3)==3)&&(Condition(i,9)==1)&&(Condition(i,10)==1)&&(
Condition(i,11)==0)
    Confidence(i,3)=90;

elseif(Condition(i,3)==3)&&(Condition(i,9)==0)&&(Condition(i,10)==1)&&(
Condition(i,11)==1)
    Confidence(i,3)=80;

elseif(Condition(i,3)==3)&&(Condition(i,9)==1)&&(Condition(i,10)==0)&&(
Condition(i,11)==0)
    Confidence(i,3)=75;

```

```

elseif(Condition(i,3)==3)&&(Condition(i,9)==0)&&(Condition(i,10)==0)&&(
Condition(i,11)==1)
    Confidence(i,3)=70;

elseif(Condition(i,3)==3)&&(Condition(i,9)==0)&&(Condition(i,10)==1)&&(
Condition(i,11)==0)
    Confidence(i,3)=60;

elseif(Condition(i,3)==3)&&(Condition(i,9)==0)&&(Condition(i,10)==0)&&(
Condition(i,11)==0)
    Confidence(i,3)=40;

elseif(Condition(i,3)==4)&&(Condition(i,4)==1)&&(Condition(i,5)==1)&&(C
ondition(i,9)==1)&&(Condition(i,10)==1)&&(Condition(i,11)==1)
    Confidence(i,3)=100;
    TotalAgreementCounter=TotalAgreementCounter+1;

elseif(Condition(i,3)==4)&&(Condition(i,4)==1)&&(Condition(i,6)==1)&&(C
ondition(i,9)==1)&&(Condition(i,10)==1)&&(Condition(i,11)==1)
    Confidence(i,3)=99;

elseif(Condition(i,3)==4)&&(Condition(i,4)==1)&&(Condition(i,7)==1)&&(C
ondition(i,9)==1)&&(Condition(i,10)==1)&&(Condition(i,11)==1)
    Confidence(i,3)=95;

elseif(Condition(i,3)==4)&&(Condition(i,4)==1)&&(Condition(i,5)==0)&&(C
ondition(i,8)==0)&&(Condition(i,9)==1)&&(Condition(i,10)==1)&&(Conditio
n(i,11)==1)
    Confidence(i,3)=90;

elseif(Condition(i,3)==4)&&(Condition(i,4)==0)&&(Condition(i,5)==1)&&(C
ondition(i,9)==1)&&(Condition(i,10)==1)&&(Condition(i,11)==1)
    Confidence(i,3)=85;

elseif(Condition(i,3)==4)&&(Condition(i,4)==1)&&(Condition(i,5)==1)&&(C
ondition(i,9)==1)&&(Condition(i,10)==0)&&(Condition(i,11)==1)
    Confidence(i,3)=90;

elseif(Condition(i,3)==4)&&(Condition(i,4)==1)&&(Condition(i,6)==1)&&(C
ondition(i,9)==1)&&(Condition(i,10)==0)&&(Condition(i,11)==1)
    Confidence(i,3)=89;

elseif(Condition(i,3)==4)&&(Condition(i,4)==1)&&(Condition(i,7)==1)&&(C
ondition(i,9)==1)&&(Condition(i,10)==0)&&(Condition(i,11)==1)
    Confidence(i,3)=85;

elseif(Condition(i,3)==4)&&(Condition(i,4)==1)&&(Condition(i,5)==0)&&(C
ondition(i,8)==0)&&(Condition(i,9)==1)&&(Condition(i,10)==0)&&(Conditio
n(i,11)==1)
    Confidence(i,3)=80;

elseif(Condition(i,3)==4)&&(Condition(i,4)==0)&&(Condition(i,5)==1)&&(C
ondition(i,9)==1)&&(Condition(i,10)==0)&&(Condition(i,11)==1)
    Confidence(i,3)=80;

```





```

elseif(Condition(i,3)==4)&&(Condition(i,4)==1)&&(Condition(i,7)==1)&&(C
ondition(i,9)==0)&&(Condition(i,10)==0)&&(Condition(i,11)==0)
    Confidence(i,3)=65;

elseif(Condition(i,3)==4)&&(Condition(i,4)==1)&&(Condition(i,5)==0)&&(C
ondition(i,8)==0)&&(Condition(i,9)==0)&&(Condition(i,10)==0)&&(Conditio
n(i,11)==0)
    Confidence(i,3)=60;

elseif(Condition(i,3)==4)&&(Condition(i,4)==0)&&(Condition(i,5)==1)&&(C
ondition(i,9)==0)&&(Condition(i,10)==0)&&(Condition(i,11)==0)
    Confidence(i,3)=50;
else
    Confidence(i,3)=999999;
end
i=i+1;

end

AverageConfidence=mean(Confidence);
CL=round(AverageConfidence(1,3)/.1)*.1;

NonAgreementCounter=ii-TotalAgreementCounter;
TotalAgreementCounterPercent=(TotalAgreementCounter/ii)*100;
NonAgreementCounterPercent=(NonAgreementCounter/ii)*100;

%Condition Rating

%NBIS Rating
Pushvalue=CorEnvAreaPercent+CorrosionAreaPercent+CrackAreaPercent;

if(DelamAreaPercent==0)&&(Pushvalue<10)
    NBI=9;
elseif(DelamAreaPercent==0)&&(Pushvalue>=10)
    NBI=8;
elseif(DelamAreaPercent<=5)&&(Pushvalue<20)
    NBI=8;
elseif(DelamAreaPercent<=5)&&(Pushvalue>=20)
    NBI=7;
elseif(DelamAreaPercent<=10)&&(Pushvalue<30)
    NBI=7;
elseif(DelamAreaPercent<=10)&&(Pushvalue>=30)
    NBI=6;
elseif(DelamAreaPercent<=20)&&(Pushvalue<40)
    NBI=6;
elseif(DelamAreaPercent<=20)&&(Pushvalue>=40)
    NBI=5;
elseif(DelamAreaPercent<=40)&&(Pushvalue<40)
    NBI=5;
elseif(DelamAreaPercent<=40)&&(Pushvalue>=40)
    NBI=4;
elseif(DelamAreaPercent<=60)&&(Pushvalue<40)
    NBI=4;
else
    NBI=3;

```

```

end

%AASHTO Bridge Element Rating
AASHTOone=GoodArea+CorEnvArea;
AASHTOtwo=CorrosionArea+CrackArea;
AASHTOthree=DelamArea;
AASHTOfour=0;

AASHTOonePercent=(AASHTOone/TotalArea)*100;
AASHTOtwoPercent=(AASHTOtwo/TotalArea)*100;
AASHTOthreePercent=(AASHTOthree/TotalArea)*100;
AASHTOfourPercent=(AASHTOfour/TotalArea)*100;

%-----Output File-----
---%
fid=fopen('ConditionAssessment.txt','w');

%Header
fprintf(fid,'Results of Multi-Modal NDT Condition Assessment of a
Bridge Deck\n\n');
fprintf(fid,'Structure Carries:\t%s\n', Carries);
fprintf(fid,'Structure Spans:\t%s\n', Spans);
fprintf(fid,'City:\t%s\n', City);
fprintf(fid,'State:\t%s\n', State);
fprintf(fid,'Total Deck Area:\t%d\n\n',TotalArea);

fprintf(fid,'NBIS Rating:\t%d\n\n',NBI);

fprintf(fid,'AASHTO Rating:\tft^2\tPercentage of Total Deck Area\n');
fprintf(fid,'Condition State 1:\t%d\t%.1f\n', AASHTOone,
AASHTOonePercent);
fprintf(fid,'Condition State 2:\t%d\t%.1f\n', AASHTOtwo,
AASHTOtwoPercent);
fprintf(fid,'Condition State 3:\t%d\t%.1f\n', AASHTOthree,
AASHTOthreePercent);
fprintf(fid,'Condition State 4:\t%d\t%.1f\n\n', AASHTOfour,
AASHTOfourPercent);

fprintf(fid,'Damage Quantities (nonduplicating)\n');
fprintf(fid,'Type of Damage\tft^2\tPercentage of Total Deck Area\n');
fprintf(fid,'Sound\t%d\t%.1f\n', GoodArea, GoodAreaPercent);
fprintf(fid,'Corrosive
Environment\t%d\t%.1f\n', CorEnvArea, CorEnvAreaPercent);
fprintf(fid,'Active
Corrosion\t%d\t%.1f\n', CorrosionArea, CorrosionAreaPercent);
fprintf(fid,'Delamination/Lateral
Cracking\t%d\t%.1f\n', CrackArea, CrackAreaPercent);
fprintf(fid,'Severe
Delamination\t%d\t%.1f\n', DelamArea, DelamAreaPercent);
fprintf(fid,'Patches (Duplicating w/ Sound
Only)\t%d\t%.1f\n\n', PatchNONDUPArea, PatchNONDUPAreaPercent);

fprintf(fid,'Damage Quantities (duplicating)\n');
fprintf(fid,'Type of Damage\tft^2\tPercentage of Total Deck Area\n');

```



## APPENDIX 3 – SAMPLE OUTPUT FROM CONDITION ASSESSMENT CODE

## Results of Multi-Modal NDT Condition Assessment of a Bridge Deck

Structure Carries: State Route 15  
 Structure Spans: Interstate 66  
 City: Haymarket  
 State: Virginia  
 Total Deck Area: 10392

NBIS Rating: 5

AASHTO Rating:	ft <sup>2</sup>	Percentage of Total Deck Area
Condition State 1:	5632	54.2
Condition State 2:	2420	23.3
Condition State 3:	2340	22.5
Condition State 4:	0	0

## Damage Quantities (nonduplicating)

Type of Damage	ft <sup>2</sup>	Percentage of Total Deck Area
Sound	4884	47
Corrosive Environment	748	7.2
Active Corrosion	1228	11.8
Delamination/Lateral Cracking	1192	11.5
Severe Delamination	2340	22.5
Patches (Duplicating w/ Sound Only)	100	1

## Damage Quantities (duplicating)

Type of Damage	ft <sup>2</sup>	Percentage of Total Deck Area
Sound	4884	47
Corrosive Environment	6964	67
Active Corrosion	3816	36.7
Delamination/Lateral Cracking	1476	14.2
Severe Delamination	2340	22.5
Patches	204	2

## Threshold Values

Half-Cell Potential Active (mV): -325  
 Half-Cell Potential Passive (mV): -250  
 Electrical Resistivity (kohm\*cm): 45  
 Ground Penetrating Radar (dB): -18.5

Confidence Level: 90.5

Percentage of Deck in Which all NDT Methods are in Complete Agreement: 60.2

Percentage of Deck in Which all NDT Methods are  
not in Complete Agreement:

39.8

Combined Results (Excludes Patch Areas)			Plotting Data for Severe Delaminati on			Plotting Data for Delamination/L ateral Cracking			Plotting Data for Active Corrosion			Plotting Data for Corrosive Environme nt			Plotting Data for Patches		
4	1	0	4	1	0	4	1	0	4	1	0	4	1	0	4	1	0
6	1	0	6	1	0	6	1	0	6	1	0	6	1	0	6	1	0
8	1	0	8	1	0	8	1	0	8	1	0	8	1	0	8	1	0
10	1	0	10	1	0	10	1	0	10	1	0	10	1	0	10	1	0
12	1	0	12	1	0	12	1	0	12	1	0	12	1	0	12	1	0
14	1	0	14	1	0	14	1	0	14	1	0	14	1	0	14	1	0
16	1	4	16	1	4	16	1	0	16	1	2	16	1	1	16	1	0
18	1	4	18	1	4	18	1	0	18	1	0	18	1	0	18	1	0
20	1	4	20	1	4	20	1	0	20	1	2	20	1	1	20	1	0
22	1	4	22	1	4	22	1	0	22	1	2	22	1	1	22	1	0
24	1	4	24	1	4	24	1	0	24	1	2	24	1	1	24	1	0
26	1	4	26	1	4	26	1	0	26	1	0	26	1	0	26	1	0

APPENDIX 4 –CONDITION PLOTS OF EVALUATED BRIDGES

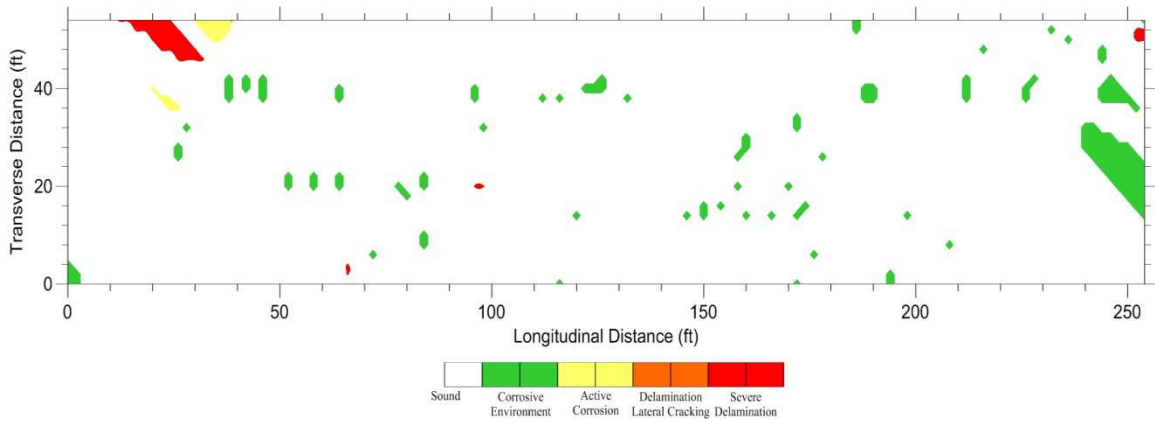


Figure 58: Condition assessment of I-495 South Bridge in Wilmington, Delaware

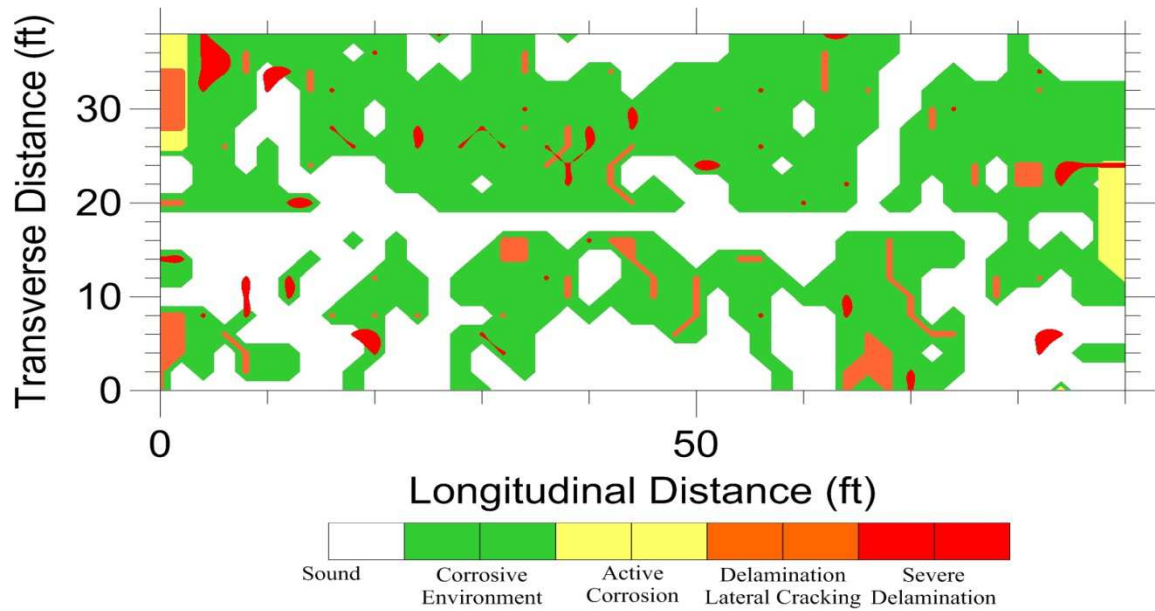


Figure 59: Condition assessment of I-195 East Bridge in Upper Freehold, New Jersey

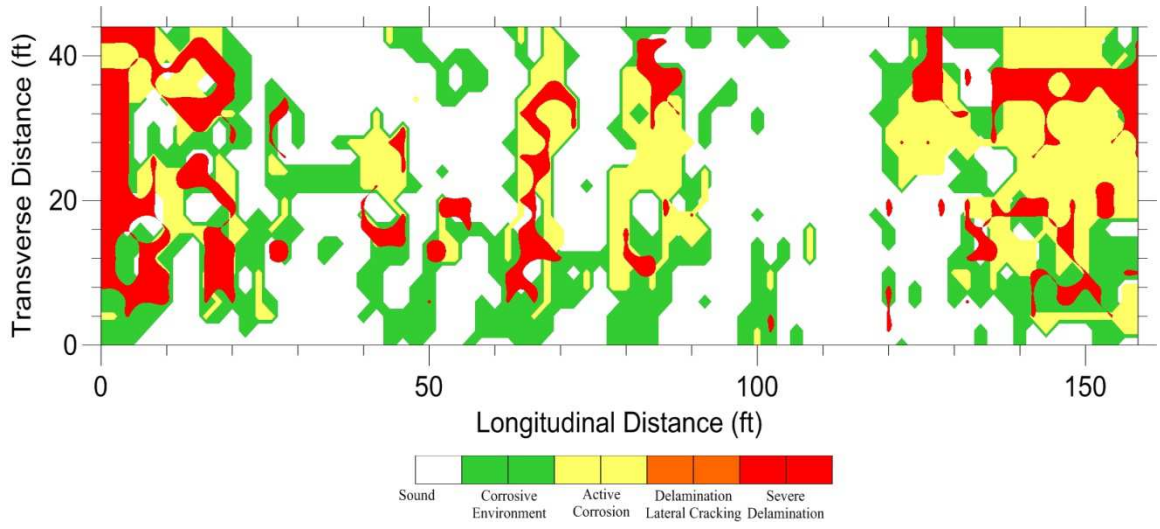


Figure 60: Condition assessment of Pequea Boulevard Bridge in Conestoga, Pennsylvania

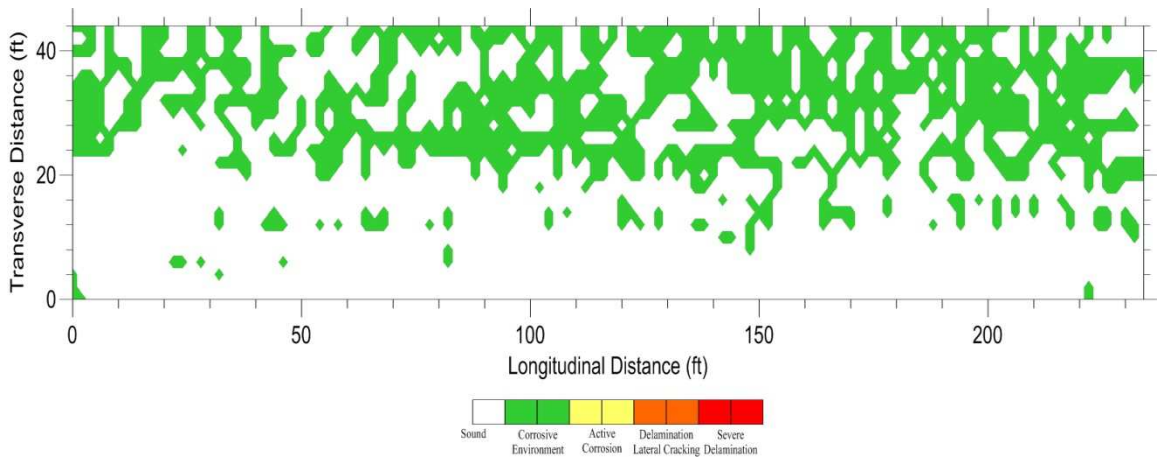


Figure 61: Condition assessment of School House Road Bridge in Middletown, Pennsylvania

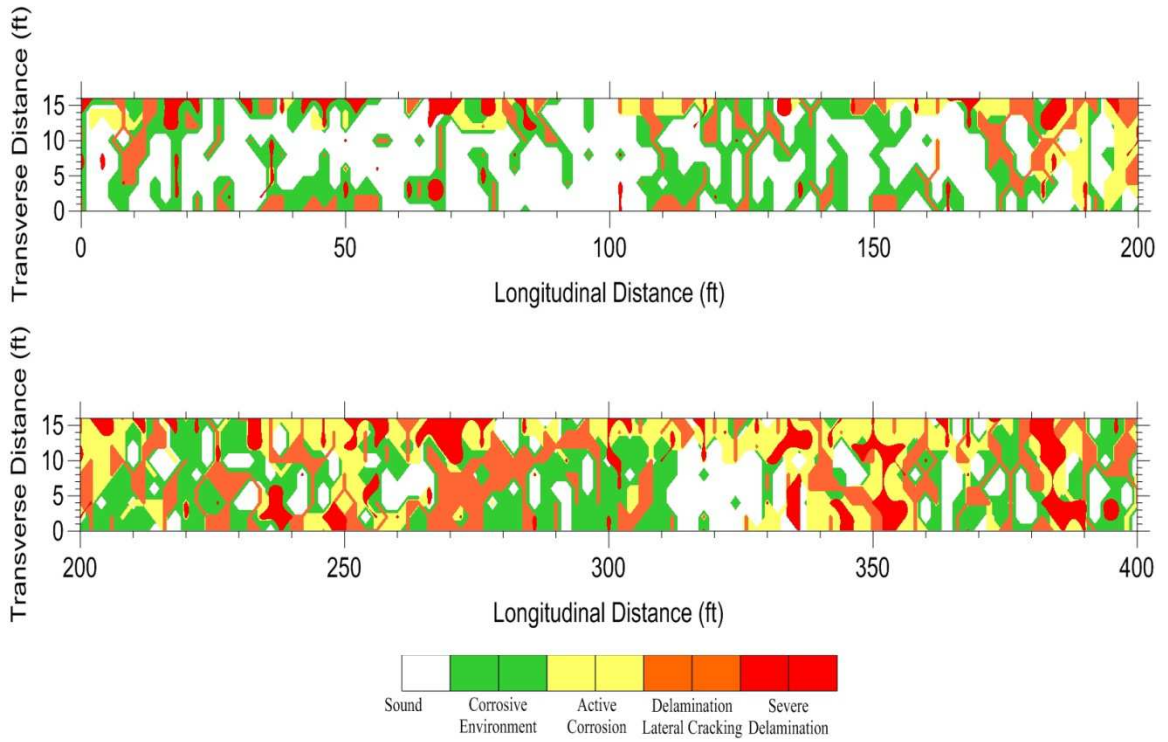


Figure 62: Condition assessment of Route 123 Bridge in Sandstone, Minnesota

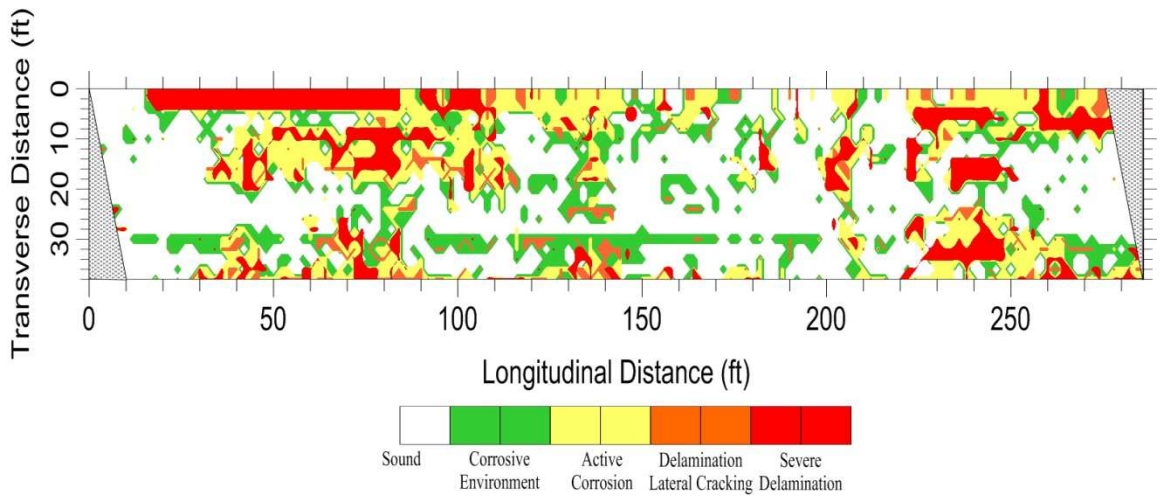


Figure 63: Condition assessment of Route 15 Bridge in Haymarket, Virginia

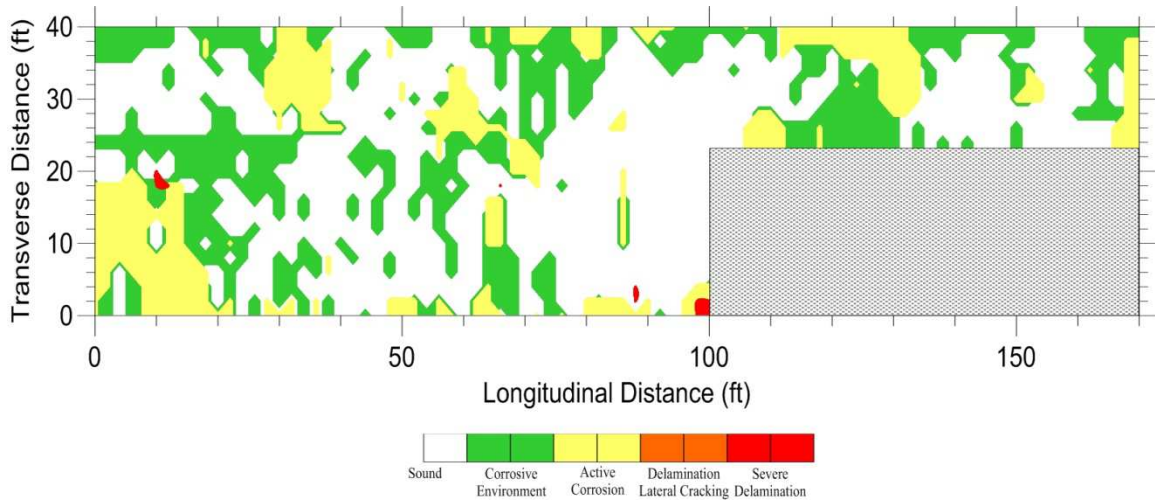


Figure 64: Condition assessment of Route 18 Bridge in Neptune, New Jersey

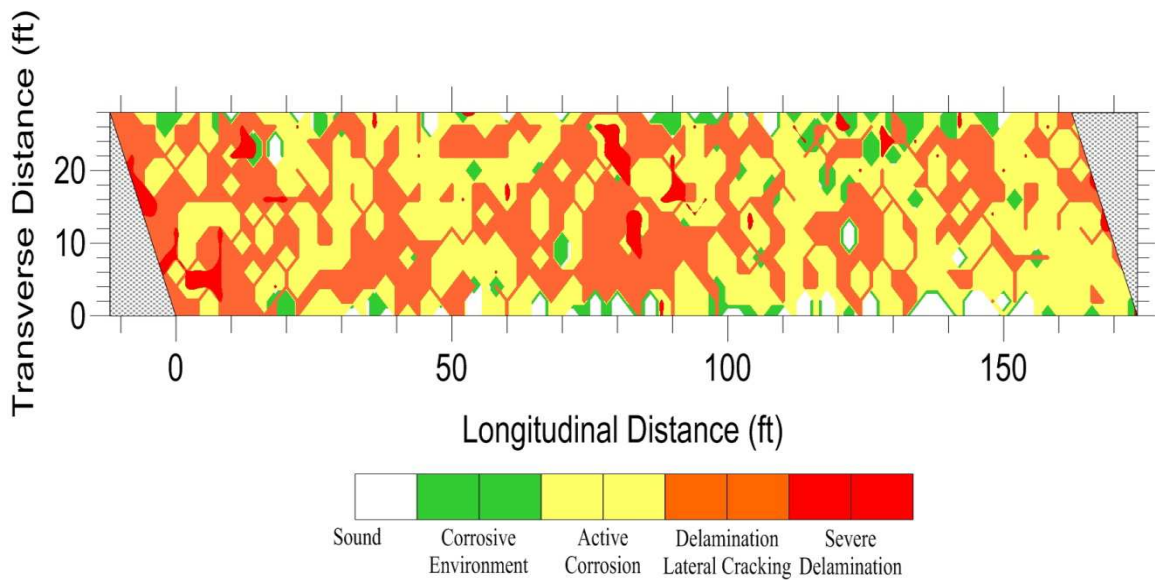


Figure 65: Condition assessment of Route 21 Bridge in Almond, New York

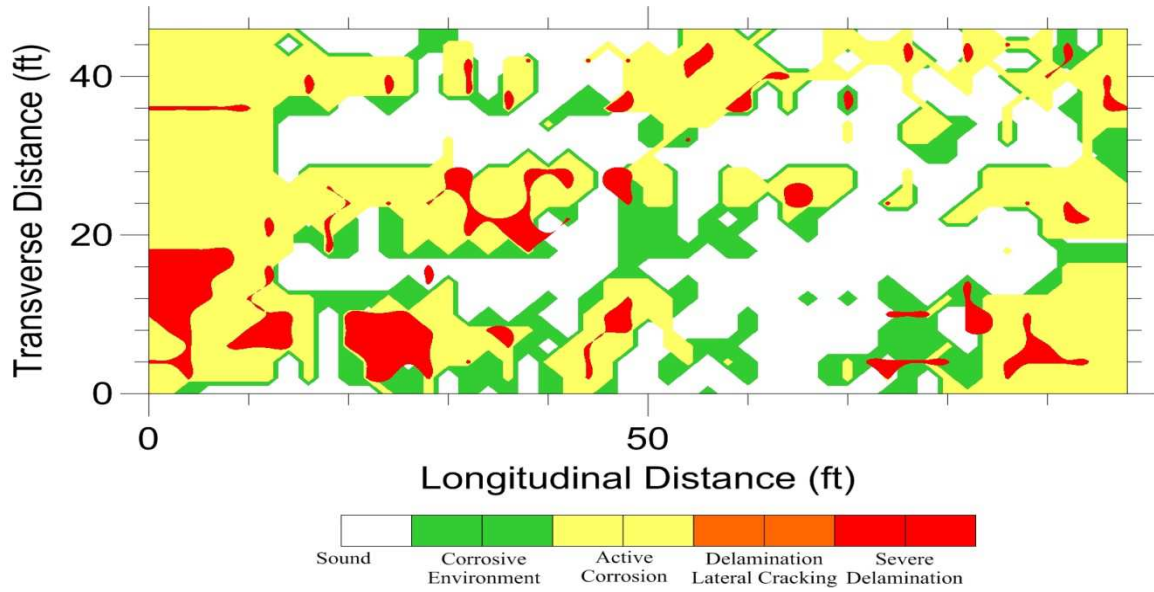


Figure 66: Condition assessment of Route 273 Bridge in Elkton, Maryland

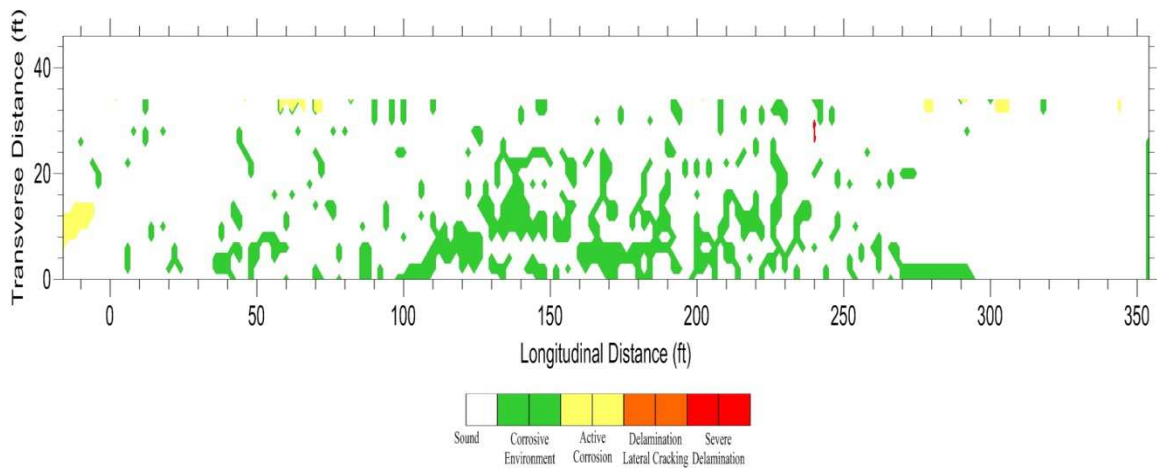


Figure 67: Condition assessment of Route 47 Bridge in Deptford Township, New Jersey

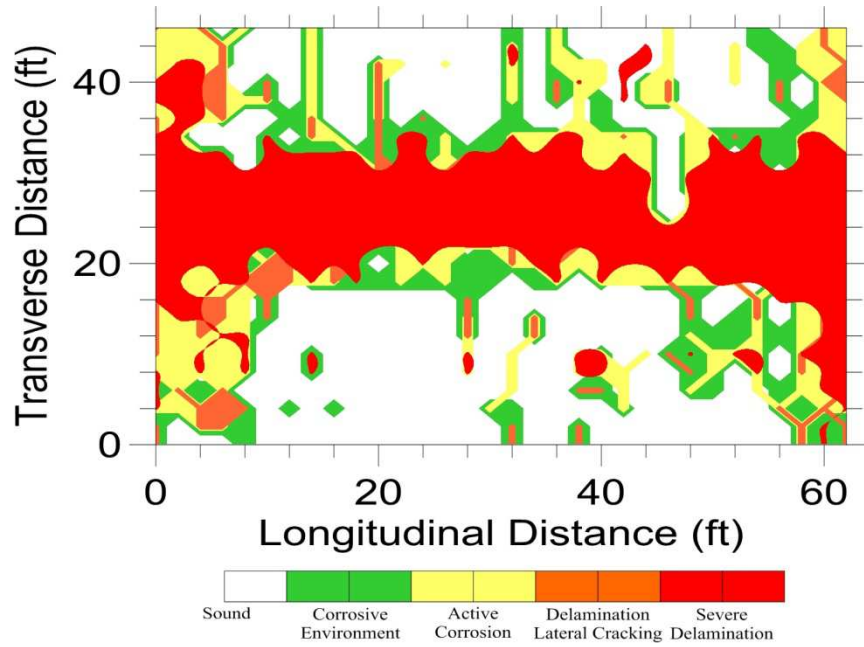


Figure 68: Condition assessment of Route 93 Bridge in Sumner, Iowa

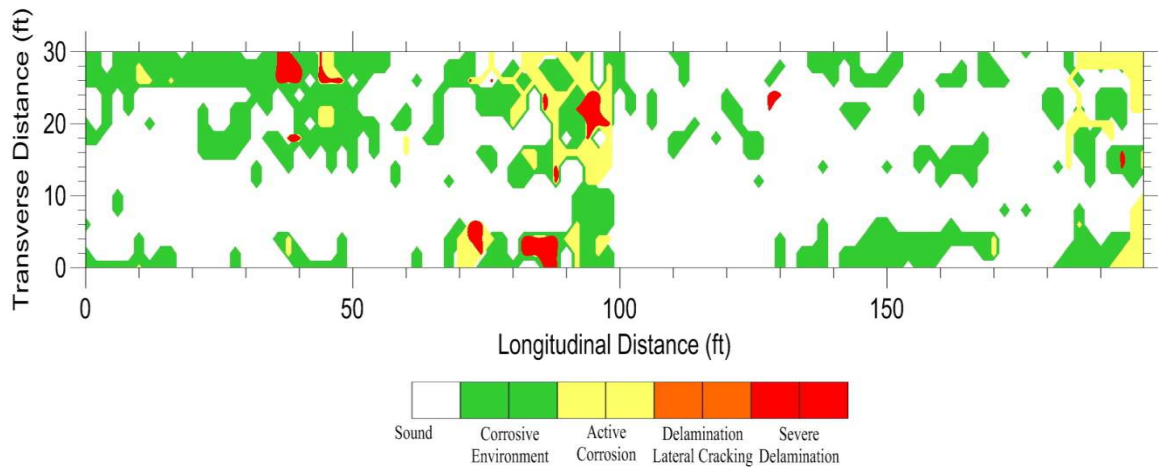


Figure 69: Condition assessment of West Bangs Ave Bridge in Neptune, New Jersey